1968

Preparation and Optical and Nmr Spectral Studies of Some Unusual Complexes of Oxovanadium (Iv).

Gerald S. Vigee
Louisiana State University and Agricultural & Mechanical College

PREPARATION AND OPTICAL AND NMR SPECTRAL STUDIES OF SOME UNUSUAL COMPLEXES OF OXOVANADIUM(IV)

A Dissertation

Submitted to the Graduate Faculty of the
Louisiana State University and
Agricultural and Mechanical College
in partial fulfillment of the
requirements for the degree of
Doctor of Philosophy

in

The Department of Chemistry

by
Gerald S. Vigee
B.S., United States Military Academy, West Point, New York, 1954
B.S., Louisiana State University, Baton Rouge, Louisiana, 1960
M.S., University of Southwestern Louisiana, Lafayette, Louisiana, 1965

May 1968

ACKNOWLEDGMENT

The author wishes to acknowledge the aid and encouragement of Professor Joel Selbin under whose direction this dissertation was accomplished.

Without the patient understanding and sacrifice of his wife, Wilhelmina, this work could not have been undertaken. A special thanks to Mrs. John Rist for many services rendered is also expressed at this time.

The author wishes also to thank the Dr. Charles E. Coates Memorial Fund of the Louisiana State University and the National Science Foundation for its financial assistance toward the completion of this dissertation.

To Willey

TABLE OF CONTENTS

LIST OF TABLES

LIST OF FIGURES

LIST OF COMMONLY USED SYMBOLS

1. Me---methyl group
2. Ph---phenyl group
3. R----alkyl group
4. Et---Ethyl group
5. o-TAS---bis(o-dimethylarsinophenyl)methylarsine
6. v-TAS---tris-1,1,1-(dimethylarsinomethyl)ethane
7. EBDPP---Ethylene bis(diphenylphosphine)
8. MBDPP---Methylene bis(diphenylphosphine)
9. EBDPA---Ethylene bis(diphenylarsine)
10. MeOH----Methyl alcohol
11. $EBDPPO_2$---Ethylene bis(diphenylphosphineoxide)
12. aca---acetylacetonate ion
13. o-phen---Orthophenanthroline
14. T---tropolonate ion
15. DMSO---Dimethylsulfoxide
16. py-----pyridine

ABSTRACT

The first chapter describes the preparation and spectral examination of some new oxovanadium(IV) complexes with phosphorus and sulfur ligands. The phosphine ligands ethylene bis(diphenylphosphine) and methylene bis(diphenylphosphine) were reacted to produce complexes with vanadyl bromide and vanadyl chloride. Impure compounds were obtained with the analogous arsenic other phosphorus ligands. The infrared and optical (visible-near infrared) spectra were used to characterize these complexes which were the first vanadyl phosphine complexes ever prepared.

The long-standing debate over the correctness of the Ballhausen and Gray energy level scheme generated the work in Chapter II. NMR paramagnetic contact shifts of the aqueous vanadyl sulfate were measured and from these data and the electron spin-nuclear spin coupling constant was determined. The results indicated the existance of π-bonding between the equatorial water molecules and the oxovanadium(II) cation. The possible existance of this type of π-bonding was ignored by the Ballhausen-Gray molecular orbital approach.

In addition, two other vanadyl complexes which might contain pi-bonding between the d' vanadyl orbital and ligand pi-orbitals were investigated. The two vanadyl complexes, of

acetylacetonate and of ortho-phenanthroline, showed very small contact shifts, especially considering that the acetylacetonate ion and the ortho-phenanthroline possess pi-orbitals which are well-suited for pi-bonding to metal ions. The absence of a large contact shift in either complex, similar to the shifts observed in other paramagnetic metal acetylacetonate complexes, probably results because the complexes fail to meet proper symmetry requirements for pi-bonding. The small contact shifts observed most likely result from a spin-polarization mechanism which is consistent with the ESR studies of similar complexes.

In Chapter III, two new complexes, vanadyl bis(tropolonate) and vanadyl bis(5-mercapto-3-phenyl-1,3,4-thiadiazole-2-thione), were found to possess certain characteristics which indicated the possibility of unusual coordination and molecularity. An extensive study of these complexes using optical (near infrared-visible), infrared, NMR, ESR, solubility, molecular weight determination and magnetic moment measurements was undertaken and most of the experimental evidence bore out the hypothesis that the two complexes contain unusual coordination and molecularity.

CHAPTER I

COMPLEXES OF OXOVANADIUM(IV) WITH PHOSPHORUS AND SULFUR LIGANDS

PHOSPHINE COMPLEXES OF OXOVANADIUM(IV)

INTRODUCTION

It is generally recognized that the organic phosphines, arsines and sulfide ligands act as weak sigma-pair donors toward Pearson hard acids. If the metal atom to which the ligands are bonded contains filled or even partially occupied pi-bonding d-levels, the metal-ligand bond may be strengthened by the donation of metal electron density to the ligand $d\pi$ orbitals. The result is that many complexes which might otherwise be unstable, are found to be very stable. The early transition elements, i.e., those in Groups III, IV, V and VI, possess little or no ligand field stabilization energy in their common (high) oxidation states, and bonding is mainly the result of a combination of ionic and sigma-bonding. These metal atoms, having vacant pi orbitals, are capable of bonding to ligands such as the oxide ion, which possesses filled, low energy pi-orbitals, and electron donation of the ligand-to-metal type is thus possible. It is not surprising that few complexes[1-3] of these early transition elements have been prepared with phosphorus-, arsenic- and sulfur-donor ligands. In most cases, the complexes of phosphorus, arsenic and sulfur donor ligands

are prepared with the metal atoms in a lower-than-usual oxidation state, in which presumably the d-electron repulsion facilitates some pi-bonding.

Complexes such as $V(Me_2PCH_2CH_2PMe)_3$, $[V(Ph_3P)_2(CO)_4]$, and $[V(Ph_3P)(NO)(CO)_4]$ which have vanadium in the zero valent state appear to be more common and better characterized than those higher-valent types represented by $[Ph_3PH][VCl_4(PH_3P)]$ and $[VCl_3(R_3P)]_x$[1,2]. The only well-characterized complexes of tetravalent vanadium (a d^1 system) in which the vanadium atom is bonded to either an arsenic or a phosphorus atom (sulfur will be covered later in the chapter) are the following arsenic-donor complexes:

$VCl_4 \cdot x[o\text{-}C_6H_4(AsMe_2)_2]$ (x = 1 or 2)[4]

$VCl_4 \cdot [o\text{-}C_6H_4(AsEt_2)_2]$[5]

$VCl_4 \cdot$o-TAS and $VCl_4 \cdot$v-TAS[6]

where: o-TAS = bis-(odimethylarsinophenyl)methylarsine

v-TAS = tris-1,1,1-(dimethylarsinomethyl)ethane

The latter two complexes, upon exposure to air, are reported to yield the corresponding oxovanadium(IV) complexes, $VOCl_2 \cdot$o-TAS and $VOCl_2 \cdot$v-TAS, but these compounds were not very well characterized and apparently not preparable from a VO^{2+} starting material[6].

As a result of the present investigation, it is quite certain that the report[7] of a bis-(triphenylphosphine), (Ph_3P), complex of $VOCl_2$ is erroneous and that the product reported as $VOCl_2 \cdot 2Ph_3P \cdot 2H_2O$ is in reality a complex of triphenylphosphine oxide. To refute the claims of Majundar et al.[7], that they had prepared a true phosphine complex, the complex in question was synthesized using their procedure. In addition, the phosphine oxide, $Ph_3P = O$, was prepared by oxidizing Ph_3P in benzene with hydrogen peroxide. Much of the benzene was boiled off and then allowed to cool. Upon cooling, a white precipitate was produced from the benzene solution which analysed to be the phosphine oxide. The $Ph_3P = O$ was reacted with aqueous $VOCl_2$ to give a product similar in appearance to the complex made by the procedure of Majundar et al.[7]. The I.R. spectrum of the known phosphine oxide complex and that of the complex made by the method of Majundar et al.[7] were identical. The same report[7] claims complexes of U(IV) and U(VI) with this phosphine ligand, but these claims have been similarly refuted by two other laboratories[8,9], which also find the ligand to be the phosphine oxide.

In light of the foregoing, it was of particular interest to see if phosphine and arsine complexes could be prepared directly

from VO^{2+} starting materials. No pure arsine complexes were obtained but preparations of the first solid phosphine complexes of oxovanadium(IV) are reported here.

EXPERIMENTAL

A. Preparation of Compounds

The two ligands, obtained from Aldrich Chemical Co., which led to pure VO^{2+} complexes, their formulas and abbreviations used in this work, are the following:

Ethylenebis(diphenylphosphine) ; $(C_6H_5)_2PCH_2CH_2P(C_6H_5)_2$; EBDPP,

Methylenebis(diphenylphosphine) ; $(C_6H_5)_2PCH_2P(C_6H_5)_2$; MBDPP.

Other ligands investigated which led to impure green-colored VO^{2+} complexes, i.e., complexes which could not be satisfactorily purified to a state which yielded acceptable analytical analyses, were ethylenebis(diphenylarsine), methylenebis(diphenylarsine), tri-n-butylphosphine, triphenylphosphine, triphenylarsine and tri-n-octylphosphine. It is not clear why the phosphorus ligand, EBDPP, forms acceptable VO^{2+} complexes while the EBDPA, the analagous arsenic ligand, consistently gave a low carbon-hydrogen analysis. The low carbon-hydrogen analysis cannot be explained by assuming that the arsenic ligand was oxidized to the arsine oxide, although this might be a contributing factor. There is a

possibility that the arsenic ligand is a poorer ligand than the phosphorus ligand but forms a bond of about the same strength as a bond formed between two molecules of $VOBr_2 \cdot xH_2O$, the starting material. The result is that a mixture of $(VOBr_2 x'H_2O)_x$ and $VOBr_2 \cdot EBDPA$ is produced, which would account for the low carbon-hydrogen analyses. Probably the most logical conclusion that can be reached is that the starting material, $VOBr_2 xH_2O$, is hydrated and the arsenic ligand cannot successfully compete with the water molecules as ligands regardless of the amount of EBDPA ligand used in the starting material. If a mixture of the desired product and some other species exist in the green product, an adsorption column might be used to separate some of the desired product, but this was not attempted in this investigation.

The carbon-hydrogen analyses of the complexes is prepared with triphenylphosphine, triphenylarsine, tri-n-octylphosphine and tri-n-butylphosphine indicated that the carbon and hydrogen contents were extremely low. Again, as in the case of the EBDPA, these ligands failed to yield acceptable results probably because they could not compete with water as a ligand for the starting material $VOBr_2$. In addition, since these ligands are monodentate, no entropy effect is available to give

their complexes added stability as is the case with the bidentate ligands EBDPP and EBDPA. Therefore, only the complexes of the first two ligands listed above will be described here.

The oxovanadium(IV) starting materials used were solid $VOBr_2 \cdot xH_2O$ and syrupy $VOC\ell_2 \cdot xH_2O$. The former was prepared from commericial $VOSO_4 \cdot 4H_2O$. Reaction of the sulfate with aqueous ammonia produced first a brown precipitate of $VO(OH)_2 \cdot xH_2O$, which was washed rapidly with water and then reacted with aqueous HBr to produce a blue solution with a pH of about 6. The solution was evaporated over a steam bath to a blue-green slurry. The slurry was heated at 110°C under vacuum until a dark green highly hygroscopic solid was produced. $VOC\ell_2 \cdot xH_2O$ was produced in the same way except that it was not possible to dry it to a solid. It was used as a thick syrupy liquid.

Reactions were carried out in degassed solvents and efforts were made to prevent air from coming into contact with the phosphine ligands during the course of their reactions with oxovanadium(IV). In spite of precautions of this type, some phosphine oxide compounds were formed (possibly as a result of the water present in the starting materials).

1. Preparation of $VOBr_2(EBDPP)\cdot H_2O$

One gram (.003 moles) of $VOBr_2\cdot xH_2O$ (x assumed to be 5) was added to 25 ml of absolute methanol. The complex will not all dissolve in this volume of solvent, but previous experience had shown that too little of the MeOH led to too low a product yield, and too much led to unwanted products. This mixture was added to a solution of 1.8 g (0.0045 moles) EBDPP ligand dissolved in 125 ml of methylene chloride. Higher ligand-to-metal ratios were found to lead to impure oily products. The color of the stirred mixture turned from very light green to a deep green and stirring was continued overnight in the airtight reaction vessel. A blue-green precipitate was separated by filtration from a green solution. The solid was washed with acetone, then hot (70^oC) $CC\ell_4$, and then dried under vacuum. Elemental analysis (Table I) suggests a product of empirical formula $(VOBr_2)_2\cdot EBDPPO_2\cdot H_2O$. The phosphine ligand appears to have been oxidized to the diphosphinedioxide, which is abbreviated $EBDPPO_2$. This formulation is supported by infrared spectral data which will be discussed later. The green solution was evaporated to dryness under vacuum and a green powder remained. It was washed repeatedly with hot (70^oC) portions of $CC\ell_4$. This

treatment was shown to remove unreacted ligand from the green product. Finally the powder was dried in vacuum. Elemental analysis (Table I) leads to the empirical formula $VOBr_2(EBDPP)\cdot H_2O$ and this is supported by infrared spectral data (vide infra).

2. Preparation of $VOBr_2(MBDPP)\cdot H_2O$

The same procedure used to prepare the analogous EBDPP complex, described above, was used to obtain the MBDPP compound. However, no blue-green solid was isolated since only a green solution resulted when the starting materials were mixed and stirred. This green solution yielded, upon evaporation, a green solid from which the excess ligand was washed by means of hot $CC\ell_4$. Elemental analysis (Table I) leads to the empirical formula $VOBr_2(MBDPP)\cdot H_2O$.

3. Preparation of $VOC\ell_2(EBDPP)\cdot H_2O$

The preparation of this compound follows exactly the procedure outlined in 1 above for the preparation of the analogous bromide compound, with the exception that syrupy $VOC\ell_2\cdot xH_2O$, rather than solid $VOBr_2\cdot xH_2O$, was used. A blue-green solid formed as in the case of the bromide, and its elemental analysis (Table 1) suggests that it is a phosphineoxide product having the empirical

formula $(VOC\ell_2)_2(EBDPPO_2)\cdot 4H_2O$.[7] The green solid isolated from the filtrate was the desired product and it has the empirical formula $VOC\ell_2(EBDPP)\cdot H_2O$.

B. Spectral Studies

Infrared spectra were obtained by both the nujol mull and KBr pellet techniques, using a Beckman IR-7 spectrophotometer, employing $NaC\ell$ optics for the 4000-650 cm^{-1} range. Visible spectra were obtained with a Cary Model 14 spectrophotometer, using $CH_2C\ell_2$ solutions of the phosphine complexes and acetone solutions of the phosphineoxide complexes. The latter were not soluble in inert solvents such as $CH_2C\ell_2$.

RESULTS AND DISCUSSION

The three phosphine complexes prepared are listed in Table I with their elemental analyses. All are green in color. The phosphineoxide complexes are blue-green, the same color as the presumed Ph_3P complex reported earlier[7] and the color of $VOC\ell_2\cdot 2Ph_3PO$ crystals reported by Horner *et al.*[10].

Infrared spectral data of the five compounds listed in Table I are given in Table II. The I.R. spectral data clearly

verified (a) the presence of H_2O, (b) the presence of the organic ligands, and (c) the presence of the oxovanadium(IV) entity ($\nu_{V\equiv O}$ in the 992-1005 cm^{-1} range). The appearance of a great many bands in the 1100-1300 cm^{-1} region, however, makes a clear-cut distinction between the presence of or absence of the P=O bond difficult. In an effort to determine if the complexes prepared contained phosphines or phosphineoxides as ligands, the I.R. spectrum was made of the $EBDPPO_2$ ligand obtained by the oxidation of EBDPP with H_2O_2. Furthermore, the organic ligands contained in $(VOBr_2)_2 \cdot EBDPPO_2 \cdot H_2O$ and $VOBr_2 \cdot EBDPP \cdot H_2O$ were recovered from their complexes by decomposing the complexes with dimethylsulfoxide, DMSO. I.R. spectra of these ligands were made. The three foregoing I.R. spectra (Figures 1-3) were then compared (in the critical 1100-1300 cm^{-1} region) with the I.R. spectrum of fresh EBDPP, (Figure 4) which analysis had shown to be an unoxidized product. The I.R. spectrum of the ligand oxidized by H_2O_2 and that of the ligand recovered from the proposed phosphineoxide, $(VOBr_2)_2 \cdot EBDPPO_2$, were very similar in the 1185 cm^{-1} region where both displayed a broad band characteristic of a P=O stretching frequency. The I.R. spectrum of fresh ligand and that of the ligand recovered from the $VOBr_2 \cdot EBDPP$, the proposed phosphine complex containing the P-V bond, were also

Figure 1

The infrared spectrum of EBDPP ligand after it was oxidized to $EBDPPO_2$ with H_2O_2. The portion of the spectrum shown is the P=O stretching region between 1100 cm^{-1} and 1300 cm^{-1}.

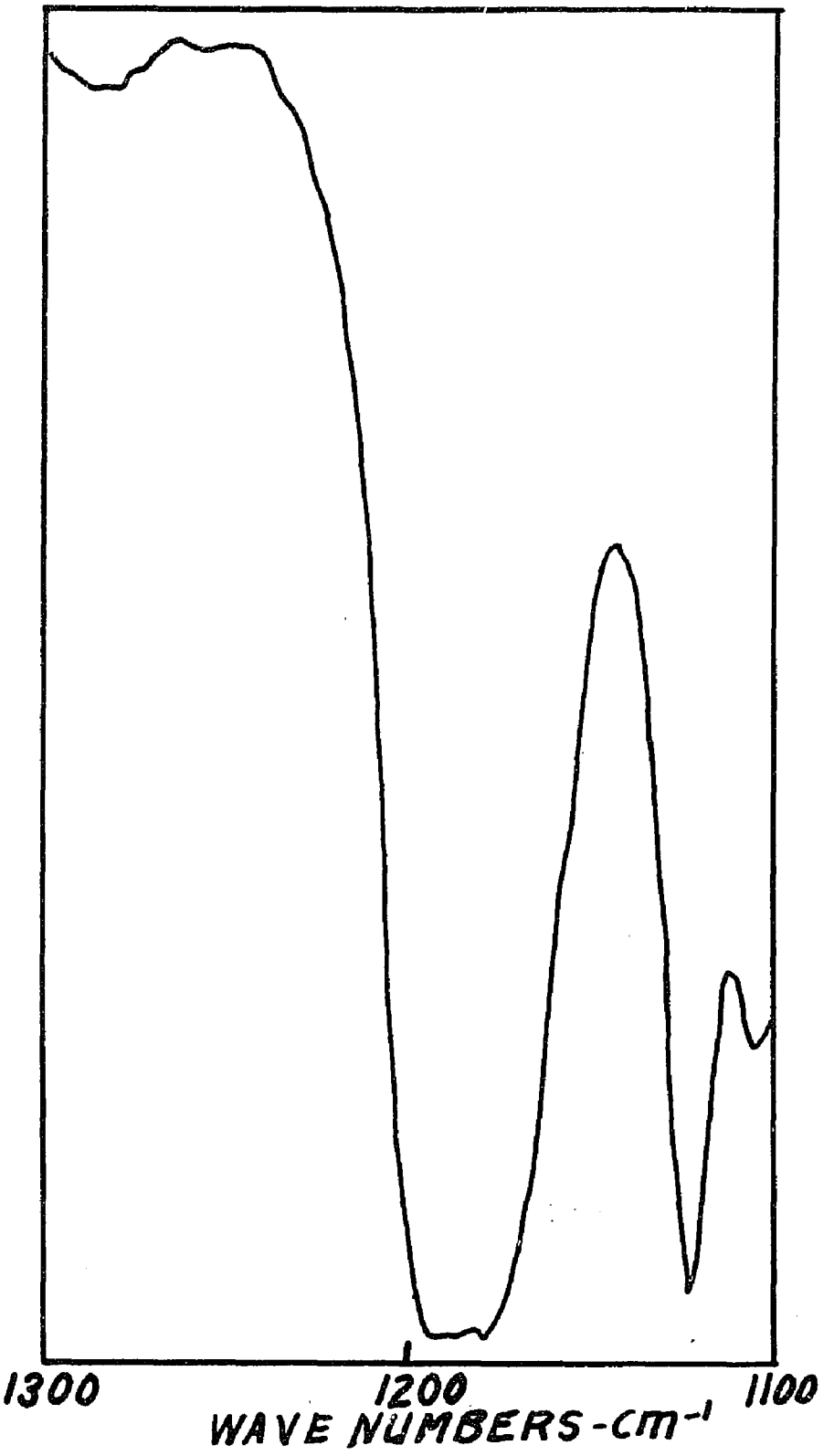
1300
1200
1100
WAVE NUMBERS - CM⁻¹

Figure 2

The infrared spectrum of the ligand recovered from $(VOBr_2)_2 \cdot EBDPPO_2 \cdot H_2O$ in the P=O stretching region between 1100 cm^{-1} and 1300 cm^{-1}.

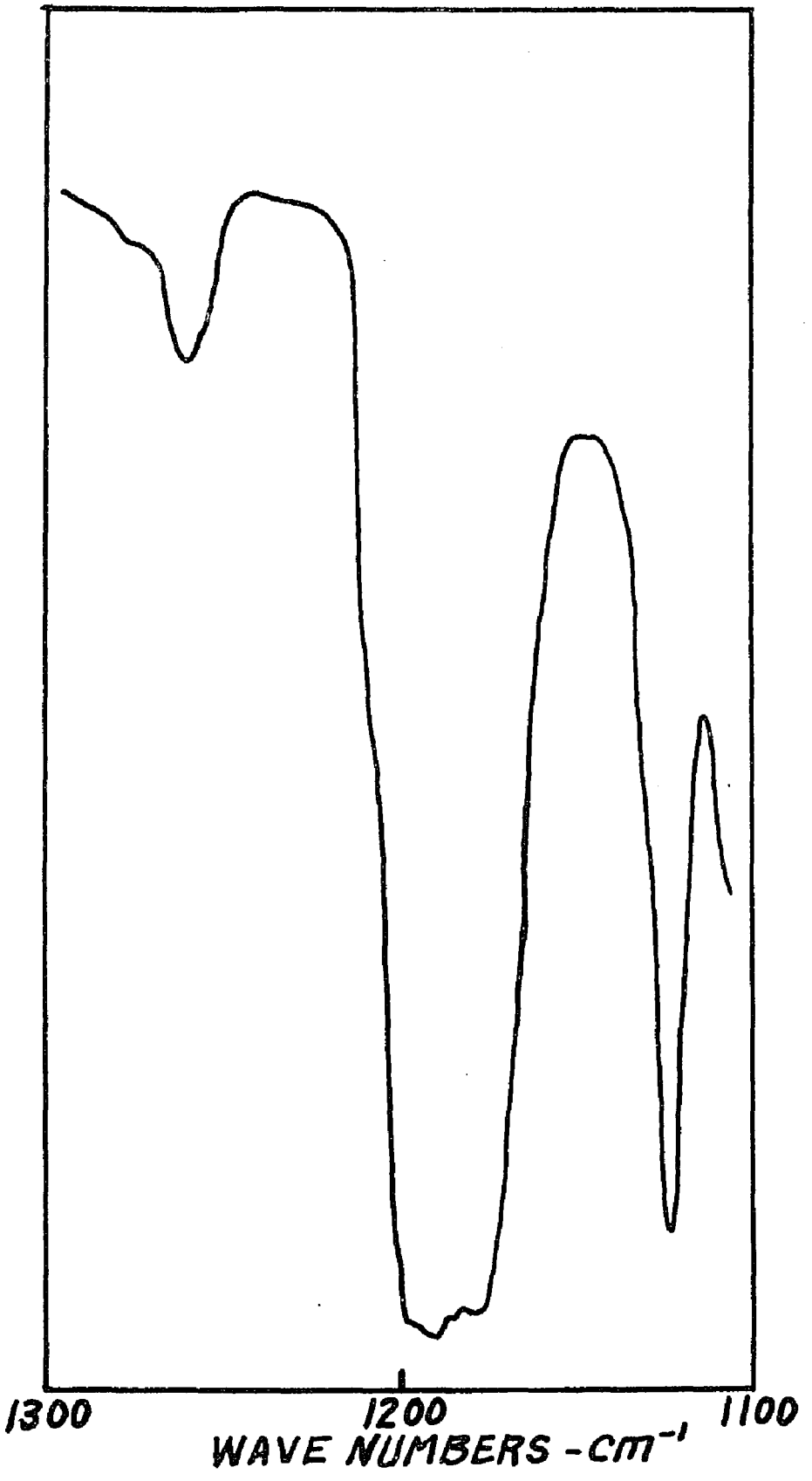
1300
1200
1100
WAVE NUMBERS - CM⁻¹

Figure 3

The infrared spectrum of the ligand from $VOBr_2 \cdot EBDPP \cdot H_2O$ in the P=O stretching region between 1100 cm^{-1} and 1300 cm^{-1}.

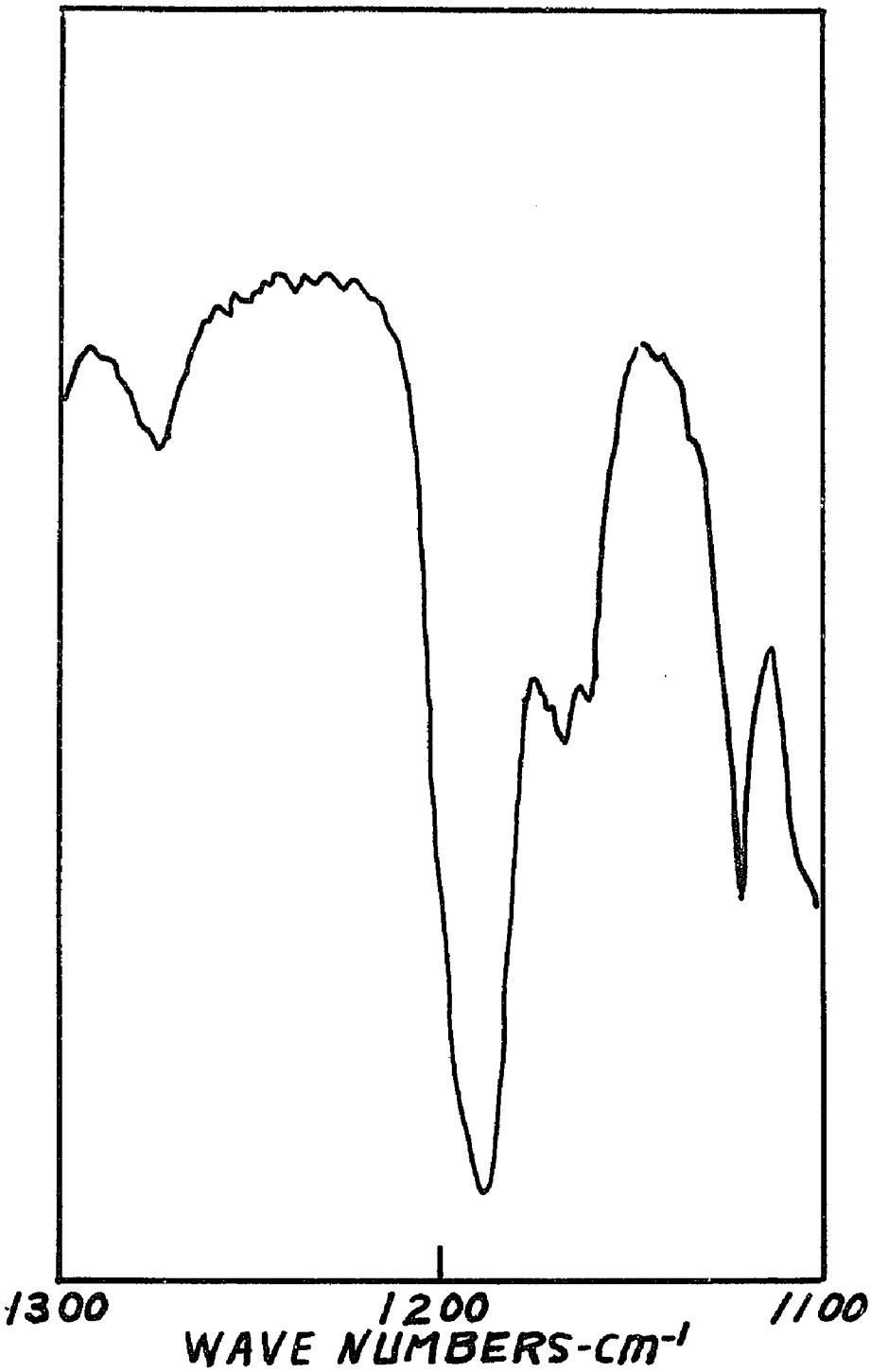
1300
1200
1100
WAVE NUMBERS-cm-1

Figure 4

The infrared spectrum of the fresh ligand EBDPP in the region between 1100 cm^{-1} and 1300 cm^{-1}.

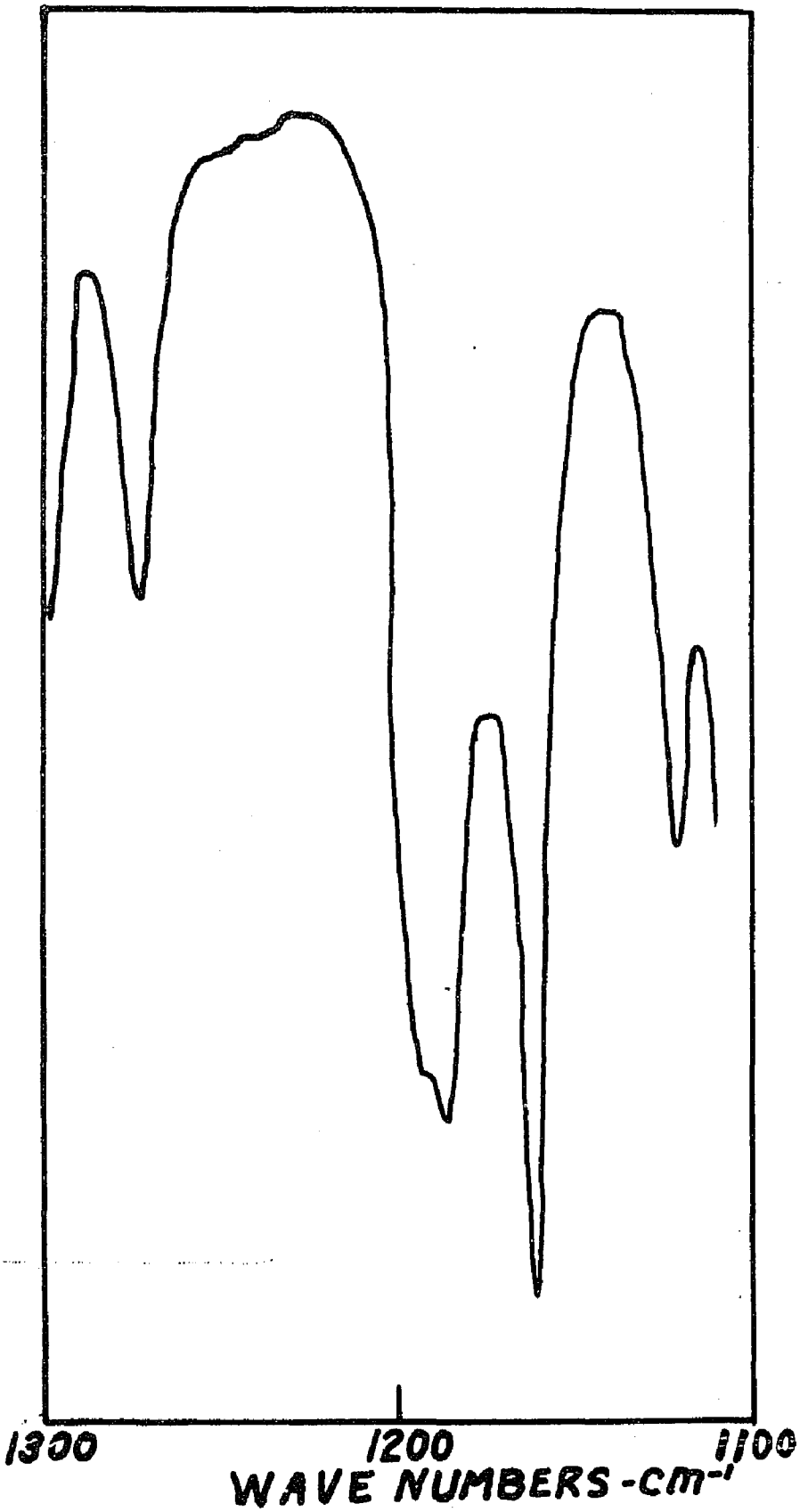
1300
1200
1100
WAVE NUMBERS - cm⁻¹

similar. These two ligands did not display the broad band around 1185 cm^{-1} which is characteristic of the P=O stretching frequency. From the above discussion, it is concluded that not only have new phosphineoxide complexes been prepared but also the first VO^{2+} complexes containing direct phosphorus-metal bonds.

The electronic spectral data in the 10-25,000 cm^{-1} region, presented in Table III, are fairly characteristic of VO^{2+} complexes.[3] A typical electronic spectrum of phosphine complexes of $VOBr_2$ and $VOC\ell_2$ is shown in Figure 5. The position of the first two bands appears to result from d-d transitions within the vanadium atom whoe d-orbital energies have been most significantly split apart by the strong axial field due to the multiple-bonded oxygen. The equatorial ligands appear to exert little influence upon the relative ordering of these levels. However, the third band (III) appears at lower energies than usually found for oxygen and nitrogen-donor ligands, and this strongly suggests that it has a charge transfer (ligand-to-metal) origin. This proposal is supported by analogous data from a series of sulfur donor complexes recently prepared[11], as well as others[12]. There is an ill-defined shoulder on the low energy side of band I (footnote b, Table III) which has previously been reported[13] in other VO^{2+} complexes. More will be said about this band later in this work.

Figure 5

The electronic spectrum of $VOBr_2 \cdot EBDPP \cdot H_2O$ in solution of $CH_2C\ell_2$ recorded between 10,000 cm^{-1} and 25,000 cm^{-1}. This spectrum is typical of the other phosphine complexes of oxovanadium(IV) prepared in this work.

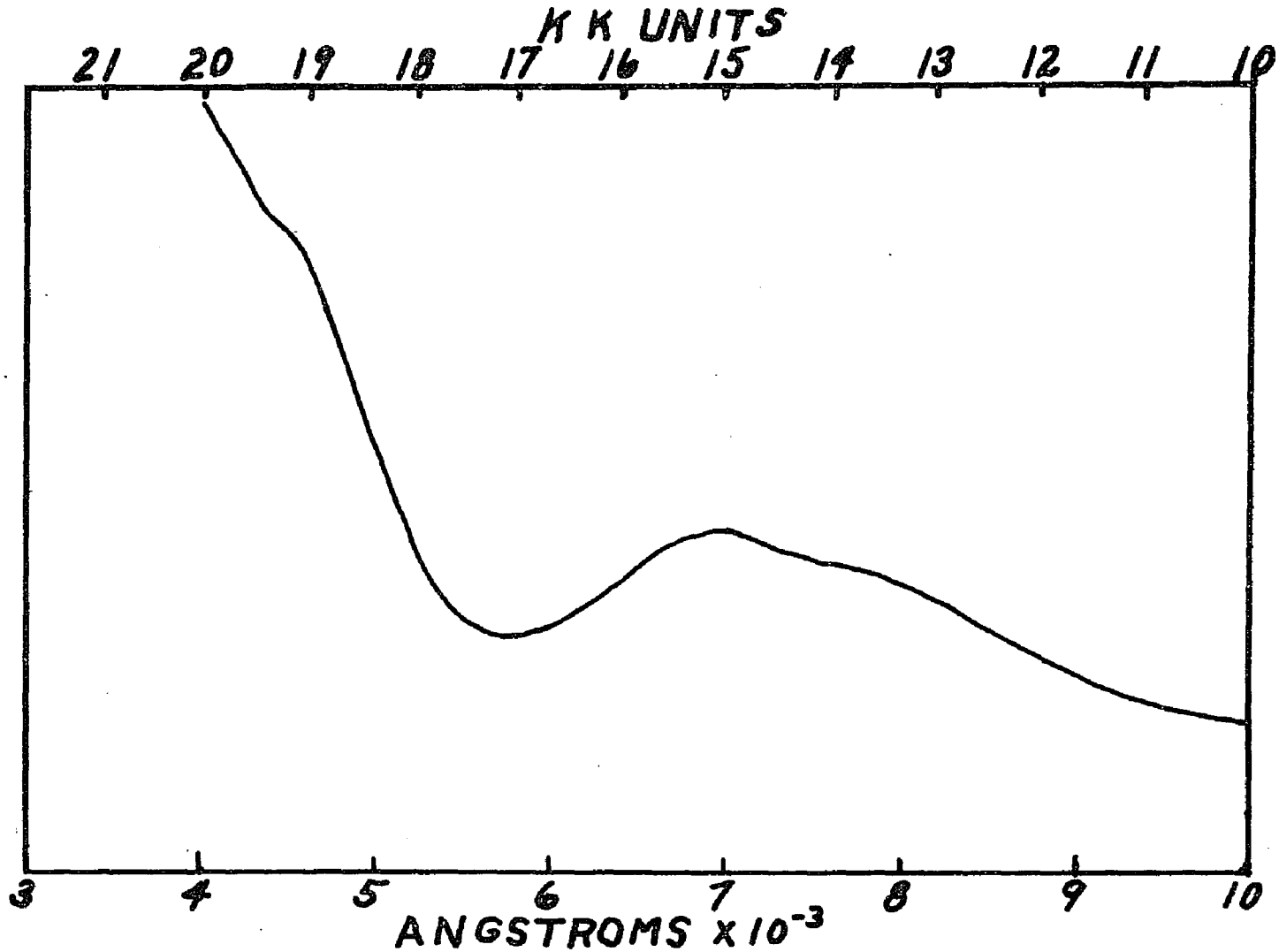
K K UNITS
21
20
19
18
17
16
15
14
13
12
11
10
3
4
5
6
7
8
9
10
ANGSTROMS X 10⁻³

TABLE I

NEW PHOSPHINE AND PHOSPHINEOXIDE COMPLEXES OF OXOVANADIUM(IV)

Complex	Color	Calculated			Found		
		C	H	P	C	H	P
$VOCl_2 \cdot EBDPP \cdot H_2O$	Green	56.32	4.75	11.19	57.10	4.66	11.50
$(VOCl_2)_2 \cdot EBDPPO_2 \cdot 4H_2O$[10]	Blue-green	40.10	4.11	7.96	39.13	5.30	7.54
$VOBr_2 \cdot EBDPP \cdot H_2O$	Green	48.52	4.09	9.64	48.51	4.46	9.69
$(VOBr_2)_2 \cdot EBDPPO_2 \cdot H_2O$[10]	Blue-green	35.56	2.99	7.07	35.84	4.59	7.08
$VOBr_2 \cdot MBDPP \cdot H_2O$	Green	47.69	3.85	9.86	48.79	4.64	9.54

TABLE II

The infrared spectra of the phosphine and phosphineoxide complexes listed in TABLE I. The spectra were made in nujol mulls. The values are given in cm^{-1}, and s = strong, m = medium, w = weak, sh = shoulder and b = broad.

$VOCl_2 \cdot EBDPP \cdot H_2O$: 698s, 734s, 745sh, 800w, 875w, 890w, 1003ν(V≡O), 1030w, 1070w, 1104s, 1127s, 1158s, 1184sh, 1315w, 1370sh, 1381s, 1442s, 1467s, 1594w, (+H_2O bands).

$(VOCl_2)_2 \cdot EBDPPO_2 \cdot 4H_2O$: 695s, 732s, 745s, 755sh, 765sh, 795w, 850w, 890w, 975sh, 995sh, 1005ν(V≡O), 1027m, 1075sh, 100s, 1125s, 1185sb, 1195s, 1270w, 1317w, 1380s, 1404m, 1440s, 1465s, 1590w, (+H_2O bands).

$VOBr_2 \cdot EBDPP \cdot H_2O$: 665w, 692s, 700s, 725s, 735s, 745s, 750s, 786w, 820w, 845w, 865w, 925w, 952s, 975w, 992 (V≡O), 1025s, 1070m, 1090s, 1125s, 1140w, 1150s, 1169s, 1187sh, 1197m, 1285w, 1313w, 1336w, 1440w, 1417w, 1435s, 1438s, 1484m, 1575m, 1589m, (+H_2O bands).

$(VOBr_2)_2 \cdot EBDPPO_2 \cdot H_2O$: 657w, 685w, 694s, 700s, 709sh, 730sh, 740s, 748s, 790w, 827w, 850w, 865m, 925w, 957m, 977s, 997, (V≡O), 1025m, 1075m, 1098s, 1127m, 1165m, 1190m, 1208w, 1262m, 1315w, 1338w, 1418m, 1435s, 1463s, 1478s, 1575m, 1585m, (+H_2O bands).

$VOBr_2 \cdot MBDPP \cdot H_2O$: 700s, 750s, 795s, 900w, 935m, 980s, 1000 (V≡O), 1029s, 1075sh, 1150sb, 1325w, 1340m, 1360s, 1435s, 1443s, 1455w, 1485m, 1592s, (+H_2O bands).

TABLE III

ELECTRONIC SPECTRAL BANDS[a], cm^{-1}

	I[b]	II	III
$VOBr_2 \cdot EBDPP \cdot H_2O$	12,850(79)	14,410(85)	21,800sh
$VOC\ell_2 \cdot EBDPP \cdot H_2O$	12,900	14,600	23,800sh
$VOBr_2 \cdot MBDPP \cdot H_2O$	13,070	14,500	21,200sh
$(VOBr_2)_2 \cdot EBDPPO_2 \cdot H_2O$	13,000	14,700	24,400sh
$(VOC\ell_2)_2 \cdot EBDPPO_2 \cdot 4H_2O$	12,800	14,700	23,800sh

(a) The spectra of the first three compounds were run in $CH_2C\ell_2$ as solvent, the remaining two compounds were run in acetone.

(b) There is a very weak, very broad shoulder on the low energy side of the first band. Its maximum position cannot be established accurately, but it lies in the 10,500-11,500 cm^{-1} range.

SULFUR COMPLEXES OF OXOVANADIUM(IV)

The success of phosphines and arsines as ligands for preparing complexes of the early transition elements, that is, those in the Groups III, IV, V and VI, has encouraged inorganic chemists to explore the possibility of employing sulfur ligands to form complexes with these early transition metals. As in the case of phorphorus and arsenic ligands, the interest in sulfur ligands was in the possibility of stabilizing low oxidation states of metal atoms. Many of these low oxidation state metal complexes had been prepared using ligands such as CO, $RN{\equiv}C$, R_3P, R_3As and others[14]. Although these ligands possess small to moderate sigma donor properties, they are all reasonably good pi acceptors. The pi bonds which may form between these ligands and the metals of low or negative oxidation state offer a mechanism for the removal of high electron density from the metal atoms. A metal atom so pi-bonded is thus able to accept more sigma electron donation from the ligands; in this way the pi-bonding system compliments the sigma-bonding system (synergistic effect), resulting in a stronger metal-ligand bond.

The CO ligand has its weak sigma orbital on the carbon atom while the pi acceptor orbital, which probably gives the CO-metal

bond most of its bond strength, is a pi-antibonding orbital distributed over both the carbon and oxygen atoms. The phosphorus, arsenic and sulfur ligands may use empty $d\pi$ orbitals to form pi-bonds with a metal atom. Although the pi-bonds formed between these $d\pi$ orbitals are weaker than the CO pi-bonds, the sigma-bonding abilities of phosphorus, arsenic and sulfur ligands are much greater, with the result that they form many complexes as stable as those formed by CO. A comparison of the pi accepting abilities of phosphorus, arsenic and sulfur ligands with the accepting ability of the carbon monoxide ligand might be gleaned from the ordering of ligands according to their trans effects given by Orgel[14].

trans effect ordering

$$H_2O < OH^- < NH_3 \text{ pyridine} < C\ell^- < Br^- < NCS^-$$
$$\sim I^- \sim NO_2^- \sim SO_3H^- < PR_3 \sim R_2S \sim SC(NH_2)_2$$
$$< NO < CO \sim C_2H_4 \sim CN^-$$

One can see from this series that the sulfur ligands, although not as good as pi-acceptors as the CO ligand, rate about equal with the phosphorus ligands in their pi-bonding abilities. The above relations are certainly not quantitative and are only one measure of the

abilities of various ligands to pi-bond; they are, however, at least indicative.

Sulfur ligands commonly appear not only as neutral species but also as mono- and divalent species while phosphorus and arsenic ligands appear mostly as neutral species, although some phosphide (R_2P^-) species are known. Attempts to make a vanadium complex with a neutral sulfur ligand have been largely unsuccessful. Only one report, by Fowles[15], has been uncovered in the literature of a purely neutral sulfur ligand bonded to a vanadium atom. Fowles attempted to react the ligands of the type R_2S (where R = Me, Et, Pr and Bu) with $VC\ell_4$, but in each case the V(IV) was reduced to V(III) to give the $VC\ell_3 \cdot L_2$. Attempts by this author to make $VOBr_2$ complexes of thiourea and propane dithiol were likewise unsuccessful.

Vanadium complexes of mono- and divalent sulfur ligands have been successfully prepared. King[16] has prepared complexes of the type $(C_5H_5)_2V_2(CH_3S)_4$, and dithiocarbamates of the VO^{2+} entity have recently been reported[17,18]*. Thus, it seems that the additional ionic character of ionic sulfur ligands leads to a more stable complex, although Fowles has apparently demonstrated that the neutral ligand will bond to vanadium when it is below the

---

*The dithiocarbamates prepared in this work were synthesized before the discovery of references 17 and 18.

oxidation state of four. Because sulfur ligands can be used more extensively as ionic ligands, particularly as multidentate ligands, they appear to be more versatile and more interesting than the phosphorus and arsenic ligands. Because of this difference, sulfur ligands have recently raised some interesting questions which have not appeared with phosphorus and arsenic ligands. Recently, Holm et al.[19] and Gray et al.[20] prepared some complexes of Ni, Pd, Pt, Co, Mo, W and V with ligands of this type:

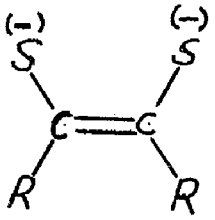

I

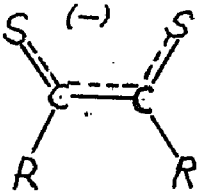

III

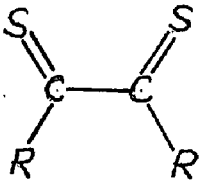

II

ESR data of these metal complexes raised the problem of ambiguity in the definition of metal oxidation states when the ligand has relatively stable oxidized and reduced forms. If two molecules of form I combined with a metal ion, the ion would possess a formal +4 oxidation state. The metal could conceivably combine with form II and form III, in which case the metal would have the formal oxidation

states of zero or +2. The complexes prepared by Holm *et al.* and by Gray *et al.* could not easily resolve this ambiguity.

It would be desirable, then, to prepare and characterize VO^{2+} complexes with sulfur donor ligands, not only because very few have previously been prepared, but also because of the interesting possibilities one might encounter from the standpoint of the formal oxidation state of the vanadium in the VO^{2+} entity. With this mind, efforts were made to prepare complexes of VO^{2+} with ligands which would bond, not only through sulfur atoms, but also through a combination of sulfur and oxygen and through sulfur and nitrogen atoms. A complete study of these compounds was not possible, but a cursory look at data derived from some of these new complexes suggests some interesting avenues for future research in this area.

EXPERIMENTAL

Preparation of Complexes

Solvents used in the preparation of the VO^{2+} complexes of 5-mercapto-3-phenyl-1,3,4-thiadiazole-2-thione, orthomercaptobenzoic acid, dithiosalcylic acid and 2,3-dimercaptotoluene were of reagent grade or better and were used "out of the bottle" with no further purification. Manufacturers of the ligands used were as

follows: Thione ligand by Aldrich Chemical Company; orthomercaptobenzoic acid by Eastman Organic Chemicals; and dithiosalcylic acid and 2,3-dimercaptotoluene by K & K Laboratories. No attempt was made to purify the foregoing ligands; they were used as purchased from the manufacturer. In the preparation of the dithiocarbamate complexes, however, special attention to the purity and oxygen content of the solvents was given, the details of which will be presented later. Except as noted, the source of VO^{2+} was $VOSO_4 \cdot 4H_2O$ which was used as purchased without further attention to its purity.

1) Thiourea, Triphenylphosphinesulfide, Propane Dithiol

In an attempt to make complexes of thiourea, triphenylphosphine sulfide, and propane dithiol with $VOBr_2 \cdot xH_2O$, a large excess of ligand (4:1 mole ratio) was treated with 1 gr. (0.003 moles) $VOBr_2 \cdot xH_2O$ (x assumed to be 5) in a mixture of 125 ml $CH_2C\ell_2$ and 25 ml CH_3OH for various lengths of time ranging from 2 hours to approximately one week. There was no indication that either the thiourea or the triphenylphosphine sulfide combine or reacted with the $VOBr_2$. However, about one hour after mixing, the solution in the mixture containing the propane dithiol gave a slight color change, turning from light green to a deeper green. A green solid

was isolated from the green solution by evaporation, and its elemental analysis proved it to be too low in carbon content to indicate the existance of a pure compound. It is likely that the charge on the vanadium atom was too high[15] to accommodate these neutral sulfur ligands.

2) 5-mercapto-3-phenyl-1,3,4-thiadiazole-2-thione

A solution of 1.1 gr. (0.041 mole) ligand in 150 ml of 95% CH_3OH was mixed with 0.65 gr. (0.02 mole) of $VOBr_2 \cdot x5H_2O$ and allowed to stand for two hours. A green precipitate appeared which was filtered from the solution and washed with three 50 ml portions of CH_3OH and two 20 ml portions of CS_2 (with some product being lost to the CS_2). The green product was dried under vacuum and its elemental analysis was:

	Elemental Analysis Found	Theoretical for $VO[(C_6H_5)N_2C_2S_3]_2 \cdot H_2O$
%C	35.76	35.88
%H	2.35	2.24
%H	10.12	10.47
%S	37.56	35.88

3) Ortho-mercaptobenzoic acid

(a) A solution of 1.5 gr. (0.1 mole) ligand in 150 ml of 95% CH_3OH was mixed with 1.4 gr. (0.045 mole) of $VOBr_2 \cdot 5H_2O$. The

solution was stirred while a saturated KOH-in-methanol solution was added until the solution reached a deep green color. The green solution was filtered and dioxane was added to the solution until a muddy green precipitate appeared. The precipitate was filtered and washed well with water and then dried in vacuum.

Elemental Analysis Found		Theoretical for $K_2VO[(C_6H_4)COOS]_2 \cdot H_2O$
%C	38.41	39.25
%H	3.00	2.34

(b) An aqueous suspension of $VO(OH)_2$ was prepared according to the procedure described on page 7. A methanolic solution of the ligand was added to the $VO(OH)_2$ suspension until the solution turned green and no more brown suspension remained. The green solution was allowed to stand for 1½-2 hours, in which time a precipitate was formed. The precipitate was filtered and washed with water, dried in vacuum, and again washed three times with 50 ml portions of $CHC\ell_3$. The product was then dried in vacuum.

Elemental Analysis Found		Theoretical for $VO[(C_6H_4)COOSH]_2$
%C	45.23	44.91
%H	3.70	2.67

4) Dithiosalcylic acid

The potassium salt of the ligand was prepared by mixing together 3.4 gr. (0.023 moles) of ligand to 2.5 gr. (0.046 moles) of KOH in aqueous solution (which would presumably give the dianion of the ligand). An aqueous solution of 150 ml H_2O and 2.5 gr. (.011 moles) $VOSO_4 \cdot 4H_2O$ was mixed with the ligand solution to produce immediately a muddy gray precipitate. The precipitate was filtered and washed well with water and dried in vacuum.

	Elemental Analysis Found	Theoretical for $VO(C_6H_5COS_2) \cdot 3H_2O$
%C	29.40	28.99
%H	2.88	3.45

5) 2,3-Dimercaptotoluene

A solution of 1.2 gr. (0.0084 moles) of ligand in 50 ml of CH_3OH was mixed with a solution of 1 gr. (0.0042 moles) of $VOSO_4 \cdot 4H_2O$ in 150 ml H_2O. An alcoholic solution of 0.4 gr. (0.0084) moles)KOH was slowly added to the stirred $VOSO_4 \cdot 4H_2O$ solution. A gray precipitate appeared which was filtered and washed well with 50% water-methanol solution.

	Elemental Analysis Found	Theoretical for $VO[CH_3C_6H_3S_2H]_2 \cdot H_2O$
%C	43.10	42.53
%H	3.68	4.05

6) Preparation of Dithiocarbamate Ligands

The ligands used in the preparation of VO(dithiocarbamate)$_2$ were prepared by the method of Welcher[21], with the exception that CH_3OH was added to the water solution of the ligand to decrease the crystallization time.

7) N,N-Dithiocarbamate, potassium salt

The ligands N,N-RR' dithiocarbamate, potassium salt where R and R' are Ethyl and Ethyl; Piperdine; Ethyl and Phenyl; Cyclohexyl and Cyclohexyl; and n-butyl and n-butyl, were used to prepared complexes of the type $VO(R_1R_2NCS_2)_2$. The same procedure was used to prepare all of the complexes except as noted. To a reaction flask which could be purged of air was added the following:

(a) 0.0012 moles of $VOSO_4 \cdot 4H_2O$

(b) 0.002 moles of the ligand dissolved in 50 ml of $CH_2C\ell_2$ which had previously been purged of oxygen by bubbling dry nitrogen through it for 20 minutes. It was noted that not all of the ligand and $VOSO_4 4H_2O$ dissolved in the $CH_2C\ell_2$.

The mixture was again purged with dry nitrogen and immediately sealed to leave the solution in the flask blanketed with nitrogen. The mixture was shaken in a "cocktail fashion" for five minutes every

half hour for about three hours during which time the solution turned deep red. The colored solution was filtered from the unreacted $VOSO_4$ under a blanket of dry nitrogen gas. A quantity of 150 ml of petroleum ether, which had been previously purged of oxygen by dry nitrogen, was added to the red solution to cause the VOL_2 (L = N,N-RR' dithiocarbamate) to precipitate. The precipitate was washed with three 50 ml portions of purged petroleum ether and then dired under vacuum. The product was then wax-sealed in a flask under a nitrogen blanket. The colors of the complexes prepared were slightly different for different R and R' groups, but could best be described as colors ranging between dirty green and dirty brown. The following complexes were made by the processes described above:

Complex	Elemental Analysis					
	Found			Theoretical		
	C	H	S	C	H	S
bis(N,N-diethyldithiocarbamate) oxovanadium(IV) $VO[(C_2H_5)_2NCS_2]_2 \cdot H_2O$	32.79	5.75	32.68	31.49	5.77	33.59
bis(piperidine dithio carbamate)oxovanadium(IV) $VO[C_5H_{10}NCS_2] \cdot H_2O$	35.46	5.66		35.73	5.45	
bis(N,N-methylcyclohexyldithio carbamate)oxovanadium(IV) $VO[CH_3C_6H_{10}NCS_2] \cdot H_2O$	41.77	6.48		41.83	6.10	
bis(N,N-dicyclohexyldithio carbamate)oxovanadium(IV) $VO[(C_6H_{10})_2NCS_2]_2 \cdot H_2O$	51.36	8.11		52.62	7.08	

RESULTS AND DISCUSSION

The infrared spectrum of $VO[(C_2H_5)_2NCS_2]_2 \cdot H_2O$ was recorded in nujol mull. A sharp strong peak at 950 cm^{-1} was found which is assigned to the $\nu(V{=}O)$, which is generally found in this region in all VO^{2+} complexes.[22] An optical spectrum of the same complex was made in nujol mull, using the filter paper technique, between the regions 10,000 cm^{-1} and 25,000 cm^{-1}. There was a conspicuous absence of the normally observed ligand field bands which usually occur in VO^{2+} complexes in the 14,000-16,000 cm^{-1} region. A broad peak, however, was found centered at about 23,800 cm^{-1}.

It would seem, then, that the infrared spectrum suggests the existence of the normal VO^{2+} complex of the dithiocarbamate spectrum, however, is not that of a normal VO^{2+} complex. It is possible that the electronic spectrum of the dithiocarbamate complex indicates the same ambiguity of metal valency which existed in the complexes of sulfur ligands prepared by Holm *et al.*[19] and Gray *et al.*[20].

TABLE IV

The following ligands were used to prepare complexes with oxovanadium(IV) entity:

1. 5-mercapto-3-phenyl-1,3,4-thiadizaole-2-thion, potassium salt

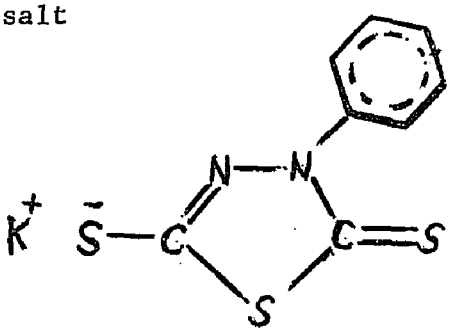

2. Ortho-mercaptobenzoic acid

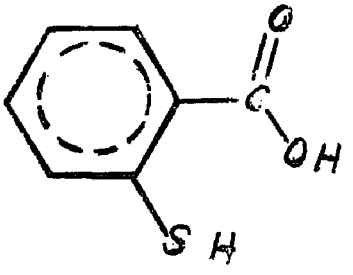

3. Dithiosalicylic acid

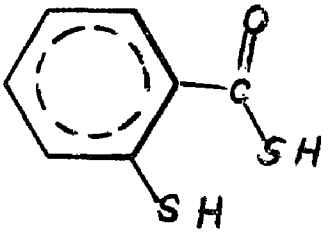

Table IV (Continued)

4. 2,3-Dimercaptotoluene

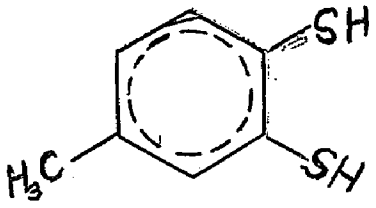

5. Diethyldithiocarbamate

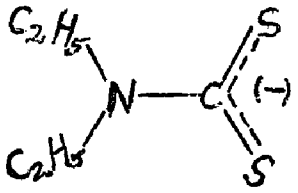

6. Piperidine dithiocarbamate

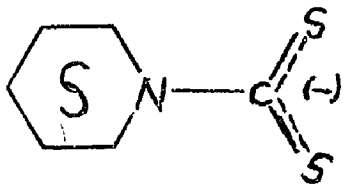

7. Ethyl aniline dithiocarbamate

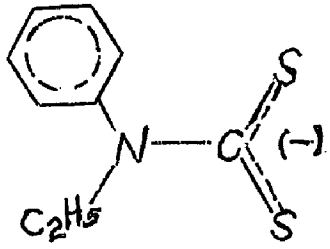

Table IV (Continued)

8. Dicyclohexyldithiocarbamate

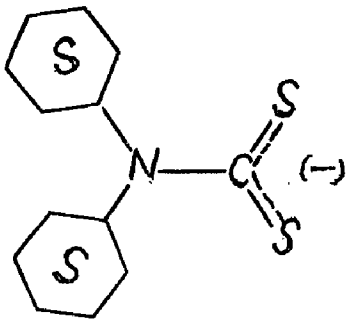

9. Di-n-butyldithiocarbamate

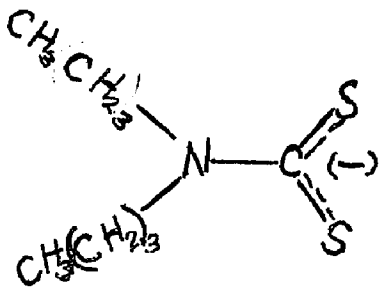

CHAPTER II

AN NMR STUDY OF π-BONDING IN OXOVANADIUM(IV) COMPLEXES

A DISCUSSION OF THE PRINCIPLES OF NMR CONTACT SHIFTS

INTRODUCTION

The use of nuclear magnetic resonance as a means of studying paramagnetic complexes is still in its infancy. Until recently it was widely thought that it was impossible to do meaningful NMR experiments on compounds possessing unpaired electrons.[23] The failure to observe NMR shifts of paramagnetic complexes was due mainly to the extremely large shifts and large line broadening which occurs under these conditions and the lack of a satisfactory explanation for these unusual phenomena. The early NMR workers concentrated on the fertile field of organic chemistry, using NMR as a tool to identify and elucidate the structure of non-paramagnetic molecules. Inorganic and, in particular, paramagnetic complexes were virtually ignored. Bloembergen[24], however, as early as 1950 drew attention to the importance of NMR studies of nuclei of non-magnetic atoms in paramagnetic complexes. His words made little impression on workers in the inorganic field, probably because of the lack of acceptance of a theoretical foundation to explain the various phenomena observed; consequently, little was done in this area. Attempts to explain these phenomena were partially

successful for crystals, but it remained for McConnell[25] in his paper on indirect hyperfine interactions in the paramagnetic resonance spectra of aromatic free radicals to explain the mechanisms by which the line broadening and the large shifts (by now called contact shifts) could take place in aromatic systems. A "follow up" paper by McConnell[26] further explained the existence of two components of the large shifts which became known as the isotropic contact shift (or simply contact shift) and the pseudocontact shift. As is the case with most theories, their main value lies not in the theory itself, but rather in the fact that they give rise to experiment and research to prove or disprove their validity and usefulness. Such was the case with contact shifts, for after the classic paper by Shuman and Jaccarino[27] on the investigation of MnF_2 crystals by NMR, there was a noticeable increase of activity in this area by Orgel, Taube, Shuman, Benson and Eaton, and later by Horrocks, LaMar and Drago. Eaton summed up the cautious optimisim prevailing in this field of research when he stated that "these studies have yielded a considerable amount of useful information on the electronic structures and magnetic properties of transition metal complexes. However, a number of questions regarding the extent of applicability of this NMR technique and the interpretation of the results still

remain."[28] Considering the large amount of work having been done in the contact shift field since this quotation (1965), it is obvious that some researchers are even more optimistic than Eaton.

REQUIREMENTS FOR CONTACT SHIFTS

There are two main mechanisms, and possibly a third, which occasionally prevent the observance of paramagnetic complex NMR spectra. The first two mechanisms, the dipolar and the electron spin-nuclear spin coupling mechanism, are the most important. A third mechanism, the quadrupole coupling, which also appears in diamagnetic complexes, is less important.[23,26,29,30]

The dipolar mechanism results when paramagnetic ions or complexes tumble through solution and in so doing set up large magnetic fields which interact with the nuclear magnetic moment (μ). Interaction of this high electron induced field with the μ of the resonant nucleus causes a dipolar spin-lattice relaxation of the nucleus. As a result, T_1, the longitudinal relaxation time, is decreased. The line width W of the NMR spectrum, which is proportional to $\frac{1}{T_1}$, becomes broader with decreasing T_1 and is often "washed out".

The electron spin-nuclear spin mechanism frequently decreases both T_1 and T_2 (the latter being the transverse relaxation time), which results in considerable line broadening and possible wash-out of the spectrum. This mechansim occurs when an unpaired electron in the vicinity of the resonating nucleus gives rise to a fluctuating field at the nucleus with a resulting decrease in T_1. If the electron relaxation time τ_S between states $S = +\frac{1}{2}$ and $S = -\frac{1}{2}$ is long, coupling of the electron and nucleus will give rise to two proton resonance peaks. A short relaxation time will produce only one NMR peak. If, however, the relaxation time lies somewhere in between, a time average peak will result which in effect shortens T_2 and causes severe line broadening.

Since quadrupole moments generally play only a minor role, they will not be discussed further here.

It can be seen from the above that the longitudinal relaxation time T_1 and the transverse relaxation time T_2 have to be short in order to observe an NMR line spectrum since the line width W depends on the relaxation time of the resonating nucleus. T_1 and T_2 are short if one or sometimes both of the following requirements are met:

$$\frac{1}{\tau_S} \gg A_n \qquad \frac{1}{\tau_B} \gg A_n \qquad \ldots.1$$

where

$\frac{1}{\tau_B}$ = exchange rate between the coordinated species and the bulk species (τ_B is the lifetime of the coordinated species).

$\frac{1}{\tau_S}$ = spin relaxation rate for the electron coupled to the resonating nucleus. Relaxation is between S_1 spin states of $-\frac{1}{2}$ and $+\frac{1}{2}$.

A_n = the electron spin-nuclear spin coupling constant.

It should be noted at this point that conditions favorable to observing an ESR spectrum are generally opposed to those necessary for observing an NMR spectrum. There is, however, a gray area between the two conditions in which both ESR and NMR spectra are possible. For the few paramagnetic complexes which exist in this area, the A_n values determined by both ESR and NMR agree very well.

CONTACT SHIFTS

When an unpaired electron is induced into the neighborhood of a resonating nucleus, it changes the diamagnetic field about the nucleus because of the great charge density and magnetic moment of the electron. As a result of this large change in the field

about the nucleus, the nucleus resonance frequency (or field) is shifted either upfield or downfield from its diamagnetic field position, usually by an exceptionally large amount (as much as 5000 cps).[23,26,28,29,31,32,33]

McConnell[26] gives as the proper Hamiltonian for the description of the shift resulting from the electron spin-nuclear spin interaction, the following:

$$\mathcal{H} = (A_n S \cdot I) + (S \cdot G \cdot I) + (S \cdot C \cdot I) \qquad \ldots.2$$

where: first term = Spin coupling term

second term = Symmetric dyadic with zero trace

third term = Skew-symmetric dyadic.

Of particular interest is the quantity A_n, the electron spin-nuclear spin coupling constant, found in the spin coupling term. It is unfortunate that A_n does not result from only one mechanism such as the Fermi contact coupling, but rather from three different mechanisms.

The Fermi contact coupling or electron spin-nuclear spin coupling term is usually the most dominant term, especially in the first row transition metal complexes. The electron orbit-nuclear spin coupling and the electron spin-electron orbit (spin-orbital coupling) interactions contribute to the resonance shift to a

lesser extent.

To avoid the complications of an obviously complex system, the A_n resulting from the three mechanism can be divided into two effects: A_c, the contact shift, and A_p, the pseudocontact shift. Thus:

$$A_n = A_c + A_p \qquad \ldots.3$$

The contact shift term A_c is due mainly to the Fermi contact coupling; that is, the electron spin-nuclear spin coupling. Simply put, the unpaired electron density must find its way to the neighborhood (an s orbital possessed by the resonating nucleus) of the resonating nucleus via the bond system between the source of the unpaired electron density and the resonating nucleus. The sigma system can be used to carry unpaired density through the molecule, but its ability to do so attenuates rapidly with the number of bonds between the unpaired electron source and the resonating nucleus.[31,32] The effect is found to be small[28,31,32,34,35] for most ligand systems, but for ligands like H_2O, NH_3, etc., the sigma-transfer of spin density could be appreciable.

The main effects to be considered in contact shifts are those due to the transfer of electron density through the pi systems.

The phenomena of distributing the unpaired electron density around a delocalized pi system is well understood. There remained, however, the need for a mechanism by which electron spin density (of proper spin) could be transmitted from the pi system to the sigma system in which the resonating nucleus resided. McConnell[25] in his classic paper on hyperfine interaction of paramagnetic systems illustrates how a pi orbital electron-spin polarization can be transmitted through a strong electron exchange mechanism to the sigma bonding electron system. Take as an example the following protion of a β-diketone system showing the pi orbitals of the ring atoms and the sigma orbitals of the hydrogen and the center carbon atom:

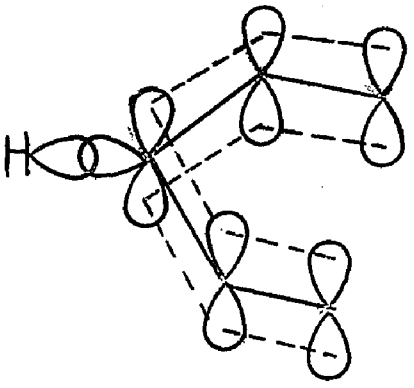

If a ring proton is attached to a carbon of the pi system which contains the unpaired electron, the three orbitals s, sp^2 and

p_x can be combined to give:

$$\phi_1 = A\theta(s, sp^2, p_x)\beta\alpha\alpha$$
$$\phi_2 = A\theta(s, sp^2, p_x)\alpha\beta\alpha$$
$$\phi_3 = A\theta(s, sp^2, p_x)\alpha\alpha\beta$$

These orbitals combine to give the following molecular orbitals:

$$\Psi_1 = \frac{1}{\sqrt{2}}(\phi_1 - \phi_2) = \text{Bonding ground state}$$
$$\Psi_2 = \frac{1}{\sqrt{2}}(\phi_1 + \phi_2 - 2\phi_3) = \text{Excited state}$$

Ψ_2 ↑

Ψ_1 ⇅

The energy difference between Ψ_1 and Ψ_2 is small enough that the exchange mechanism can take place between Ψ_1 and Ψ_2, thus transmitting electron spin between the pi system and the s orbital of the resonating proton. This large unpaired spin results in the large paramagnetic shifts observed.

The amount of unpaired spin density at the ring carbon to which the proton is attached is given by:

$$A_n = Q\,\rho_n \qquad \ldots.4$$

A_n = electron spin-nuclear spin coupling

Q = proportionality constant, e.g.,
-22.5 gauss for C - H
+27 gauss for C - CH_3

ρ_n = unpaired electron density at carbon nucleus

Of course, it must be understood that the carbon atom nucleus sees not only unpaired electron density from the pi system but also from the sigma system. This, coupled with the fact that shifts result from pseudocontact mechanisms, makes the above relation only approximate. In a strong pi system, however, where sigma effects are non-existent, or can be ignored, and pseudocontact effects are small (which is normally the case in the first row transition series), the above relation seems to hold. The contact shifts resulting from this mechanism may be as high as 5000 cmps or even larger.

Pseudocontact shifts arise from the anisotropy in the g-tensor of the paramagnetic complex; thus, the pseudocontact shift for a nucleus depends on its geometrical position in the molecule.[28,29,31,32] The shift is described by:

$$\frac{\Delta H_i}{H} = -\frac{\beta^2 S(S+1)}{27kT}\frac{(3\cos^2\theta-)}{r_i^3}(g_{||} + 2g_{\perp})(g_{||} - g_{\perp}) \qquad \ldots.5$$

θ -- angle between the radius vector and the crystal axis

i -- the ith proton

r_i -- the length of the ith radius vector

$g_{||}$ -- the g factor $||$ to the crystal axis

$g_{\perp}$ -- the g factor $\perp$ to the crystal axis

β -- Bohr Magneton

k -- Boltzman Constant

T -- absolute temperature

S -- electron spin of the molecule

The proton shifts around the same pi system due to pseudocontact effects can be related in the following way:

$$\left(\frac{\Delta H}{H}\right)_i : \left(\frac{\Delta H}{H}\right)_j : \cdots = \frac{3\cos^2\theta_i - 1}{r_i^3} : \frac{3\cos^2\theta_j - 1}{r_j^3} : \cdots \quad \ldots.6$$

The usual description of the pseudocontact shift mechanism is that it results from a coupling of the electron and the nucleus through space rather than as a result of a bond carrying mechansim. Eaton[28] predicts that shifts resulting from unpaired electron density (4f electrons) of the rare earth metal complexes would be

predominantly pseudocontact, since the 4f electrons are so deeply buried in the electron cloud of the atoms. Generally, the pseudocontact shifts are small compared to contact shifts. For the first row transition metal complexes, pseudocontact shifts of protons may range from 0-20 cps; while in the second row transition metal complexes, they may range from 200-800 cps.[28] The direction of the shift will be upfield or downfield depending on the relative size of $g_{||}$ and $g_{\perp}$.

When one produces a spectrum of a paramagnetic complex, the NMR shift is due to both the pseudo as well as the contact shift. The total contact shift of the paramagnetic system can be described by the following relation:

$$\frac{\Delta H}{H} = -\frac{4}{9} A_n \frac{\gamma_e \, g\beta I(I+1)S(S+1)}{kT} = \frac{\Delta \nu}{\nu} \qquad \ldots.7$$

and for proton shifts specificially:

$$\frac{\Delta H}{H} = -A_n \frac{\gamma_e}{\gamma_n} \frac{g\beta S(S+1)}{3kT} \qquad \ldots.8$$

where:

H -- field strength

ν -- resonating frequency (60 mc or 100 mc)

A_n -- electron spin-nuclear spin coupling constant

γ_e -- electron gyro-magnetic

γ_n -- nuclear gyro-magnetic

g -- ratio of $\frac{\mu \text{ mag. mom.}}{\mu \text{ tot. ang. mom.}}$ of electron

β -- Bohr magneton constant

k -- Boltzman constant

T -- absolute temperature

I -- nuclear spin

S --- electron spin

The shift $\frac{\Delta H}{H}$ is a total shift made up of the sum of both the pseudocontact shift and the contact shift, and the resulting electron spin-nuclear spin coupling constant A_n is the sum of A_c and A_p. A_c and A_p may be either plus or minus depending on the sign of the electron spin (in relation to the magnetic field) which induces the contact shift. If A_n is positive, the shift of the nucleus from its "diamagnetic position" is downfield. This is because the unpaired electron spin, which is coupled with the shifted nucleus, has its moment in the same direction as the magnetic field and thus reinforces the field. With less applied field to cause resonance of the nucleus, the contact shift is at a lower field

(downfield). When A_n is determined to be negative, just the opposite of the above is true, and the resultant shift is found to be upfield. It will be shown later that the magnitude and sign of A_n provide considerable insight into the elucidation of magnetic and structural properties of paramagnetic systems.

SPIN DENSITIES

The mechanism for distributing unpaired spin densities, ρ_n, about a molecule containing a paramagnetic species was previously described. The spin density ρ_n was shown to be related to the electron spin nuclear spin coupling constant by:

$$A_n = Q\ \rho_n \qquad \ldots\ldots 4$$

From the NMR spectrum of a paramagnetic molecule, we are able to determine the sign of A_n for the contact shift of a nucleus in the molecules. Drago and others[23,31,32] have determined that if the resonating nucleus is a proton and is bonded to an atom which forms a system transmitting unpaired electrons through its sigma bonds, the sign will be α spin and the spin remains the same throughout the sigma system. Thus, if a metal ion transfers α spin density (the spin moment is in the direction of the magnetic field

and sometimes called + spin density) to the ligand through its sigma bond network, the spin density distributed at each atom will be α spin. Therefore, Q for all sigma systems is positive and the spin density ρ_n will have the same sign as A_n.

For a pi system, two types of groups attached to the pi system have been investigated.

ring proton
opposite electron
spin transmitted

and

methyl proton
same electron spin
transmitted

It has been shown that the Q for the ring proton is about -22.5 gauss and that Q for the methyl proton ranges between 5 and 30 gauss, although on a benzene type ring, it is usually about 27 gauss. Thus, we see from the above that when A_n is determined to be positive from the NMR spectrum, the spin density at the carbon atom of the ring proton group is β spin or negative spin. The Q value for a CH_3-group is positive, however, when A_n is positive the ρ_n at the ring carbon is positive (or α spin).

Spin density distribution about a pi system can be demonstrated by using the important resonance forms of valence bond structures for the pi systems. All positions at which a major contributing resonance form places unpaired electrons will have spin density of one type (α or β spin). All other positions on the molecule may have either the same spin or opposite spin, depending on spin correlation in the pi system, although usually the spin is opposite. Take the following example:

Allyl radical[23]

$$\underset{\underset{(1)\quad(2)\quad(3)}{\text{a}}}{CH_2 = CH - CH\uparrow} \quad \leftrightarrow \quad \underset{\underset{(1)\quad(2)\quad(3)}{\text{b}}}{\uparrow CH - CH = CH_2}$$

Two important valence bond structures for the allyl radical can be drawn putting electron density at positions (1) and (3). No valence bond structure can be drawn which will place α electron density at position (2); thus, it is assumed to have β spin density. Now consider the following example:

Nickel(II)bis(aminotroponeimineate)[23,36] (showing only one bidentate ligand)

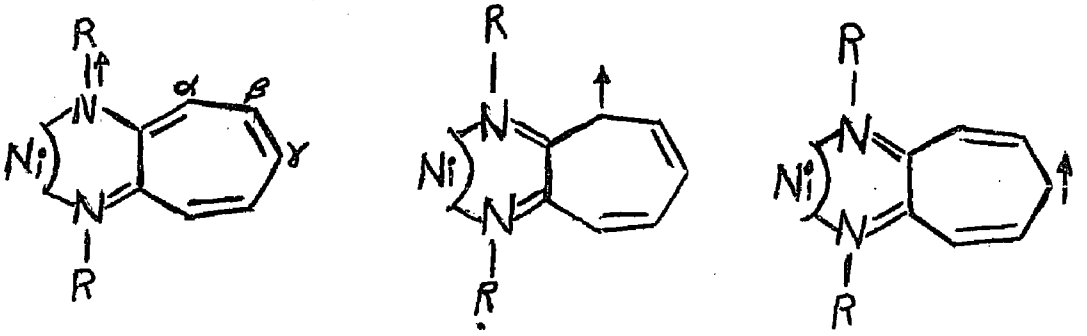

(a) (b) (c)

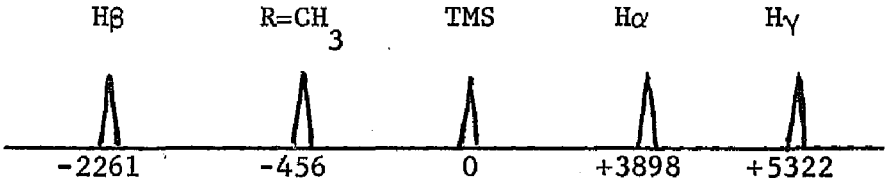

(d) - chem shifts in cps

The three structures (a), (b), and (c) represent the three valence bond structures which can be drawn for the Ni(II) complex. These valence bond structures show electron density distributed at the nitrogen atoms and at the α and γ ring positions. Position β will probably have the opposite spin density. One makes the above analysis by assuming that the ligand can be treated as a radical and that Ni(II) ion, the source of the unpaired electron

density, causes α spin to be transmitted to the radical. One would then expect α spin at the two nitrogen atoms and ring positions α and γ. If spin correlations in the ring are not too great, one would expect opposite spin at the β position.

The relation $A_n = Q\ \rho_n$, where Q is negative for the C-H group, indicates that with α spin at the carbon atom, the spin at the proton should be β spin, that is, electron spin which opposes the applied magnetic field H_o. The field strength H_o must then be raised to a higher field $H_o + \Delta H$ in order to produce resonance, and thus, the protons attached to carbon (or other atoms of pi character) are resonated at a higher field. The observed contact shift will then be upfield. The opposite is true of protons attached to ring carbons with β unpaired spin. The NMR spectrum (d) bears out this analysis. In Figure (a), R was allowed to be CH_3. The Q for $C\text{-}CH_3$ (or $N\text{-}CH_3$) is known to be positive, and from an analysis similar to that above, one would expect the CH protons to be shifted downfield. This shift was observed in the NMR spectrum. When the CH_3 on the N was replaced by a phenyl group, the following valence bond structure could be drawn.

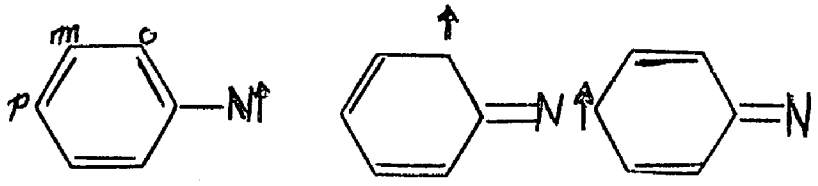

a b c

In this case, α spin density would be distributed on the o (ortho) and p (para) ring positions, while the m (meta) position would contain β spin. The NMR spectrum of the phenyl group would be analyzed in the same way as the seven-membered ring system considered above.

A valence bond calculation was performed on the aminotroponeimine radical by Eaton[36] to determine the spin densities at each position. These spin densities were adjusted to fit the spin density distribution found by NMR techniques.

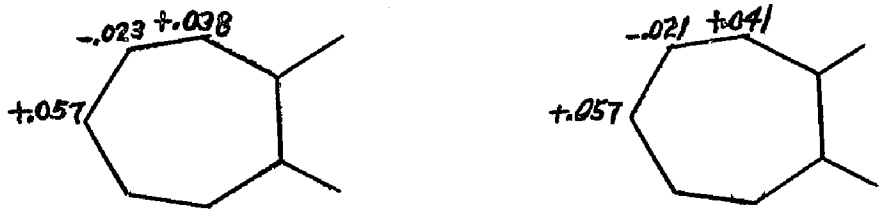

calculated for .10 electron experimental

It was found that if $\frac{1}{10}$ electron was allowed to be transferred to the pi system from Ni(II), the claculated and experimental spin densities were in good agreement. One can deduce from these results that the Ni(II) transferred $\frac{1}{10}$ of an electron to the ring in pi bonding. A similar technique can be used to determine the amount of covalent bonding in the sigma system. A

word of caution is appropriate at this point. As seen previously, many factors are at work which determine the sign and magnitude of A_n. Only when these other factors can be either properly accounted for or ignored will the above method provide a quantitative answer. In general, however, a qualitative answer, i.e., the sign and relative magnitude of A_n, can be determined. This qualitative answer in itself provides a great deal of understanding of a paramagnetic system.

METAL AND LIGAND CHARGE TRANSFER

An earlier discussion of the total contact shifts of paramagnetic complexes revealed that shifts could occur through the coupling through space of an unpaired electron with a proton in the complex. This relatively simple mechanism was called the pseudo-contact shift. The second part of the total contact shift, known simply as the contact shift, is not nearly as simple. The contact shift, sometimes referred to as the Fermi contact shift, requires the transmittance of the unpaired electron density through the molecular bonding system. It has been shown[28-32] that the distribution of unpaired spin density occurs in both the pi network and the sigma network of the molecule and it is possible to envoke

hyperconjugation to explain transmittance of ρ_n from sigma to pi and from pi to sigma systems.[28,36] Generally, the energetically unfavorable mechanism of hyperconjugation compared to the pure pi or sigma transmission can be ignored. Through each of the pi and sigma networks, unpaired electron density can be transmitted as a result of metal-to-ligand charge transfer (M → L) or through ligand-to-metal charge transfer (L → M). The spin of the electron density can either be α or β spin.

A summary of the metal and ligand charge transfers to produce contact shifts are shown to be:

Network	Types of Transfer
sigma	αM → L
	αL → M
	βL → M
pi	αM → L
	αL → M
	βL → M

A sigma model was proposed by Horrocks.[32] "If unpaired spin density resides in metal orbitals of sigma symmetry and is transferred to the sigma orbitals of the ligands, the magnetic field of the protons is reinforced by the electron spin magnetic field and the proton resonances are all shifted to lower applied

fields. These shifts attenuate rapidly as the number of bonds between a given proton and the metal increase."

Note that when Horrocks speaks of metal electron density, he is referring to density with α spin since all unpaired electron densities on the metal atoms "line up" with the magnetic field. β spin density, therefore, is never transferred from the metal to the ligand in a sigma network. The same results attained by ($\alpha M \rightarrow L$) could also be accomplished by having the ligand donate β spin to the metal ($\beta L \rightarrow M$). This would cause an excess of α spin on the ligand which would result in the same downfield shift of the sigma protons (provided both mechanisms affected the same ligand pi orbitals). A transfer of α spin from ligand to metal ($\alpha L \rightarrow M$) would have just the opposite shift as the above two cases. A knowledge of the position of all the d electrons in the metal ion and the energy relations between the d orbitals and ligand orbitals is necessary to properly analyze the type of charge transfer expected. This will be discussed under charge transfer in the pi system.

Charge transfer in the pi system was reasonably well studied by Eaton and many others.[28,30,36] Eaton's studies of paramagnetic transition metal acetylacetonates[28], coupled with

the studies of others, provides the information necessary to arrive at a technique for predicting the type of transfer which occurs in the pi system of transition metal complexes. Eaton gives the following analysis of the charge transfer in the pi system of the transition metal acetylacetonates.

"The smooth change in NMR shifts from Ti(III) to Fe(III) suggests strongly that there is no abrupt change in mechanism along the series and it would seem to be a fair assumption that the shifts in the Mn(III) compound are also predominately contact in nature. Pseudocontact effects will therefore be neglected in the ensuing discussion of this series.

"The contact mechanism implies that the electron spin has been partly delocalized from the metal atom to the ligand. This can occur either through the sigma orbitals or through the pi orbitals. The results of Forman, Murrell and Orgel[37] suggest that the spin is in the ligand pi system, and this is perhaps the more likely situation since all the sigma orbitals will be either strongly bonding or strongly antibonding and therefore distant in energy from the basically nonbonding metal d orbitals. The positions of the relevant orbitals are shown diagrmatically in Figure 5.

"There are two possible types of interaction, namely, between the metal d orbitals and the bottom antibonding ligand

	D_3 Symmetry
Ligand π^*	$a_2 + e$
	$a_1 + e$
Metal d	e
Orbitals	$a_1 + e$
Ligand π	$a_2 + e$
	$a_1 + e$
	$a_2 + e$

TABLE 5

ORBITALS OF THE (D_3) POINT GROUP IN METAL ACETYLACETONATES

pi orbitals, and between the metal d orbitals and the top bonding ligand pi orbitals. The former will correspond to charge transfer from the metal to the ligand. It may be noted that in this point group (D_3) both types of interaction with either set of d orbitals are allowed by symmetry. The metal-to-ligand charge transfer must result in the delocalization of positive spin. The ligand-to-metal charge transfer must result in the delocalization of positive spin if the d shell is half-filled or more, since only the β electrons can be accepted, leaving an excess of α electrons on the ligand, but will probably result in negative spin delocalization for a less than half-filled d shell since the maximum spin multiplicity will be preserved by the transfer of an α electron."[28]

The analysis scheme proposed by Eaton may be summarized in the following steps. (The shifts apply to the aca ring proton).

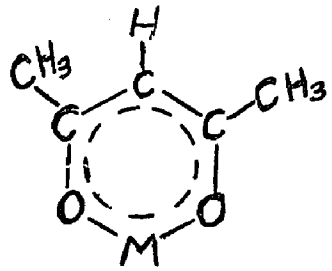

(a) For metal-to-ligand (M → L) charge transfer, the unpaired spin will be α spin on the ligand at the oxygen.

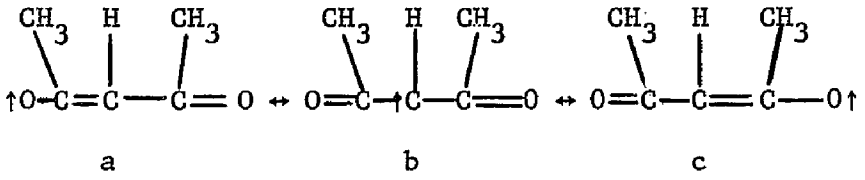

Drawing the major valence bond structures of the aca radical, one sees that α spin on the ligand places α spin at the C-H group or β spin at the proton. The shift at the proton due to β spin will be upfield.

(b) For $\alpha L \rightarrow M$, β spin will be left on the ligand. The β spin on the ligand will result in α spin at the C-H proton and the shift is expected to be downfield.

(c) For $\beta L \rightarrow M$, α spin will be left on the ligand and the result will be opposite that of b, i.e., the shift will be upfield.

As an example of the use of the above rules, let us consider $Ti(III)(aca)_3$, which is a d^1 system with unpaired electrons lying in the t_{2g} orbitals. It is expected that there will be $\alpha L \rightarrow M$ charge transfer into the t_{2g} orbitals since the t_{2g} orbitals are less than half full and would accept parallel electron spin rather than have the donated electron density pair up or go into the higher e_g orbital. This results in β spin on the ligand, and as per (b) above, the shift should be downfield. The NMR shift was observed by Eaton to be downfield.

If one considers $Mn(III)(aca)_3$, there will be a choice of either $\beta L \rightarrow M$ donation to the lower half-filled d orbitals or

$\alpha L \rightarrow M$ donation to the upper empty d orbitals. The preferred possibility will depend on the relative magnitude of the exchange interaction and the ligand field splitting. The observed shift for Mn(III) complex was downfield, which would indicate $\alpha L \rightarrow M$. This would tend to indicate that the effect of ligand field splitting is less than the exchange interaction effects.

With $Fe(III)(aca)_3$, the only possibility is donation of $\beta L \rightarrow M$ because of more than half-filled d orbitals. This results in unpaired α spin density on the ligand with the requirement that the shift be downfield. The shift was so observed.

We can see from the above examples that the rules for pi bonding work well. To say that these rules are general enough to have wide application remains to be seen. There are some factors such as sigma contact shifts, molecular symmetry, crystal field splitting, pseudocontact shifts, and others, which together might contribute more to the shift than that of the pi contact shift. Therefore, based on a knowledge of ligand orbital energies, d orbital energies, symmetry, etc., one must make an analysis of the contact shift for each individual case.

CONTACT SHIFTS AS A TOOL

The exploratory phase of contact shifts is in full bloom. Enough useful information is known to begin using contact shifts as something more than phenomena of our scientific curiosity. A search of the contact shift literature, which was by no means complete, shows that as a tool, it is very versatile and useful. Finally, then, it would be pertinent to briefly mention some aspects of chemistry to which contact shifts have been applied.

1. Bonding Systems

a. Eaton, Ref.28: By comparing the ρ_n distribution about a pi system determined by both NMR and a McLachlan MO calculation, Eaton was able to determine the degree of metal - ligand covalent bonding.

b. Fackler, Ref.38: Hydrogen bonding in inorganic complexes was studied.

c. Horrocks, Ref.39: Horrocks investigated the pi bonding systems of isoquinoline-2-oxide and isoquinoline-1-oxide.

d. Eaton, Ref.30: Eaton developed a new approach to the study of extended pi systems, conjugation and hyperconjugation. He demonstrated the conjugation linkage of biphenyl, stillbene, azobenzene and ---SO_2---.

e. Eaton, Ref.36: Eaton compared the C-H sp^2 and sp^3 bond with the C-F sp^2 and sp^3 bond.

2. Stereo Chemistry and Structural Determination

a. Holtzclaw, Ref.40: Holtzclaw studied the cis and trans species of diaquobis(ethylenediamine) Co(III) ion.

b. Drago, Ref.1: Using the relationship $\frac{\Delta\nu}{\nu} = -Ai\frac{\gamma_e}{\gamma_n}\frac{S(S+1)}{3kT}g\beta$, by plotting $\frac{\Delta\nu}{\nu}$ vs $\frac{1}{T}$, Drago was able to investigate the temperature range over which some metal complexes changed from octahedral to tetrahedral.

c. Horrocks, Ref.41: Horrocks was able to determine the M-N-O angle of Ni(II) and Co(II) acetylacetonate pyridine-N-oxide complexes.

d. Drago, Ref.42: Drago studied cis and trans complexes.

e. Drago, Ref.43: Drago demonstrated that contact shifts are transmitted through halogen ions coordinated to the metal and thus provided a method for determining whether or not certain halogens are in the coordination sphere.

f. Eaton, Ref.28: Eaton determined whether complexes such as $Ni(aca)_2$ were polymerized in certain solvents.

3. Kinetics

a. Holtzclaw, Ref.40: Holtzclaw suggested a method of studying the kinetics of metal complexes.

b. Adams, Ref.44: Adams studied the exchange interaction of metal complexes in various solvents.

c. Ref.45, Ref.30, Ref.26: Similar to studies made in Ref.26.

4. Solvent Effects

a. Happe and Ward, Ref.8: Happe and Ward studied the solvent effects of $Ni(aca)_2$ and $Co(aca)_2$.

b. Drago, Ref.43: Drago demonstrated the effect of hydrogen-bonding of chloroform used as a solvent for metal complexes.

5. Magnetic Properties

a. Shuman, Ref.27: Shuman investigated the ferromagnetic and antiferromagnetic properties of MnF_2 and their relation to temperature.

b. Eaton, Ref.28: Eaton investigated the low spin and high spin d electron distribution.

c. Evans, Ref.46: Determined the magnetic susceptibility of compounds by NMR.

TABLE VI

NMR DEFINITIONS

1. Contact Shift - unusually large NMR chemical shifts in paramagnetic molecules due to electron spin-nuclear spin coupling of the unpaired electron(s) with the resonating nucleus.
2. T_1 - dipolar spin-lattice relaxation or longitudinal relaxation time, resulting from the interaction between the excited nuclear spin moment and the lattic fields of atoms, molecules and ions tumbling in the neighborhood (lattice) of the excited nucleus. The relaxation energy transmitted results in an increased rotation and translation of the neighboring molecules.
3. T_2 - spin-spin relaxation or transverse relaxation time resulting from the interaction between the excited nuclear spin moment and other spins (of both electrons as well as nuclei). This type of relaxation is prevalent in solids.
4. $1/\tau_B$ - exchange rate between the coordinated species and the bulk species (τ_B is the lifetime of a coordinated species).
5. $1/\tau_{2A}$ - the relaxation rate constant for a bulk solvent molecule. (τ_{2A} is the lifetime of a bulk solvent species in the excited state).

Table VI (Continued)

6. $1/\tau_{2B}$ - the relaxation rate constant for a coordinated species (not the same as $1/\tau_{2A}$; rather, τ_{2B} is the lifetime of a coordinated species in the excited state).

7. $1/\tau_S$ - spin relaxation rate for the unpaired electrons. (τ_S is the lifetime of unpaired electrons in the paramagnetic species). Very seldom will $1/\tau_S$ affect the line broadening (except Mn^{2+}).

8. Line width W - W is proportional to the reciprocal of the average time, t, the system spends in the excited state. $W \propto 1/t$. W is measured in cps from the NMR spectrum.

9. Quadrupole moment - an electric moment resulting from an unsymmetrical distribution of electric charge in the nucleus. The nucleus has (2I+1) orientations which couple with electrons and nuclear fields to produce line broadening.

10. A_n - electron spin-nuclear spin coupling constant (sometimes called the contact interaction constant).

11. γ_e - magnetogyric ratio of electrons; the ratio of the electron magnetic moment to the electron angular momentum.

12. γ_n - magnetogyric ratio of nucleus; the ratio of the nuclear magnetic moment to the nuclear angular momentum.

13. I - nuclear spin; for the proton $I = \frac{1}{2}$, and thus $M_I = I, (I-1), \ldots (-I+1)-I = \frac{1}{2}, -\frac{1}{2}$.

Table VI (Continued)

14. S - electron spin.

15. H - field strength, usually in gauss.

16. ν - frequency of resonance.

17. Q - proportionality constant for $A_n = Q\ \rho_n$. For example, Q = -27.5 gauss for (aromatic); Q = +27 gauss for $C\text{-}CH_3$.

18. ρ_n - spin density - fraction of an unpaired electron which appears to be localized at n. ρ_p is either + or -. Vector addition $+\rho_n$ - parallel to net spin of the species. Vector subtraction $-\rho_n$ - antiparallel to net spin of the species as a whole.

19. Exchange interaction - the unpairing of electron spins so as to reduce the energy of the system through exchange interaction of electrons having the same spin.

SOME APPLICATIONS OF NMR CONTACT SHIFTS--NMR EVIDENCE FOR PI-BONDING IN OXOVANADIUM(IV) COMPLEXES

INTRODUCTION

Ever since the publication of the molecular orbital calculation of an energy level scheme for $VOSO_4 \cdot 5H_2O$ by Ballhausen and Gray[47], this energy scheme (hereafter termed the BG scheme) has been utilized by some to explain their data and challenged and altered by others to account for their optical spectral or ESR data[3,13]. The BG energy level scheme, shown in Figure 6, takes into account pi-bonding between the vanadium atom and the axial oxygen atom, but does not take into account the possibility of pi-bonding between the equatorial water molecule oxygens and the vanadium atom. If one considers the molecular orbital scheme for the water molecule as given by McGlynn *et al.*[48] (see Table VII), one can see that both the b_1 and b_2 molecular orbitals (lying mostly on the oxygen) have the proper symmetry for bonding with the $d_{xy}(b_2)$ orbital of the vanadium atom. The BG scheme ignores any interaction between these orbitals and leaves the $d_{xy}(b_2)$ as a pure non-bonding atomic orbital.

In a primarily qualitative energy level scheme for the $VOSO_4 \cdot 5H_2O$ molecule, Selbin, Holmes and McGlynn[49] utilized the

Figure 6

Molecular Orbital Scheme for $VO(H_2O)_5^{2+}$.

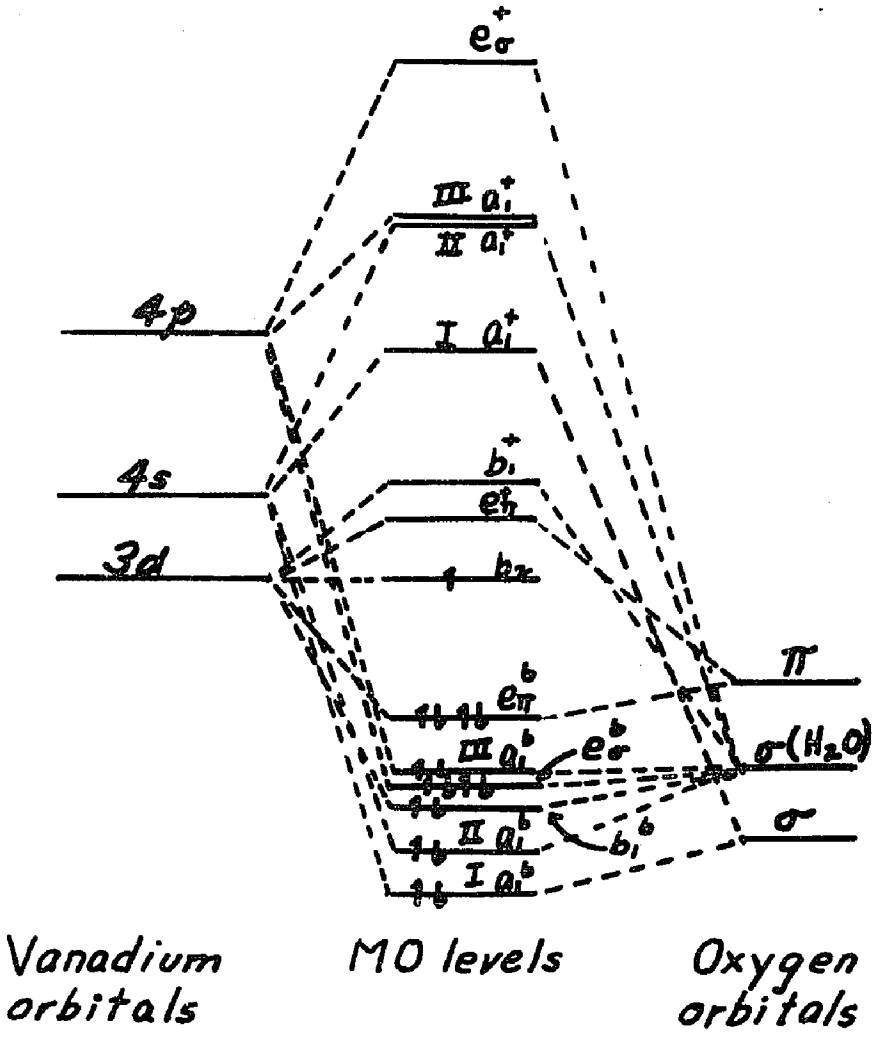
e_σ^*
III a_1^*
II a_1^*
4p
I a_1^*
b_1^*
4s
e_π^*
3d
b_2
π
e_π^b
III a_1^b
e_σ^b
σ-(H_2O)
II a_1^b
b_1^b
σ
I a_1^b
Vanadium orbitals
MO levels
Oxygen orbitals

b_2 molecular orbital of the water molecule to bond with the b_2 orbital of the VO^{2+}, and an energy level scheme quite similar to the BG scheme was deduced. Kivelson and Lee[50] examined the ESR spectra of $VO(aca)_2$ (aca=acetylacetonate ion) and [VO(tetraphenyl-porphyrin)] and carried out a somewhat more inclusive MO calculation, but in the manner of that of Ballhausen and Gray. From their experiments they deduced that the lone electron is in a b^*_{2g} orbital which is "almost completely localized on the vanadium in a d_{xy} atomic orbital" and that "in-plane pi-bonding is slight" in both complexes. Zerner and Gouterman[51] carried out more detailed "extended Hückel calculations" on VO^{2+} porphins, including in their calculations all valance orbitals of all the atoms in the porphin system. They deduced that the b_{2g} orbital is 99% an atomic $3d_{xy}$ vanadium orbital. Hecht and Johnston[52] performed ESR experiments on V^{4+} in Na_2O-B_2O_3 glass systems, and they carried out MO calculations for the VO^{2+} system in this oxide ion environment. They concluded that there is some in-plane pi-bonding, and therefore, the lone electron is not entirely localized on the vanadium atom. Thus, the square of their bonding coefficient, β_2 (i.e., $(\beta_2)^2$), in the MO wavefunction

$$\Psi_{b_2} = \beta_2(3d_{xy}) + \beta_2'(\tfrac{1}{2})(2p_{y1} + 2p_{x2} - 2p_{y3} - 2p_{x4})$$

for the b_2 orbital was in the range 0.83-0.86, rather than 1.00 as had been assumed in the BG scheme.

A more rigorous semi-empirical MO calculation carried out by Vanquickenborne and McGlynn[53] arrives at the following makeup of the b_2 MO:

$$\Psi_{b_2} = (0.93)(3d_{xy}) - (0.18)(2p_{y1} + 2p_{x2} - 2p_{y3} - 2p_{x4})$$

(where the x's and y's refer to specific oxygens 1, 2, 3 and 4, located on the x and y axes in the equatorial plane).

The specific object of this work was to determine if proton NMR studies of selected VO^{2+} complexes could experimentally substantiate pi-bonding in these complexes.

EXPERIMENTAL

$VOSO_4 \cdot 4H_2O$

The compound $VOSO_4 \cdot 4H_2O$ was purchased from the Varlacoid Chemical Company. It was dried in a vacuum and analyzed only for hydrogen. Found: 3.40%H. Calculated for $VOSO_4 \cdot 4H_2O$: 3.41%H. A stock solution of 2% $(CH_3)_3Si(CH_2)_2SO_3Na$ in water was prepared and used to make up the aqueous solutions of vanadyl sulfate for the NMR investigation. The trimethylsilane salt was chosen as an internal standard because of its solubility in aqueous solutions and because its resonance methyl peaks coincide with those of TMS (tetramethylsilane).

$VOSO_4 \cdot 2CH_3OH$

In order to prepare anhydrous solutions of $VOSO_4$ in methanol, the following procedure was employed. Ten grams of $VOSO_4 \cdot 4H_2O$ was added to 300 ml of anhydrous methanol. The solutions was refluxed until all of the solid had dissolved. Then the solution was heated until about half of the methanol had evaporated. Upon cooling, the solution yielded a blue crystalline compound whose elemental analysis indicated the formula $VOSO_4 \cdot 2CH_3OH$. Calculated: 11.5%C, 3.5%H; Found: 11.2%C, 3.0%H. This product was added to anhydrous methanol

to prepare the solutions used in the NMR studies. Tetramethylsilane (TMS) was used as the internal standard.

$\underline{VO(aca)_2}$

This compound was purchased from the Varlacoid Chemical Company. The $VO(aca)_2$ was recrystallized from hot acetonitrile. The solution of $VO(aca)_2$ was prepared with $CDC\ell_3$ as a solvent, using TMS as the internal standard.

$\underline{VOSO_4 \cdot 2(o\text{-}phen)}$

The o-phenanthroline was purchased from J.T. Baker Chemical Company. A solution of 3.5 gr. (0.02 moles) of o-phenanthroline in 100 ml CH_3OH was added to 2.4 gr. (0.01 moles) of $VOSO_4 \cdot 4H_2O$ dissolved in 150 ml of 50-50 water methanol solution. The solution was heated just to its boiling point; then allowed to cool. Upon cooling, a precipitate formed which was washed well with acetone and ether and dried in a vacuum. Analysis: Found: 43.92%C, 4.21%H; Calculated: 44.99%C, 3.15%H. The solution of $VOSO_4 \cdot 2(o\text{-}phen)$ was prepared with CH_3NO_2 using TMS as an internal standard.

A Varian HA 60 Spectrometer was used to obtain the NMR spectra of solutions of $VOSO_4 \cdot 4H_2O$, $VO(aca)_2$ and $VOSO_4 \cdot 2(o\text{-}phen)$ while a Varian HA 100 Spectrometer was used to obtain the NMR spectrum of a solution of $VOSO_4 \cdot 2CH_3OH$.

THEORY

A general theory of the NMR of paramagnetic complexes in solution is given in the first part of Chapter II and is entitled: "A DISCUSSION OF THE PRINCIPLES OF NMR CONTACT SHIFTS". The works by Drago[23] and by Benson and Phillips[54] are recommended as supplementary reading to the above discussion of contact shifts. The theory and its application to the present work is given by Wayland and Rice[55] for the protion which covers the application of NMR to the study of $VOSO_4 \cdot 4H_2O$; the work by Eaton[28] on NMR of paramagnetic transition metal acetylacetonates covers the application and theory for the protion of this work concerning $VO(aca)_2$ and $VOSO_4 \cdot 2(o\text{-phen})$.

The electron relaxation time, τ_s, for the d^1 electron in the VO^{2+} species was found to be approximately 3×10^{-9} seconds[56,57]. Although the electron relaxation time of a paramagnetic ion is affected by ligands to which it is coordinated[54], the ligand field does not significantly change the relaxation time. The value of 3×10^{-9} seconds is probably a reasonable value for most VO^{2+} electron relaxation times, regardless of the ligand to which the VO^{2+} species is attached. The τ_s has an effect on both T_1 (the longitudinal relaxation time) and T_2 (the transverse relaxation time) of resonating

nuclei in solution. If the resonating nuclei are part of the ligands which are exchanging with each other, or with other ligands in a solution containing paramagnetic ions, the relaxation time for these nuclei is given by the relation[56]:

$$\frac{1}{T_1} = C\left(3 + \frac{7}{1+W_s^2T_c^2}\right) + 2C' \frac{1}{1+W_s^2T_s^2}\ \tau_s \qquad \ldots.9$$

$$\frac{1}{T_2} = C\left(3.5 + \frac{6.5}{1+W_s^2T_c^2}\right) + C'\left(1 + \frac{1}{1+W_s^2T_s^2}\right)\ \tau_s \qquad \ldots.10$$

If T_s is large, as is the case with τ_s for the unpaired electron of VO^{2+}, this τ_s affects T_2, but has very little effect on T_1, and this relation is given as[56]:

$$\frac{1}{T_2} \approx C_1 \frac{\eta}{T} + C_2' \tau_s \qquad \ldots.11$$

where T = Temperature, η = viscosity of the solution, and C_1 and C_2 are constants. Thus, we can see that if τ_s is large, the value of T_2 is small. The effect of T_2 on the line width, W, of an NMR spectrum is given by the relation[23]:

$$W \propto \frac{1}{T_2} \qquad \ldots.12$$

If T_2 is small as a result of the large τ_s, extreme line broadening can result. This relation can be understood if one considers the uncertainty principle:

$$\Delta E \ \Delta t \sim h \qquad \ldots.13$$

As the lifetime of the excited state becomes very short (i.e., Δt is small), the uncertainty in the energy of this state, ΔE, becomes large. The lifetime of a nucleus in a particular spin state will be determined by the relaxation process. Thus, if ΔE is large, a wide range of frequencies is absorbed in transitions resulting in line broadening.

Since τ_s for VO^{2+} is large, and line broadening of the NMR spectral lines in its complexes are often too severe to be observed (as, for example, in the case of $VOSO_4 \cdot 4H_2O$), a technique to circumvent this line broadening must be employed. If the exchange of a water molecule between the bulk water and the coordination sphere of $VOSO_4 \cdot 4H_2O$ in an aqueous solution is so rapid that an average water proton peak appears on the NMR spectrum rather than two peaks representing the solvent water and the coordinated water, the chemical shift of the coordinated water protons, from the pure water proton position, $\Delta\nu_{comp}$, can be calculated from the observed average water

proton chemical shift, $\Delta\nu_{obs}$, from the relation:

$$\Delta\nu_{comp} \times f_{comp} = \Delta\nu_{obs} \quad \ldots.14$$

Here the f_{comp} is the fraction of the total water molecules complexed. In this way, the chemical shift of the water protons coordinated to the VO^{2+} can be determined even though the proton peaks of $VOSO_4 \cdot 4H_2O$ are too broad to be observed in a solvent such as dioxane. The proton peaks of $VO(aca)_2$ in $CHC\ell_3$ and $VOSO_4 \cdot 2$(o-phen) in CH_3NO_2 were broad, but not so broad that they were unobservable. Thus, it was not necessary to employ this technique to observe the NMR spectra of these two VO^{2+} complexes.

The observed chemical shift of the ligand nuclei resulting from the effect of the unpaired electron on the metal nucleus can be ascribed to either the pseudocontact or the Fermi contact shift. The pseudocontact shift is the result of the anisotropy of the g factor and is given by the relation[54]:

$$\frac{\Delta\nu}{\nu} = \frac{\beta^2 S(s+1)}{45kT}\left[\frac{3\cos^2\theta - 1}{r^3}\right](3g_{||}^2 + g_{||}g_{\perp} - 4g_{\perp}^2) \quad \ldots.5$$

where ν = frequency, S = electron spin, β = Bohr magneton, γ_e and γ_n

are magnetogyric ratios of the electron and the nucleus, respectively; θ is the angle between $g_{||}$ (which is coincident with the principal axis) and a vector of length r joining the central metal with the resonating nucleus. Thus, one can see that the pseudocontact shift of a resonating nucleus is dependent on its spatial arrangement in the paramagnetic molecule.

The Fermi contact shift, which occurs when some unpaired spin density is transferred from the ligand to the metal, or from the metal to the ligand atoms, through either the sigma or pi bonds formed between the metal and ligand atoms, makes up the greatest part of the chemical shift in most cases. The amount of spin density transferred to or from an atom to which the resonate nucleus is attached is related to the electron spin-nuclear spin coupling constant A. The latter constant, in turn, is related to the contact shift by equation 8[54]:

$$\frac{\Delta\nu}{\nu} = -A \frac{\gamma_e}{\gamma_N} \frac{g\beta S(S+1)}{3kT} \qquad \ldots.8$$

where the symbols have the same identity as they have in equation 7.

RESULTS

The average proton chemical shift of the coordinated water from uncoordinated water in the aqueous solution of $VOSO_4 \cdot 4H_2O$ was found to be 8.54 ppm (513 cps) downfield from the uncoordinated water, as shown in Table VIII. From equation 7, $\frac{A}{h}$ was determined to be 3.0×10^5 cps, and since the shift was downfield, A must therefore be positive. A typical spectrum of aqueous $VOSO_4 \cdot 4H_2O$, which demonstrates the extensive line broadening resulting from a large τ_s, is shown in Figure 7.

The proton chemical shift for -OH protons in the methanolic solution of $VOSO_4$ was determined to be 10 ppm (1000 ± 25 cps) downfield from the uncoordinated methanol (Table VIII). The value for $\frac{A}{h}$ was calculated to be 3.45×10^5. No noticeable shift was found for the methyl peak. Both the -OH and the methyl peaks were found to be broadened, but the $-CH_3$ peak not nearly as much as the -OH peak.

The methyl proton chemical shift for $VO(aca)_2$ (Figure 9a) in $CDC\ell_3$ was found to be 15 cps downfield from the diamagnetic methyl proton peak found in $Zn(aca)_2$ (Figure 9b). The peak was severely broadened, presumably by the slow relaxation of the paramagnetic ion. It was not possible to locate the CH ring peak. A peak which resembled

Figure 7

The proton NMR spectrum of $VOSO_4 \cdot 4H_2O$ in aqueous solution. TMS is used as an internal standard.

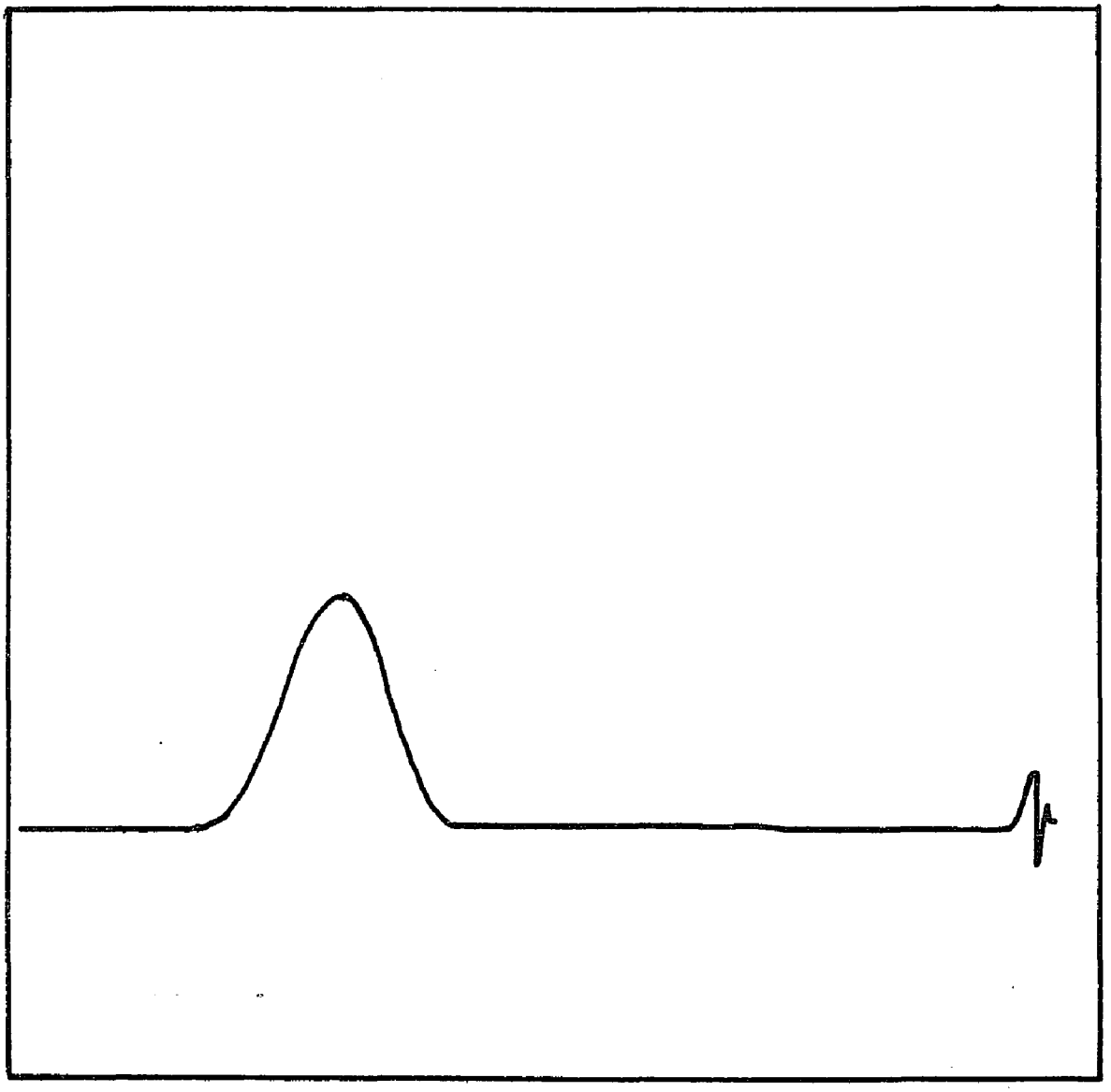

the CH peak was found just upfield from the methyl peak, but when the spectrum was run without TMS, this peak disappeared. It appears that this peak originates from TMS as a spinning side band.

Three of the four sets of equivalent hydrogens of $VOSO_4 \cdot 2$(o-phen) were found to be broadened (Figure 10), but they were found to be very little shifted from the resonate position of the same hydrogens of the diamagnetic ligand (Figure 10). A fourth peak, which lies nearest the VO^{2+} species in the molecule, could not be located on the NMR spectrum.

DISCUSSION

ESR measurements[50,58] place the unpaired electron of VO^{2+} in the d_{xy} orbital, in support of the BG scheme. This assignment is accepted as fact and used by all other workers in the field.[3,13,47,51,52,53]. There is little doubt then that the unpaired electron is in the d_{xy} orbital in the ground state. If one accepts the symmetry group C_{4v} as the point group of the V atom in the $VOSO_4 \cdot 4H_2O$ molecule in solution[47,53], then the d_{xy} orbital has b_2 (or b_2^*) symmetry. From symmetry considerations alone, it can only pi bond with either the b_1 or b_2 MO's on the equatorial water molecules (Table VII).

Wayland and Rice[55] demonstrated the existence of π-bonding between coordinated water molecules and the metal ions Co^{2+}, Fe^{2+}, Mn^{2+} and Fe^{3+}. The proton NMR of these ions in aqueous solution was run along with aqueous solutions of Co^{2+} and Ni^{2+} whose unpaired electrons are in orbitals of only sigma symmetry. The contribution due to sigma unpaired electron transfer, taken as the effect given by Ni^{2+}, was "stripped" out of the results found for Co^{2+}, Fe^{2+}, Mn^{2+} and Fe^{2+} leaving only the effect contributed by pi-bond unpaired electron transfer. Good correlation between the electron spin S in the t_{2g} orbitals and the electron spin-nuclear spin coupling constants was

found, a summary of which is given in Table IX.

Wayland and Rice used a MO energy level scheme of water similar to that of McGlynn[48] to deduce that both the b_1 and the b_2 water MO's have the appropriate symmetry for pi-bonding between the metal ion and the water molecule. Indeed, the paramagnetic shifts observed by Wayland and Rice are interpreted using both b_1 and b_2 water MO's bonded to the t_{2g} orbitals of the metal ion.

It has been shown by Radford[59] that spin density transfer through the b_1 orbital would cause a shift upfield, whereas spin density transferred through the b_2 orbital would cause a shift to be downfield. Since the observed shift for the metal ions was downfield, Wayland and Rice concluded that although the b_1 orbital must play the major role in bonding, the b_2 orbital, which is more efficient in transmitting spin density to the hydrogen, is responsible for the observed shift. The reason that the b_2 orbital is more efficient for transferring spin density is because it is made up of both the oxygen 2p and the hydrogen 1s orbitals, and thus, any spin density transferred through this orbital goes directly into the hydrogen orbital. The b_1 orbital, however, is less efficient because hyperconjugation (or spin polarization) must be involved (a much less efficient process) to transfer spin density to a hydrogen

orbital. In any case, delocalization of unpaired pi electron density into the water molecule is present.

The observed shift for the VO^{2+} ion in water is found to be downfield, but of much smaller magnitude than those shifts observed by Wayland and Rice for transition metal ions with more d (i.e., t_{2g}) electrons. However, it can be concluded on the basis of the foregoing results and discussion that there is indeed experimental proton NMR support for pi-bonding between the VO^{2+} and water molecules. The observed shift cannot be interpreted as arising from the tumbling of the VO^{2+} ions in solution because a dipolar shift of this type would result in an upfield shift, whereas the observed shift is actually downfield. Therefore, as in the case demonstrated by Wayland and Rice, the shift is most likely due to bonding between the b_2 MO of VO^{2+} and the b_1 and b_2 MO's of H_2O.

The compling constant $(\frac{A}{h})$ was determined to be 3.0×10^5 cps, whereas the coupling constants for the other transition metal ions were about 14×10^5 cps. The smaller observed coupling constant for VO^{2+} cannot be due to σ transfer (which is normally much smaller than pi transfer), since σ transfer would result in an $(\frac{A}{h})$ value of about 1.5×10^5 cps. (See Table IX results for Co^{2+} and Ni^{2+}). Furthermore, the unpaired electron is unambiguously placed in VO^{2+}

in a primarily d_{xy} orbital anyway, which is not suitable for sigma bonding.

Other recent ^{17}O NMR work supports the conclusion of pi-bonding presented here. Wuthrich and Connick[60] examined the ^{17}O NMR spectrum of VO^{2+} in water and found that the $(\frac{A}{h})$ for ^{17}O water oxygens was 3.8×10^6 cps. This coupling constant is an order of magnitude larger than that found in this study for the proton-electron coupling, and this is understandable, since the ^{17}O is bonded directly to the VO^{2+}, while the protons are two bonds away and the attenuation of the coupling due to distance would account for the smaller coupling. From earlier ^{17}O NMR data, Connick[60] *et al.* found that the $(\frac{A}{h})$ values for the ions Mn^{2+}, Fe^{2+}, Co^{2+} and Ni^{2+} in aqueous solution were much larger than the $\frac{A}{h}$ found for the VO^{2+} ion. This is consistent with the comparison of the $(\frac{A}{h})$ proton coupling found in this study to the $\frac{A}{h}$ proton couplings found by Wayland and Rice[55].

Hausser and Laukien[56] measured the relaxation times T_1 and T_2 of VO^{2+} in aqueous solution by proton NMR. No coupling constant was given; however, if their data for T_1 and T_2 are used to calculate a value for $(\frac{A}{h})$, one obtains $(\frac{A}{h}) = 1.65 \times 10^6$. This value is somewhat larger (by a factor of five) than the value found here, but the larger value was determined by assuming a "good value"

for the τ_s (electron relaxation time). In addition, exchange (correlation) times must be determined before $(\frac{A}{h})$ can be determined from relaxation times. The method used here, that of chemical shifts developed by Wayland and Rice, is a more direct approach which does not require any assumptions. There is, however, no disagreement on inferences of Hausser and Laukien and the conclusions of this work that pi-bonding exists between the water molecules and the VO^{2+} ion.

There still remains the question of why the $(\frac{A}{h})$ constants for the VO^{2+} (found in this work and by Connick[60] et al.) are smaller than the $(\frac{A}{h})$ found for other ions. From the previous discussion, one could make a case for the "play off" of the b_1 orbital effect against the b_2 orbital effect. Since each of these orbitals has the effect of shifting the proton peak in opposite directions, the b_2 orbital could be assumed to have less bonding than the b_1 orbital in the VO^{2+} complex, while in aqueous complexes of Co^{2+}, Fe^{2+}, Mn^{2+} and Fe^{3+}, just the opposite is true. More likely, however, is the fact that the VO^{2+} complex has a square pyramide configuration, whereas the other ions in aqueous solution possess the octahedral configuration. The octahedral configuration permits both the b_1 and b_2 water MO's to bond to the metal ions at

the same time, since the metal ions possess t_{2g} orbitals. In the VO^{2+} complex, however, a water molecule can bond to the VO^{2+} d_{xy} orbital, either with the b_1 or the b_2, but not with both at the same time, since these two orbitals are orthogonal on the water molecule. A third consideration, which cannot be overlooked, is the effect that structure has on the bonding. It is known that VO^{2+} complexes form a square pyramid[13] with the VO^{2+} species sitting above a rectangular base formed by the four equatorial bonding atoms (Figure 8). As a result, the ligand bonding orbitals (b_1 or b_2) are pulled down and away from the VO^{2+} ion. The overlap possible between bonding pi orbitals of the VO^{2+} ion and the b_1 or b_2 water MO's is not as great as the overlap possible in the other metal ions of octahedral symmetry. Probably all of these effects contribute to producing the small $(\frac{A}{h})$ value observed for $VOSO_4 \cdot 4H_2O$.

In an effort to add new evidence for pi-bonding to that cited above, the proton NMR spectrum of $VOSO_4 \cdot 2CH_3OH$ in methanol was obtained. It was assumed in this case that the MO's of the methanol oxygen atom would bond to VO^{2+} in a way similar to that of the water oxygen atom. Thus, observing the methanol-OH peak, one should expect it to behave similarly to the water proton in aqueous $VOSO_4$. Indeed, the water proton and the methanol-OH proton do have similar

Figure 8

The Structure of $VO(H_2O)_4^{2+}$.

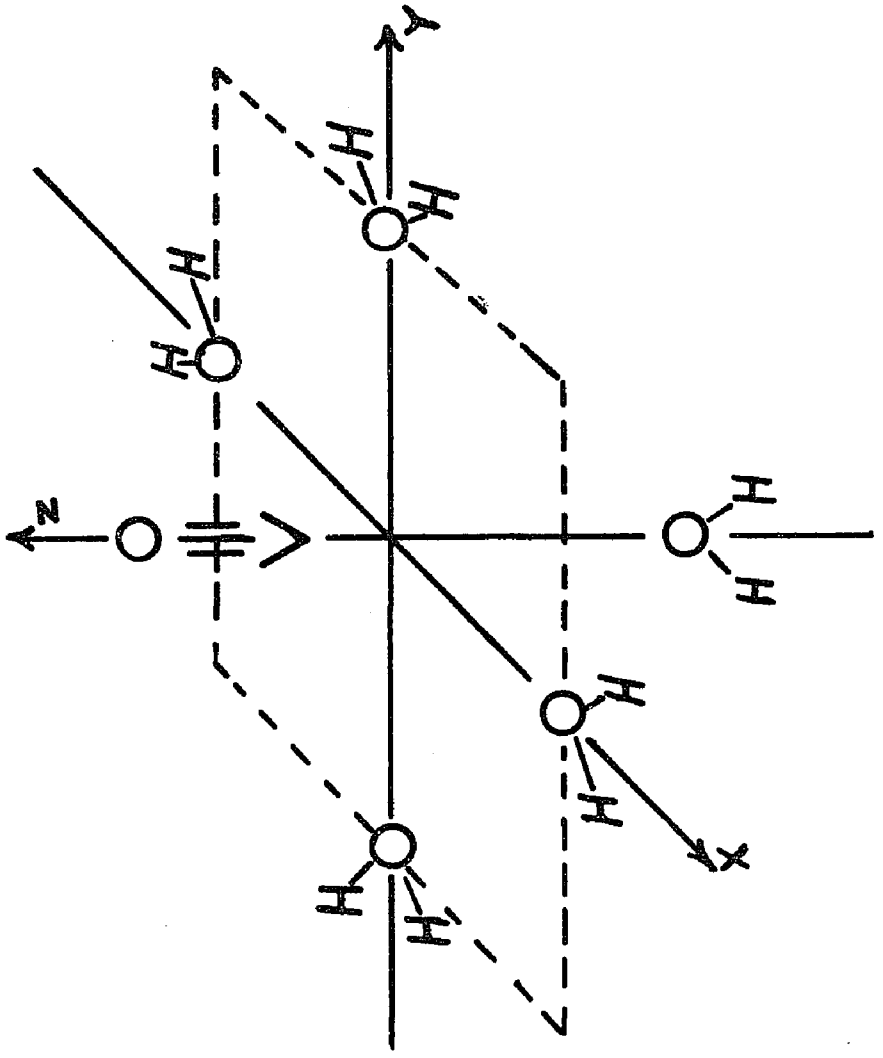
Y
Z
X
H
O

coupling constants (see Table VIII), and thus it appears that pi-bonding from methanol to VO^{2+} is also occurring.

In an effort to further investigate the pi-bonding in other types of VO^{2+} complexes, the NMR spectrum of $VO(aca)_2$ was obtained in $CDC\ell_3$ as a solvent with TMS as an internal standard (Figure 9a). An earlier attempt to obtain such a spectrum by Eaton[28] failed. Because of the judicious selection of sweep rate, gain and filter settings made on the HA60 NMR spectrometer by Mr. William Wegner of the Louisiana State University Department of Chemistry, it was possible to obtain a spectrum of the methyl peak of $VO(aca)_2$. The peak was extremely broad and the center of the peak could be determined to about ±3 cps. The methyl peak was found to be shifted 15 cps <u>downfield</u> from the diamagnetic methyl peak of $Zn(aca)_2$ (Figure 9b) indicating that A is positive. No peak for the C-H ring proton of the $VO(aca)_2$ was found, however.

Table IV gives the contact shifts for the acetylacetonates of Ti(III), V(III), Cr(III), Mn(III) and Fe(III) measured by Eaton[28], and the mechanism by which these contact shifts occurred were well described earlier in Chapter II. To reiterate the conclusions reached by Eaton, the contact shifts shown in Table X are the result of metal-to-ligand charge transfer of unpaired spin density (α spin)

Figure 9

a. The proton NMR spectrum of $VO(aca)_2$ with TMS as an internal standard.

b. The proton NMR spectrum of $Zn(aca)_2$ with TMS as an internal standard.

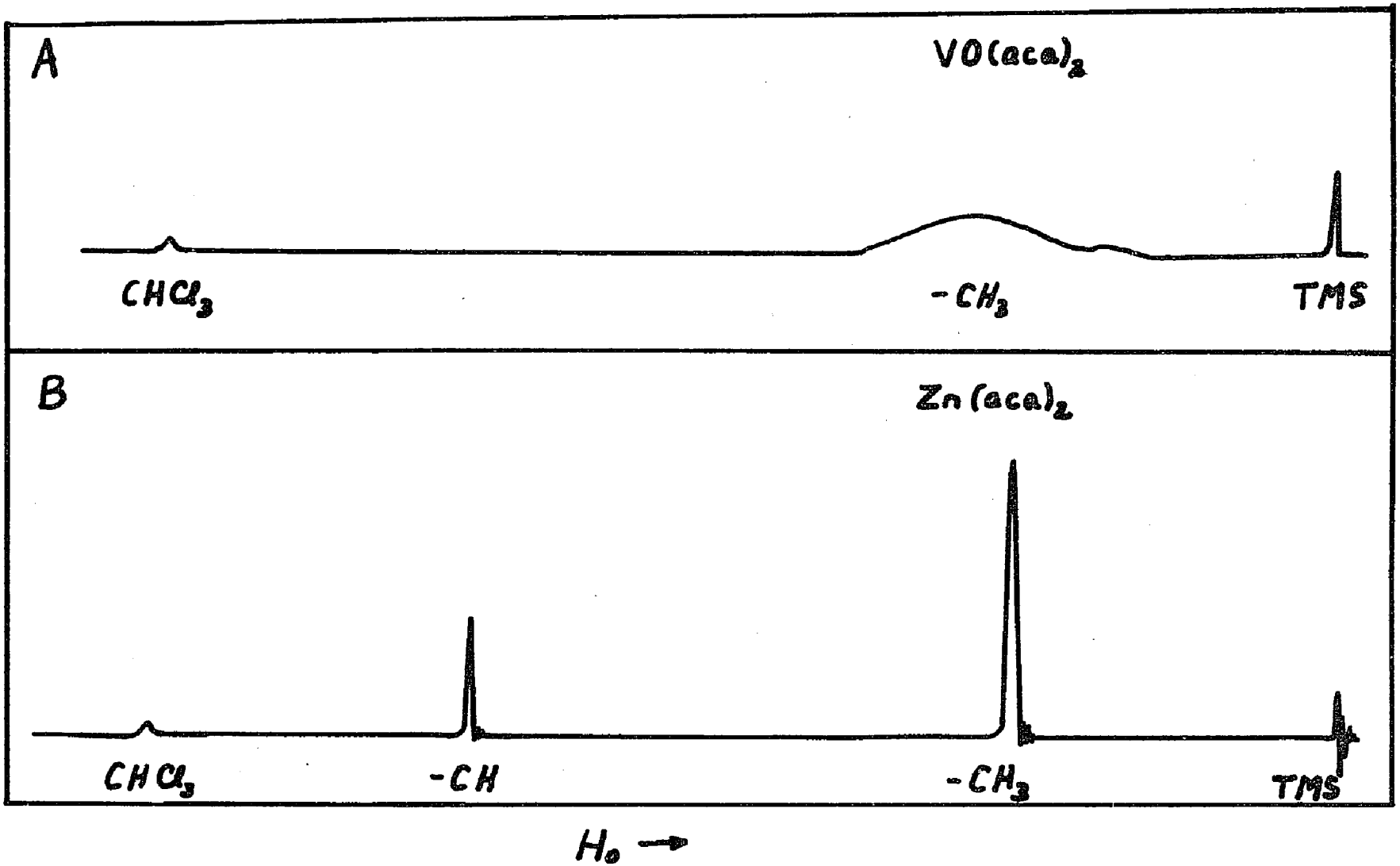
A
VO(aca)2
CHCl3
-CH3
TMS
B
Zn(aca)2
CHCl3
-CH
-CH3
TMS
Ho →

from the metal t_{2g} orbitals to the lowest antibonding (unfilled) orbitals of the acetylacetonate ligand. If one examines the results of molecular orbital calculations given in Table XI (McLachlan), one can see that spin density transferred into the lowest antibonding ligand orbitals will have a much greater effect on the methyl peak than on the ring C-H peak. In addition, the transfer of α spin density will cause both the C-H and the methyl peaks to be shifted downfield.

The $VO(aca)_2$ energies should not be too different from the other metal acetylacetonates of the first row transition series, and a hurried conclusion would lead one to believe that the contact shifts of $VO(aca)_2$ should be of the same order of magnitude as those of the other metal acetylacetonates. Experimental evidence has shown otherwise. The C-H ring peak could not be found and the methyl peak was shifted only 15 cps. It is probable, then, that the chemical shift of $VO(aca)_2$ does not follow the mechanism which was responsible for the smooth increase in chemical shifts observed for the methyl peaks of Ti(III) through Fe(III).

Earlier[50], it was established that the d^1 electron in $VO(aca)_2$ is almost completely localized in the $b_2(d_{xy})$ orbital. Since $VO(aca)_2$ can be considered to be in the C_{4v} point group, the

acetylacetonate ion ligand must supply orbitals which will properly overlap with the b_2 orbital in order to have an electron transfer mechanism similar to the other metal acetylacetonates. No such molecular orbital exists on the acetylacetonate ligand. Thus, for symmetry reasons, it is improbable that the shift of the methyl protons on $VO(aca)_2$ originates from the same mechanism as the other metal acetylacetonates. One must now turn to a more exotic explanation of the observed shift. In Kivelson and Lee's[50] work on a vanadyl prophyrin, they observed a small hyperfine splitting of the ESR signal due to the porphyrin nitrogens. They first suggested the possibility of the mixing of the b_2 ground state with a higher state whose symmetry could account for the delocalization of the d^1 electron onto the porphyrin nitrogen. They discounted this reasoning in favor of a polarization mechanism. They reasoned that the unpaired electron in the b_2 orbital, when in a magnetic field, has α spin. The d^1 electron interacted with the paired electrons in the highest filled porphyrin pi orbital (located primarily on the nitrogen) resulting in a polarizing of the electron with β spin. The nitrogen then experiences a surplus of α spin density and through polarization interaction, the hyperfine splitting on the ESR spectrum could be explained. If one applies this same

reasoning to the $VO(aca)_2$ molecule, this should result in the introduction of α spin onto the acetylacetonate oxygen. Thus, the polarization mechanism, as well as the spin density transfer mechanism, through orbital overlap described by eaton, places α spin on the ligand oxygen, but the effect that the two mechanism have on the chemical shifts of the methyl protons and C-H are different. The spin density transfer through orbital results in the interaction between the t_{2g} orbitals of the metal and the empty antibonding pi orbital. If one considers the spin densities given in Table XI and the effect that unpaired spin density would have on the methyl protons and C-H chemical shift, one can see that the spin density on the carbon attached to the methyl (+0.4979) would be much larger than the spin density of the C-H (-0.1658) by this mechanism. The polarization mechanism, however, required that the lone electron in the d_{xy} orbital interact with one electron of the paired electrons in the top bonding ligand molecular orbital. Table XI shows that any spin density transferred to this orbital would have the greatest effect on the C-H carbon (spin density = 0.7291), whereas the effect on the carbon attached to the methyl group would be rather small (+0.0640). This explanation would account for the observations of the $VO(aca)_2$ NMR spectrum. First the methyl peak is

only shifted 15 cps downfield from its diamagnetic position while the methyl peaks of the other metal acetylacetonates are shifted from 1110 cps to 3367 cps because spin density transfer in $VO(aca)_2$ is in the top bonding molecular orbital which has little effect on methyl group spin densities, while the spin density transfer in the other metal acetylacetonates involves the lowest antibonding orbital which causes large spin densities to be placed on the methyl group. A second reason for such a small methyl proton chemical shift is the fact that a polarization interaction of this type is rather weak[50]. Since the polarization interaction permits little electron-spin nuclear spin coupling between the d^1 and the methyl protons, this would explain why the slow relaxing d^1 electron broadens the methyl proton peaks but does not completely wash them out.

The C-H proton, however, is much more affected by the polarization mechanism given above (see Table XI), and this would account for a much larger electron spin-nuclear spin coupling between the d^1 electron and the C-H proton. With this larger coupling, it is not unreasonable to assume that the C-H peak was broadened to the point that it could be located. Since the polarization mechanism predicts α spin on the CH group carbon, equation 5 ($A = Q\ \rho_c$; Q is

negative for CH group) would predict the CH peak to lie upfield from its diamagnetic position. Thus, it seems the polarization is able to explain, not only the magnitude, but also the correct direction of the observed chemical shift.

In general, the spin orbit coupling accounts for the anisotropy of the g factor in metal ions. This anisotropy of the g factor makes possible the pseudocontact shift which was given earlier by equation 5.

$$\frac{\Delta\nu_i}{\nu} = -\frac{\beta^2 S(S+1)}{45kT}\left[\frac{3\cos^2\theta-1}{r^3}\right]\left[3g_{||}^{\,2} + g_{||}g_{\perp} - 4g_{\perp}^{\,2}\right]$$

In his work on acetylacetonates, Eaton[28] ignored the effect of pseudocontact shifts because of the large shifts observed and because the first row transition metal ions are known to possess small anisotropies which account for only small pseudocontact shifts. Since the chemical shifts for the methyl protons of $VO(aca)_2$ were observed to be small, pseudocontact shifts cannot be discounted. Equation 6 above was used to calculate the chemical shift of the methyl protons using the following:

r = 6Å (this is a conservative estimate; r is probably near 7Å).

$g_{||}$ = 1.948 ref.6

$g_{\perp}$ = 1.981

θ = 102° ref.6

The chemical shift was found to be approximately 0.6 cps downfield. This value is probably smaller than 0.6 cps because of the conservative distance assumed for r. In any case, the pseudocontact shift cannot account for the observed chemical shifts of the methyl protons, which is in agreement with the assumptions made by Eaton[28]. One must conclude that the spin polarization mechanism is the most probable mechanism accounting for the contact shift.

The NMR spectrum of $VOSO_4 \cdot 2$(o-phen) was also obtained in order to investigate the possibility of pi-bonding between the b_2 metal orbital and the sp^2 nitrogen ligand atom. Figure 10 is the NMR spectrum of the free ligand in CH_3NO_2, and it shows the four chemically different peaks, H_1, H_2, H_3 and H_4. The peaks are well resolved, especially H_1, which is closest to the ligand atom nitrogen. Since nitrogen has a quadrupole moment, it characteristically broadens protons peaks of protons attached to it, but the proton H_1 is apparently too far removed (two bonds away) to have any broadening effect. If, however, one observes the NMR spectrum of $VOSO_4 \cdot 2$(o-phen), in CH_3NO_2, from Figure 10 one can see that H_1 has disappeared from its position in the free (diamagnetic) ligand, and that H_2, H_3 and H_4 are broadened and ill-defined. One important observation is that H_2, H_3 and H_4 of the VO^{2+} complex are shifted only slightly downfield

Figure 10

A. The NMR spectrum of o-phen ligand.

B. The NMR spectrum of $VOSO_4 \cdot 2$(o-phen).

TMS (not shown is used as an internal standard.

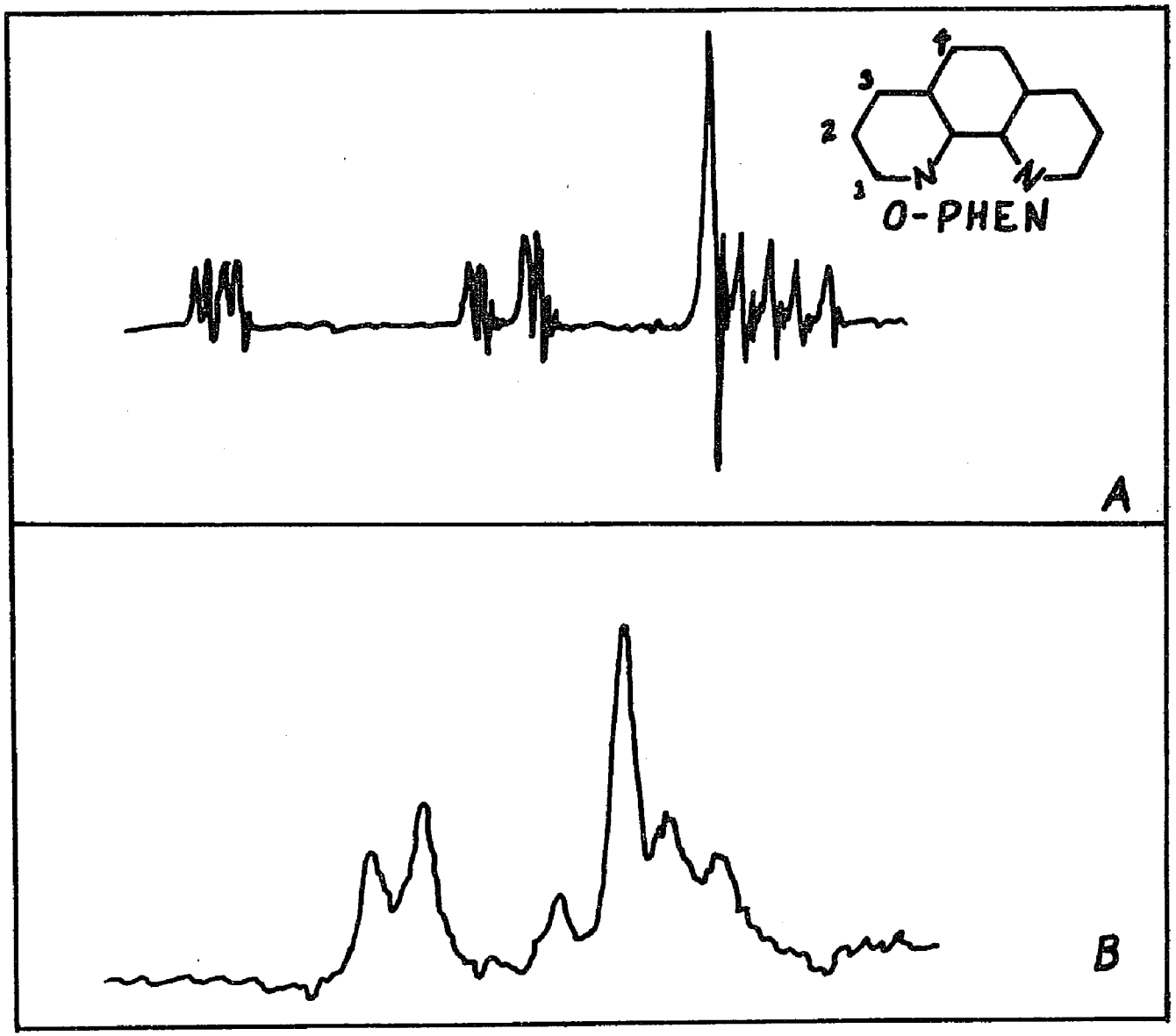
4
3
2
1
N
N
O-PHEN
A
B

from their positions in the free ligand. The large peak left of the center of H_3 and H_4 was shifted 10 cps while the H_2 peak was shifted 13 cps. Again, employing the polarization mechanism which was used to explain the observed shifts in $VO(aca)_2$ in the previous discussion, and also used by Kivelson and Lee[50] to explain the hyperfine splitting of a vanadyl porphyrin, one can explain the chemical shifts observed for the NMR spectrum of $VOSO_4 \cdot 2$(o-phen). The disappearance of the H_1 peak, which is that of the ligand proton closest to the VO^{2+} ion, can result from a combination of two effects. It is much closer to the VO^{2+} ion than the other protons in the molecule, and is more susceptible to both polarization effects and to pseudocontact effects than are the other protons of the ligand.

CONCLUSIONS

The $VOSO_4 \cdot 4H_2O$ and $VOSO_4 \cdot 2CH_3OH$ both possess some degree of pi-bonding between the b_2 orbital on the VO^{2+} ion and the b_1 and b_2 orbitals of the ligand. These conclusions are contrary to one of the assumptions of the BG energy scheme. No quantitative determination of the amount of bonding could be predicted because the contact shift, from which such a determination could be made, results from two competing mechanisms rather than from just one mechanism. A comparison of the electron spin-nuclear spin coupling constant $(\frac{A}{h})$ indicates that there is probably less pi-bonding between the VO^{2+} ion and its attached water molecules than between the metal ions Co^{2+}, Fe^{2+}, Mn^{2+} and Fe^{3+} and the water ligands attached to them.

Consistent with the ESR studies of Kivelson and Lee[50], on $VO(aca)_2$ and vanadyl porphyrin, the NMR studies of $VO(aca)_2$ and $VOSO_4 \cdot 2$(o-phen) show very little in-plane π-bonding between the d_{xy} metal orbital (which possesses the d^1 electron) and the in-plane ligands.

These conclusions suggest that monodentate ligands such as H_2O and CH_3OH pi bond to the b_2 metal orbital because they are

able to rotate in such a manner that symmetry requirements for overlap are met. The bidentate ligands, such as the acetylacetonate ion, the porphyrin ion or the o-phen molecule bond in such a way that symmetry requirements for pi-bonding between the b_2 orbital and the ligand orbitals cannot be met.

TABLE VII

MOLECULAR ORBITAL CALCULATIONS FOR H_2O[48]

MO	2s	$2p_x$	$2p_y$	$2p_z$	3s	1s (hydrogen)
$1a_1$	0.804(0.786)	---	---	-0.020(0.0)	-0.012(0.0)	0.167(0.108)
$1b_2$	---	---	-0.646(0.582)	---	---	-0.450(0.209)
$2a_1$	-0.433(0.054)	---	---	0.793(0.732)	0.019(0.0)	0.296(0.106)
$1b_1$	---	1.0(1.0)	---	---	---	---
$3a_1$	0.627(0.074)	---	---	0.517(0.156)	-0.649(0.482)	-0.489(0.144)
$4a_1$	-0.723(0.085)	---	---	-0.487(0.112)	-0.776(0.517)	0.582(0.142)
$2b_2$	---	---	-0.965(0.418)	---	---	0.937(0.291)

TABLE VIII

NMR CONTACT SHIFT DATA FOR THE AQUEOUS SOLUTIONS OF $VOSO_4 \cdot 4H_2O$[a] AND THE METHANOLIC SOLUTION OF $VOSO_4 \cdot 2CH_3OH$[b]

	Moles $VOSO_4$	Total moles of H_2O[a] or CH_3OH[b]	$\Delta\nu$ in cps[c] at 43°C or 40°C[b]	$(\frac{A}{h})_\pi$[d]
1	0.00120	0.275	524	---
2	.00139	.274	501	---
3	.00181	.277	514	---
			Average = 513	3.0×10^5
4	8.28×10^{-5}	0.0822	1000[e]	$3.4_5 \times 10^5$

a. These data are for runs 1, 2 and 3.

b. These data are for run 4.

c. Resonance frequency = 60 Mc for aqueous solutions and 100 Mc for methanolic solution.

d. See the note under Table IX.

e. 1000 ± 25 cps.

TABLE IX

NMR CONTACT SHIFT DATA OF PARAMAGNETIC IONS IN AQUEOUS SOLUTION[55](a)

Ion	S_{total}	$(\frac{A}{h})$ x 10^{-5}	$S_{t_{2g}}$	$(\frac{A}{h})_{\pi}$ x 10^{-5}
Cu^{2+}	1/2	1.5	0	---
Ni^{2+}	1	1.1	0	---
Co^{2+}	3/2	4.2	1/2	18.3
Fe^{2+}	2	5.0	1	14.0
Mn^{2+}	5/2	5.9	3/2	12.7
Fe^{3+}	5/2	7.7	3/2	16.5

(a) $(\frac{A}{h})$ is the coupling constant resulting from the total shift; $(\frac{A}{h})_{\pi}$ (or the π-only contribution) was determined by "stripping out" the σ contribution, which can be taken from the Ni^{2+} value for $(\frac{A}{h})$ values of Co^{2+}, Fe^{2+}, Mn^{2+} and Fe^{3+}.

TABLE X

CONTACT SHIFT DATA FOR METAL ACETYLACETONATES AS GIVEN BY EATON[28]

	$\Delta\nu_{CH_3}$	$\Delta\nu/S+1$	$\Delta\nu/S \times (S+1)$	$\rho^b \times 10^2$	$Fe^c \times 10^3$
Ti	-3367	2245	4489	+28.9	68.8
V	-2611	1306	1306	+16.6	39.5
Cr	-2187	875	583	+11.1	26.4
Mn	-1372	457	229	+ 5.7	13.6
Fe	-1110	317	127	+ 4.0	9.5

(a) In cps relative to the CH_3 resonance of cobalt(III) acetylacetonate.

(b) Calculated for $A_n = Q\ \rho_c$ with Q = +27 gauss.

(c) F = the fraction of unpaired electron delocalized.

TABLE XI

MOLECULAR ORBITAL CALCULATIONS FOR THE ACETYLACETONATE ION[55]

Acetylacetonate	
Energy top bonding	+0.9417β
Energy bottom antibonding	-0.6103β

Spin Densities

	Top bonding		Bottom antibonding	
	Hückel	McLachlan	Hückel	McLachlan
O	+0.0890	+0.0710	+0.0799	+0.0852
C_1(C-CH_3)	+0.1260	+0.0640	+0.4201	+0.4979
C_2(C-H)	+0.5683	+0.7291	+0.0000	-0.1658

CHAPTER III

EVIDENCE FOR OXOVANADIUM(IV) COMPLEXES OF UNUSUAL COORDINATION

A. INTRODUCTION

Not long ago the chemistry which dealt with molecular polyhedra of high coordination number, specifically seven-, eight-, nine-, ten-, eleven- and twelve-coordinate complexes, would have been described as obscure and of limited scope.[61,62] However, with recent advances in methods and instruments of structural determination, the field of higher coordination polyhedra, even of light elements such as scandium and titanium, has become more than just an obscure curiosity.[63] It has severely challenged those chemists who deal principally in theory and it presents the possibility of challenging the present theories of bonding.

In recent years, with the advent and increased usage of x-ray and other instruments capable of structural determination, much information and data concerning the structure of polyhedra has been systematically compiled. Out of this steadily increasing store of information has come an order, in which groups and classes and certain requirements for polyhedra can be described. For instance, it has been found that chelates form more high coordination complexes than monodentate ligands. Chelates possessing oxygen and nitrogen donor atoms are well-suited because of the high electronegativities and small sizes of these ligand atoms. In addition,

ligands of phosphorus, arsenic and sulfur donor atoms are found to form many polyhedra of high coordination, but only with transition elements. The ligand size, or rather the distance or "bite" between the two donor atoms of a ligand, affects greatly its ability to form high coordination complexes. Such ligands as the tropolonate ion or the oxalate ion whose oxygen atoms are only about 2.58Å apart, make very good high-coordinating ligands. Ligands such as β-diketones are more flexible than tropolonate and oxalte ions and can more easily adjust to the requirements of the metal ion with the result that high coordination is not "forced" on the ion. A matrix of rigid bonding atoms such as the cyclopentadienyl ion also is a good example of a ligand which forces high coordination on a metal ion.

Probably, the area in which there is the greatest need for revising our thinking concerning bonding is in the requirements which the metal ion must possess in order to form high coordination polyhedra. The molecular orbital theory is incapable of predicting most cases. As an example, bonding in the octa-coordinated cube of a transition metal ion cannot be described using the valence bond theory since the best it can do is to supply seven orbitals, unless one resorts to f orbitals which is often inconsistent with observations.

At this point, it seems that the non-bonding repulsion model of Sidgwick and Powell[64] which was later extended by Gillespie and Nyholm[65] is probably the best rationale for predicting ground state geometries. There are some correlations, empirical in nature, which can be used to help predict or explain why certain ions form high coordination polyhedra and others do not. The metal-ion size-to-change ratio is a big factor. It can be shown that as the ratio of the ion size to charge increases, the coordination number also increases. In addition, the number of electrons in the d levels also has some bearing on the formation of high coordination polyhedra. Metal ions of d^o or d^x(x = 1 thru 10) electron configuration with x being low more readily form high coordination structures than do metal ions where x is high. This can be explained on the basis that the high x configuration offers fewer low-energy orbitals available for bonding. This explains why early elements of the transition series form more high coordinate polyhedra than the later and post-transition metal ions.

At this point, a word should be said about coordination number of a complex (or complexes) in the different physical states. To determine the configuration of a particular species in the gaseous state is theoretically desirable because it provides the species in

an unperturbed environment. As chemists, however, we probably would like to know what the species looks like in solution. More often than not, we are forced to determine the geometry of the species in the solid state. Solvation energies, lattic energies and various other energies are often larger than the re-organization energy of a species going from a seven- to an eight-coordinated species or vice-versa. If we are interested, then, in the geometry of a complex in solution, these facts make the thorough investigation of the geometry of the particular species very difficult.

In a recent series of five papers[66-70] by Muetterties and co-workers, a fairly detailed characterization of tropolone ion (T) complexes encompassing synthesis, structure and chemistry is presented.

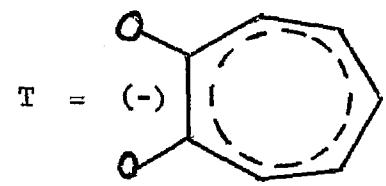

Of particular interest in this series of research papers is the question of molecularity and coordination number of the complex

polyhedra formed with the propolonate ion. Muetterties et al.[69] postulated that thorium and uranium(IV) formed complexes of coordination number ten, and these findings were strongly supported by the work of Selbin and Ortego[71]. Complexes of the tropolonate ion with scandium, yttrium, titanium, zirconium, hafnium, thorium, vanadium, niobium, tantalum, rare earth metals, indium, tin and lead were prepared by Muetterties[68]. Of equal importance was the finding that many of these unusually high-coordinated complexes also exhibit unusual molecularity which is associated with the high coordination number. In an effort to describe the high coordination number and the polymeric nature of these tropolonate complexes, Muetterties hypothesized the three-coordinated bridging oxygen. He states that many of the tropolonate complexes which might otherwise be thought of as six-coordinated complexes, have some of the chelate oxygens shared by more than one metal ion with the result that they do not form discrete six-coordinated complexes. He is thus able to explain the nature of the bonding in polymeric tropolonate complexes of Ni(II) and Co(III). One of the outstanding characteristics of these polymeric tropolonate complexes is their very low solubility in common solvents. The low solubility of these complexes makes reliable molecular weight determination almost impossible.

To pursue further the question of molecularity and coordination number put forth by Muetterties and others, particularly as it concerns the VO^{2+} species, two new complexes, VOT_2 and $VOT_2 \cdot py$ were prepared. A third complex $VO(S)_2$ {i.e., $VO[(C_6H_5)N_2C_2S_3]_2$}, which had earlier been prepared as a new complex (preparation described on page 26), was found to possess many of the same characteristics as the polymeric tropolonate complexes of Muetterties; therefore, its geometry was also investigated.

B. EXPERIMENTAL

1) Preparation of New Compounds

a) Preparation of VOT_2: Tropolone (4.8 g. 0.040 mole) was dissolved in 100 ml of 95% methanol and $VOSO_4 \cdot 4H_2O$ (4.7 g; 0.02 moles) was dissolved in 300 ml of water. The two solutions were mixed and an immediate gray precipitate was produced. The precipitate was filtered, washed well with water and methanol, and dried under vacuum. Recrystallization is possible from $CH_2C\ell_2$, but not convenient because of the very slow rate of dissolution in this solvent.

Analysis: Found: %C = 54.71, %H = 3.49. Calculated for $VO(C_7H_5O_2)_2$ is %C = 54.37, %H = 3.26.

b) Preparation of $VOT_2 \cdot py$: To a quantity of VOT_2, enough pyridine was added to dissolve the complex and produce a red-green solution. To the dark solution was added petroleum ether until a brown-red precipitate was formed. The precipitate was filtered, washed with petroleum ether, $CC\ell_4$, then again with petroleum ether.

Analysis: Found: %C = 58.88, %H = 4.35. Calculated for $VO(C_7H_5O_2)_2 \cdot C_5H_5N$: %C = 58.76, %H = 3.89.

c) Preparation of VOS_2: Preparation of VOS_2 is given on page 26 of Chapter I.

2) Spectral and Other Measurements

a) Molecular Weight Determination: The molecular weight determination of VOT_2 was made in $CH_2C\ell_2$ using a Mechrolab vapor pressure osmometer Model 302. A quantity of 0.0284 g. of VOT_2 was dissolved in 25 ml $CH_2C\ell_2$ to give 0.00037 M. solution (limit of VOT_2 solubility in $CH_2C\ell_2$ after four days dissolution period). The recommended concentration limits for accurate determinations on the vapor pressure osomometer are between 0.005 and 0.1 M. The solubility limit of VOT_2, therefore, places doubt on the outcome of the molecular weight determination. $VO(aca)_2$ was used as a calibration standard. Because of its very low solubility, no molecular weight determination could be made on VOS_2.

b) NMR Spectra: The NMR spectra were recorded on a Varian A60-A NMR Spectrometer. A special coaxial tube purchased from Wilmad Glass Company, Buena, New Jersey, was used to make the NMR spectra. The coaxial tube contains a small diameter tube centered inside a large diameter tube. A mixed solvent of $CH_2C\ell_2$ and DMSO was placed in the center tube and a solution of VOT_2 in the mixed solvent was placed in the annulus formed by the small and large tubes. The spectra were recorded at the small sweep with 50 cps

in order to spread ou the $CH_2C\ell_2$ peak in the diamagnetic solution from the $CH_2C\ell_2$ peak of the paramagnetic solution. Mixed solvents with volume concentration of $CH_2C\ell_2$/DMSO which were used were 90/10, 75/25, 50/50, 25/75 and 10/90.

FIGURE 11a--NMR spectrum of the $CH_2C\ell_2$ peaks in a solution of 50/50 $CH_2C\ell_2$/DMSO and VOT_2 recorded in a special coaxial tube. (This spectrum is typical of the other four spectra recorded to make FIGURE 11b).

FIGURE 11b--The magnetic susceptibilities of VOT_2 in varying amounts of $CH_2C\ell_2$/DMSO determined by the method of Evans.[46]

No magnetic susceptibility of VOS_2 in solution was made because of its low solubility in all solvents investigated.

c) Optical Spectra: The optical spectra were recorded on a Cary 14 Spectrophotometer. One cm matched quartz cells were used to record the spectra of VOT_2 in pyridine and VOT_2 in $CH_2C\ell_2$ (which was allowed four days to dissolve). Five cm cells were used to record the spectra of a fresh sample of VOT_2 in $CH_2C\ell_2$, VOS_2 in benzene and VOS_2 in pyridine. Both VOT_2 and VOS_2 were run as mulls in nujol on filter paper. The spectra were recorded from 10,000Å

(10,000 cm^{-1}) to 3,500Å (28,570 cm^{-1}).

FIGURE 12a--The optical spectrum of VOT_2 in pyridine.

FIGURE 12b--The optical spectrum of VOT_2 in nujol mull.

FIGURE 12c--The optical spectrum of VOT_2 in $CH_2C\ell_2$ (freshly prepared).

FIGURE 12d--The optical spectrum of VOT_2 in $CH_2C\ell_2$ (requiring a four day dissolution time).

Data from the above (FIGURES 12a-12d) have been summarized in Table XII.

FIGURE 13a--The optical spectrum of VOS_2 in pyridine.

FIGURE 13b--The optical spectrum of VOS_2 in nujol mull.

FIGURE 13c--The optical spectrum of VOS_2 in benzene.

Data from the above (FIGURES 13a-13c) have been summarized in Table XIII.

d) IR Spectra: The IR spectra were recorded on a Beckman IR-7 Spectrophotometer in the $NaC\ell$ region.

FIGURE 14a--VOT_2 was mulled in nujol and the IR spectrum was recorded between $NaC\ell$ plates.

FIGURE 14a--$VOT_2 \cdot py$ was mulled in nujol and the IR spectrum was recorded between NaCℓ plates.

e) Magnetic Moment Determination: The magnetic susceptibilities of solid VOT_2 and solid VOS_2 were determined by the Gouy method using an Ainsworth type BCT balance with a model AL7500 electromagnet produced by Alpha Scientific Lab., Inc. $VO(aca)_2$ was used as a calibration standard.

f) ESR Spectra: The ESR spectra of all samples were recorded on a model JES-3BX, X band spectrometer produced by Japan Electron Optics Laboratory Co., Ltd. All spectra were recorded at ambient temperature.

FIGURE 15a--The ESR spectrum of VOT_2 was recorded in $CH_2C\ell_2$ as a solvent.

FIGURE 15b--The ESR spectrum of VOT_2 was recorded in a sample diluted by tropolone ligand, as a dilute suspension in nujol mull and in a solution of cyclohexanol.

FIGURE 16a--The ESR spectrum of VOS_2 was recorded in a benzene solution.

FIGURE 16b--The ESR spectrum of VOS_2 was recorded as a solid diluted in the potassium salt of the organic ligand.

C. THEORY

1) Magnetic Moment - Gouy Method

A theoretical treatment of magnetic susceptibility can be found in a number of texts[72,73]. A more descriptive but less theoretical treatment is given by Drago[23]. To give adequate coverage to the theoretical treatment of magnetic susceptibility would require more space than can be justified in this dissertation; therefore, only a brief description of the procedures used to derive the magnetic susceptibilities and the relevant equations will be given.

The experimental determination of magnetic properties does not involve direct measurement of the magnetic moment, μ, but instead measurement of the magnetic susceptibility, χ, from which the moment is calculated. This is done by suspending a cylindrical sample of cross section A in a magnetic field so that one end of the sample is at the high intensity of the field H (center of the magnetic poles) while the other end of the sample projects above the magnetic poles to where the field H_o is almost negligible. The force acting on the sample is then given by the relation

$$F = \tfrac{1}{2}A(H^2 - H_o^2)(K-K') + S \qquad \ldots.15$$

where K is the magnetic susceptibility of the sample per unit volume, K' is the magnetic susceptibility of the atmosphere per unit volume and S is the force due to the sample tube alone. K' falls well within the limits of accuracy of most measuring equipment and in most cases can be ignored. Since the cross-section of the sample is uniform, the factor $\frac{1}{2}A(H^2-H_o^2)$ may be treated as a constant. Since the gram susceptibility is related to the volume susceptibility by a constant, the density (i.e., $\chi_g = \frac{K}{d}$), then Eq.15 becomes

$$10^6\chi_g = \frac{\beta F'}{w} \qquad \ldots.16$$

where χ_g is the gram susceptibility, w is the weight of the sample in grams, β is the tube calibration constant and F' = F-S. One normally finds the constant β by measuring F on a sample whose magnetic moment μ is known. Then from Eq.16

$$\mu_{eff} = 2.84(T \underline{x} \chi_M^{corr})^{\frac{1}{2}} \qquad \ldots.17$$

one can determine the corrected molar susceptibility χ_M^{corr}. By adding the Pascal's constants to χ_M^{corr} (see ref.72) one determines the χ_M (uncorrected for diamagnetism of the complex). The uncorrected

χ_M is then used to find the gram susceptibility χ_g from the relation

$$\chi_M = \chi_g M \qquad \ldots.18$$

where M is the molecular weight of the complex. The calibration constant for the tube, β, can then be found from Eq.15. The reverse process is then used to find the magnetic moment, μ, for a new complex. The constant, β, for the sample tube was determined by using $VO(aca)_2$ since its magnetic moment and other properties are most like the properties of the new complexes, VOT_2 and VOS_2.

2) Magnetic Moment - NMR Method

One criteria by which Meutterties determined complexes of tropolone to be polymeric was their very low solubility in non-polar solvents. VOT_2 and VOS_2 exhibit very low solubility in $CH_2C\ell_2$ and other inert solvents. Since the monomers, VOT_2 and VOS_2, are expected to be paramagnetic (a d^1 system), the magnetic susceptibility of their solutions could be a measure of the degree to which the complexes polymerize; that is, the polymer may provide a mechanism by which unpaired electrons can pair up. The conventional Gouy method of determining the magnetic moment in solution does not lend itself to this type of determination because of the very low

concentration of the paramagnetic ion in solution. Evans[46], however, has demonstrated a method which is well-suited for the determination of magnetic susceptibility of a paramagnetic ion of low concentration in solution. The method employs the use of proton NMR spectra. The chemical shifts from a pure reference of an uncoordinated reference molecule (either the solvent molecule or a molecule added to the solution) in solution caused by the paramagnetic substance may be given by the theoretical expression:

$$\frac{\Delta H}{H} = \frac{2\pi}{3} \Delta K \qquad \ldots.19$$

where ΔK is the change in volume susceptibility. The more useful Eq.19

$$\chi = \frac{3\Delta f}{2\pi f M} + \chi_o + \frac{\chi_o (d_o - d_s)}{M} \qquad \ldots.20$$

can be used to determine the mass susceptibility, χ, of the paramagnetic ion in solution directly from the chemical shift Δf. The quantities, f = resonate frequency of the proton (60 Mc), m - mass of substance in 1 ml of solution, χ_o = the mass susceptibility of the solvent, d_o = density of the solvent, d_s = the density of the solution, are all easily determinable. Frei and Bernstein[74] have determined that

this method will approach the classical Gouy method in accuracy if the pitfalls given by Benson and Phillips[54] are avoided. This method was used to determine the magnetic moment of $VO(aca)_2$ in $CH_2C\ell_2$ at 40°C. The μ_{eff}^{corr} was found to be 1.77 BM, very close to the balue of 1.73 found for the solid[47]. The slightly high value is probably due to a combination of solution and temperature effects.

3) Electron Spin Resonance

The extensive scope of electron spin resonance (ESR) precludes a comprehensive presentation of the subject here but a brief descriptive understanding of the principles of ESR is necessary to appreciate parts of the chapter. For a more thorough understanding of ESR, the reader is advised to consult references 75-77.

ESR is a branch of absorption spectroscopy in which microwave radiation is absorbed by the unpaired electron spin of a paramagnetic species. An electron has a spin S of ½ and its spin angular momentum quantum number can have values of $m_s = \pm\frac{1}{2}$. In the absence of a magnetic field, the spin states are degenerate but in a magnetic field the degeneracy is resolved with a lower energy level corresponding to $m_s = -\frac{1}{2}$ and the higher energy level corresponding

to $m_s = +\frac{1}{2}$.

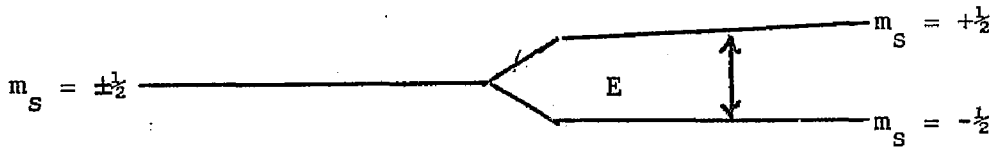

A transition between the two different energy levels occurs in a magnetic field when an electron in the state $m_s = -\frac{1}{2}$ absorbs energy of $h\nu = E$. This relation is also written:

$$E = h\nu = g\beta H_o \qquad \ldots.20$$

where h is Planck's constant, ν is the frequency of radiation, β is the Bohr magneton, H_o is the field strength of the magnetic field and g is the Lande splitting factor, a proportionality constant between the magnetic moment and the magnetic moment of an unbound electron. The quantity g is not a constant but a tensor quantity whose value depends upon the orientation of the molecule containing the unpaired electron with respect to the magnetic field. Because of its freedom of motion in the solution and gas phase, the g value is averaged over all orientations but in a crystal, movement is

restricted. The g value is also singular in a perfectly cubic crystal site and, thus is independent of crystal orientation; the g value is said to be isotropic. In a crystal site of lower symmetry, the g value depends upon the orientation of the crystal and is said to be anisotropic. In this case, two g values, $g_{||}$ which is usually taken to be parallel with the major molecular axis, and $g_{\perp}$, which is the axis perpendicular to $g_{||}$, are most often referred to. They are related to the average g value by

$$g^2 = \frac{1}{3}g_{||}^2 + \frac{2}{3}g_{\perp}^2 \qquad \ldots.21$$

If one were to record the absorption energy vs the field strength, one would find a peak similar to that found in an NMR spectrum (a). Most spectra, however, are usually recorded as the

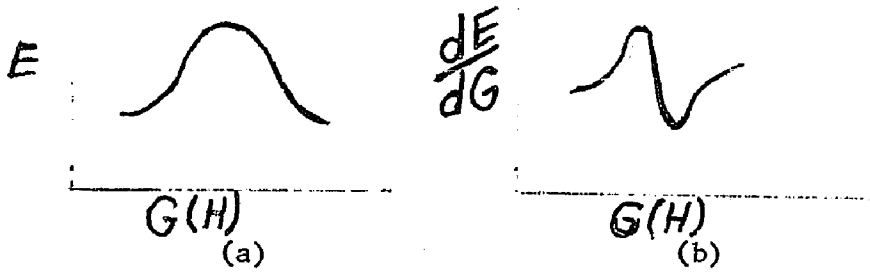

first derivative of the absorption curve against the field strength. For a single unpaired electron, the spectrum would look like (b). If, however, an unpaired electron is in the vicinity of a nucleus with spin I, an interaction takes place which causes the absorption signal to be

split into 2I+1 components. The cause of this splitting is the nuclear spin-electron spin coupling arising mainly from the Fermi contact term of the spin Hamiltonian. As an example, if one were to record the spectrum of a VO^{2+} complex, one would naturally expect to witness an eight line spectrum since the nuclear spin of ^{51}V for this d^1 complex is $\frac{7}{2}$ (number of lines = 2I+1 = $2\frac{7}{2}$ + 1 = 8). The origin of these lines may be seen to arise from the following energy level scheme:

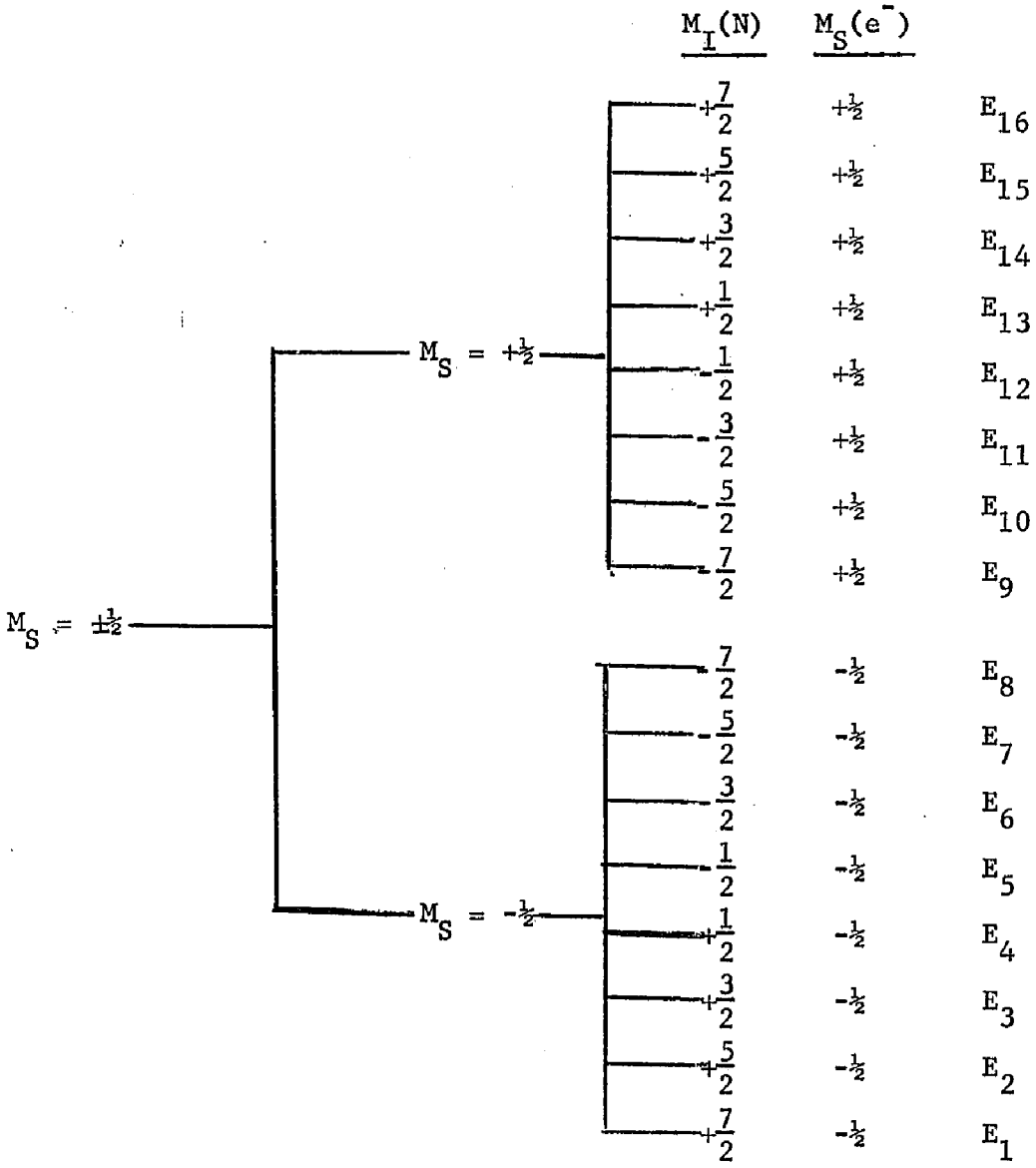

The selection rule permits transitions with $\Delta M_s = \pm 1$ and $\Delta M_I = 0$; thus, one can see that only eight lines are expected. The energies of each level are given by the relation:

$$E_{(M_S, M_I)} = g\beta H M_s + A M_s M_i \qquad \ldots.22$$

where A is the electron spin-nuclear spin coupling constant. Thus, the allowed transition energies between the various energies E_1-E_{16}, etc. can be calculated from the relation:

$$E_{16}-E_1 = [g\beta H(\tfrac{1}{2})+(+\tfrac{7}{2})(+\tfrac{1}{2})A] - [g\beta H(-\tfrac{1}{2})+(+\tfrac{7}{2})(-\tfrac{1}{2})A]$$

or

$$\Delta E = g\beta H + \tfrac{5}{2}A \qquad \ldots.23$$

There sometimes arises the case where the unpaired electron is delocalized over more than one equivalent nucleus whose nuclear spins are greater than $\frac{1}{2}$. A possibility might be an unpaired electron delocalized over two vanadium atoms which are tied together by an organic matrix. Through a diagram similar to the energy level diagram shown on page 128, one can see that the number of lines expected could be determined by the relation 2nI+1.

Applying this to the case of the two vanadium atoms, one would expect to observe fifteen lines.

D. RESULTS AND DISCUSSION

1) Solubility

The solubility of VOT_2 in inert solvents such as benzene, $CHC\ell_3$ and $CH_2C\ell_2$ was found to be very low. The solubility was quite low in CH_3OH, but in pyridine, the complex was found to be very soluble. The solubility of VOT_2 in $CH_2C\ell_2$ increased with time. It was found that up to 0.028 g. of VOT_2 would dissolve in 25 ml $CH_2C\ell_2$ in a four day period.

The solubility of VOS_2 was extremely low, not only in inert solvents such as benzene, $CHC\ell_3$ and $CH_2C\ell_2$, but also in more polar ligating solvents such as CH_3OH, THF (tetrahydrafuran), DMSO (dimethylsulfoxide) and pyridine. Very little difference in solubility was observed between $CH_2C\ell_2$ and pyridine.

As a result of their extensive work on complexes of the tropolonate ion, Muetterties *et al.*[70] proposed that the solubility of these complexes in common solvents be one of the main criteria for determining whether the tropolonate was, in fact, a polymer in the solid state. VOT_2 meets the requirements of Muetterties for being a polymer. The tropolonate complexes polymerize to dimers, trimers or higher polymers by forming three-centered bridging oxygen bonds, using the tropolonate ion oxygens. If the criteria

for predicting polymerization is valid and polymerization takes place through three-centered oxygen bonds, then VOT_2 must be at least seven-coordinated, if not greater.

No extensive work, similar to that on the tropolonate ion, has been done with the 5-mercapto-3-phenyl-1,3,4-thiadiazole-2-thion ion, but we can assumed for the moment that the low solubility of its VO^{2+} complex results from the same polymerization requirements porposed for VOT_2.

2) Molecular Weight Studies

The molecular weight determination of VOT_2 yielded a value of approximately 390. The molecular weight for the monomer is calculated to be 309. Due to the low solubility of VOT_2, the determination was made at about one-tenth the concentration recommended by the instrument manufacturer as the minimum concentration required. Although this determination indicates some polymerization in $CH_2C\ell_2$ solution, the results are very uncertain because of the too low concentration. No attempt was made to make a molecular weight determination on VOS_2 since its solubility was even lower than that of VOT_2.

3) NMR Spectra

In an attempt to determine if VOT_2 showed some evidence of polymerization in an inert solution, the method of Evans[46], described earlier, was used to determine the magnetic moment of VOT_2. In order to get sufficient VOT_2 dissolved into $CH_2C\ell_2$, the mixture was allowed to dissolve for four days. The NMR spectrum of this solution showed very little paramagnetic character since only line broadening was observed. Calculations show (assuming $\mu_{eff} = 1.75$ BM) that the $CH_2C\ell_2$ peak of the diamagnetic solution should be split form the $CH_2C\ell_2$ peak of the paramagnetic solution by an easily observable splitting ($\sim$0.7 cps). The optical spectrum showed that the solution might have oxidized since the d-d bands were either severely shifted or they were missing entirely. It thus seemed likely that the long dissolution process was in some way connected with an oxidation mechanism. Enough of the VOT_2 could be dissolved in solution, unaffected by oxidation, to record its optical spectrum in the longer 5 cm cells, but within 24 hours, all of the d-d bands exhibited by the fresh solution had disappeared. The solution of VOT_2 in pyridine was shown to be reasonably unaffected by oxidation for a matter of days. A new complex, $VOT_2 \cdot py$ was isolated from a pyridine solution of VOT_2. The stability of VOT_2 in pyridine leads the author to

conclude that the oxidation mechanism takes place at the sixth position and that pyridine, or some other polar molecule, can serve effectively to block the sixth position attack, at least for a period of time.

With the above in mind, a series of five solutions made up from dimethylsulfoxide (DMSO) and $CH_2C\ell_2$ whose volume fractions ranged from 0.9 DMSO/0.1 $CH_2C\ell_2$ to 0.1 DMSO/0.9 $CH_2C\ell_2$ were prepared. It was found that sufficient VOT_2 could be dissolved rapidly in these solutions so that the magnetic susceptibility of VOT_2 could be determined by the NMR method. A representative NMR spectrum of one of these solutions is found in Figure 11a and the results of these determinations are shown on the graph in Figure 11b. The μ_{eff} ranges from 1.82 BM in 0.9 DMSO/0.1 $CH_2C\ell_2$ to 0.94 BM in 0.1 DMSO/0.9 $CH_2C\ell_2$. The straight line extrapolation out to pure $CH_2C\ell_2$ solution shows that VOT_2 should have μ_{eff} of about 1.1 BM in pure $CH_2C\ell_2$. This is in close agreement with the magnetic moment of μ_{eff} = 1.21 determined for VOT_2 by the Gouy method. (The Gouy procedure and its results will be discussed in detail later).

In order for the above procedure to have validity, one could make two assumptions. First, one could assume an equilibrium

Figure 11a

The proton NMR spectrum of $CH_2C\ell_2$ in a coaxial set of tubes containing a solution of DMSO/$CH_2C\ell_2$ in the inner tube (peak A) and a solution of VOT_2 in DMSO/$CH_2C\ell_2$ in the annulus.

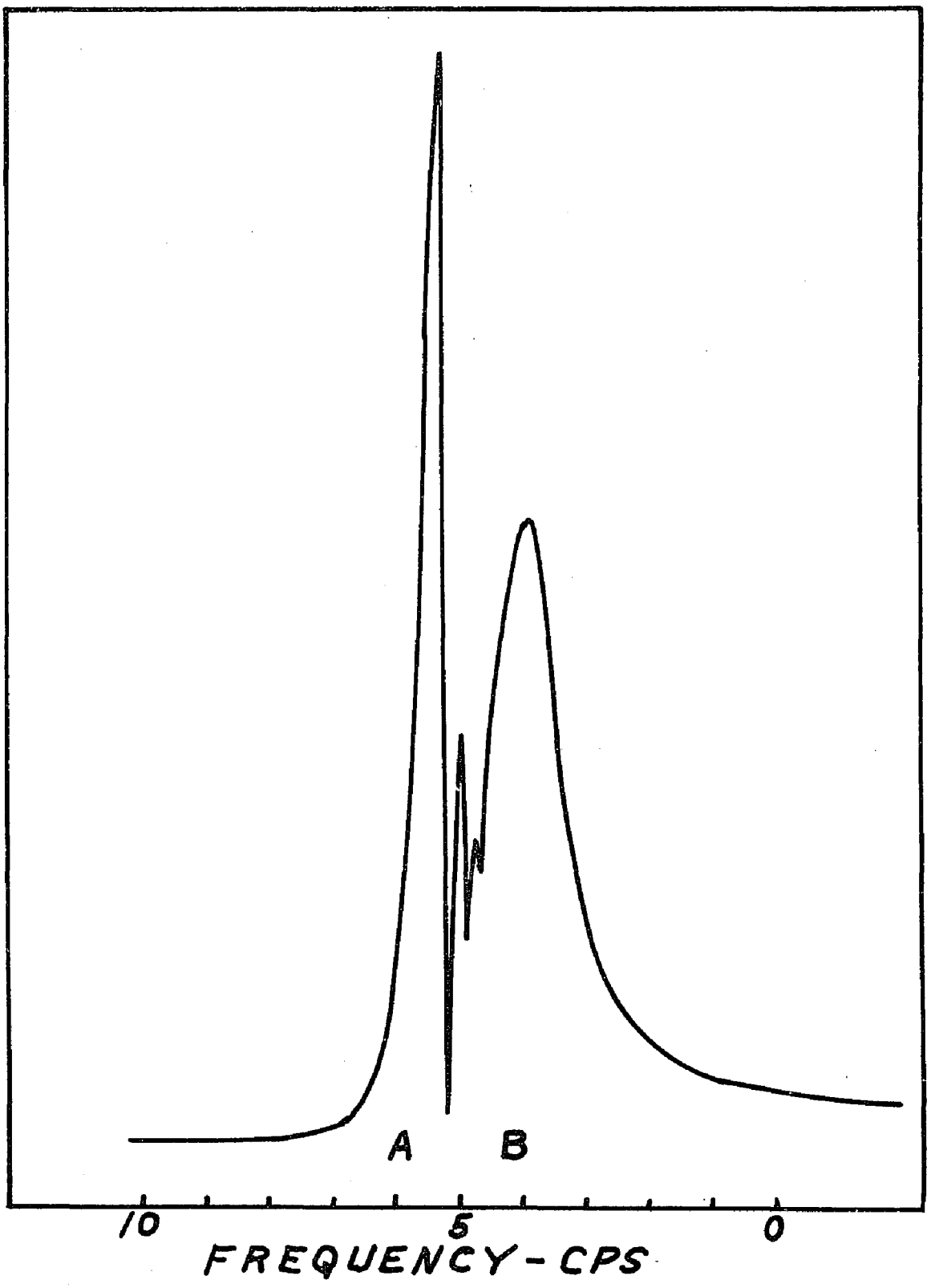
A
B
10
5
0
FREQUENCY - CPS

Figure 11b

Magnetic moment (μ_{eff}) of VOT_2 in a mixed solution of $CH_2C\ell_2$/DMSO as a function of increasing $CH_2C\ell_2$ concentration.

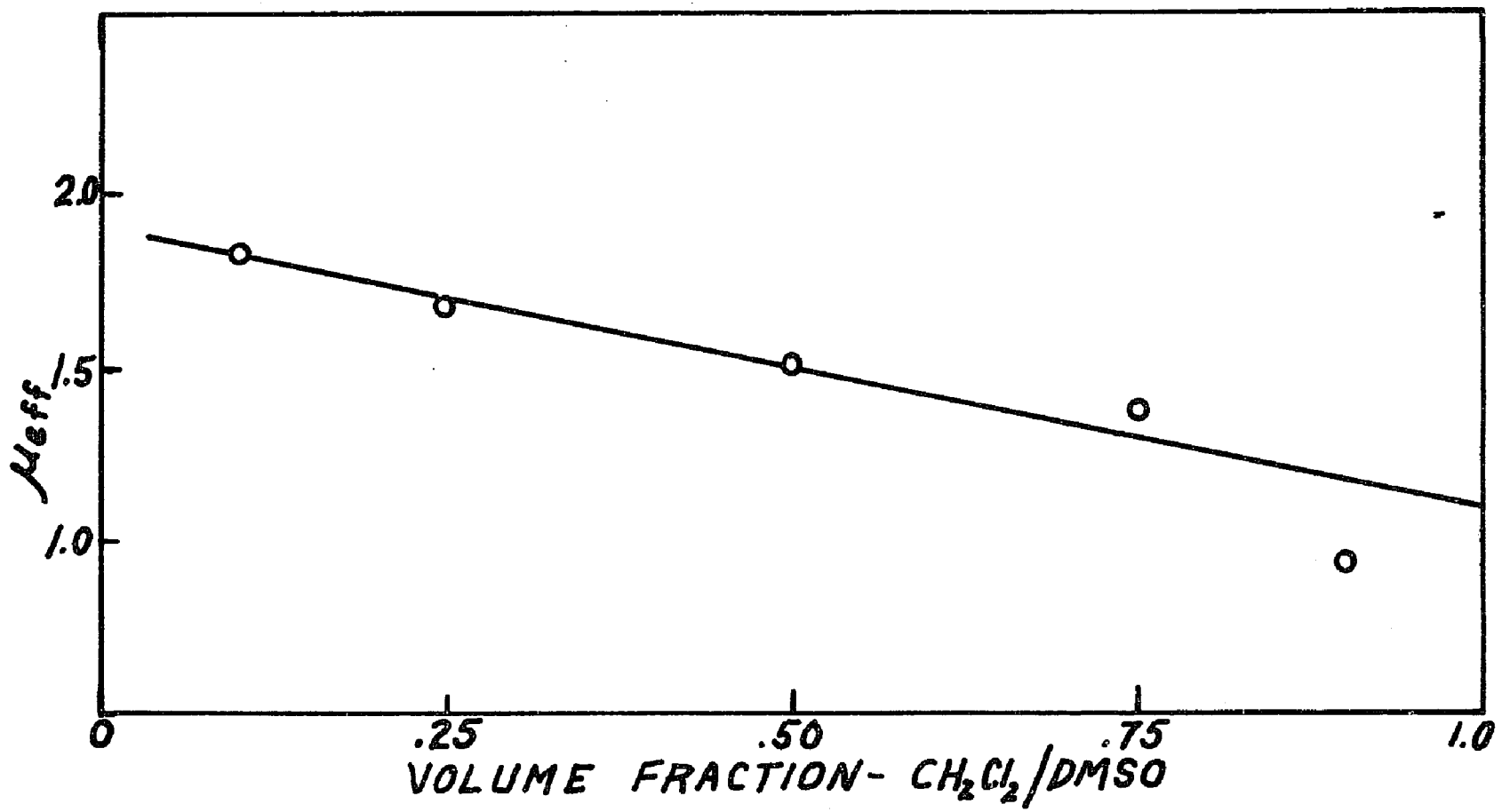
2.0
1.5
1.0
μ_{eff}
0
.25
.50
.75
1.0
VOLUME FRACTION- CH_2Cl_2/DMSO

in solution similar to:

$$a\ VOT_2 \cdot DMSO \rightleftarrows a\ VOT_2 + a\ DMSO$$

$$\Updownarrow$$

$$(VOT_2)_a$$

Thus, at zero volume fraction of DMSO there should exist in equilibrium the monomar and polymer of VOT_2 which would be reflected by the average magnetic susceptibility of the solution. The second assumption is that the average resident time of the DMSO in the sixth position limits the amount of oxidation taking place so that all (or most) of the VOT_2 in solution is unoxidized when the NMR spectra are recorded. As a precaution, only one sample was made up at a time and not over ten minutes was allowed to elapse before the NMR spectrum was recorded. Although some oxidation took place, the amount was probably not sufficient to invalidate the findings of Figure 11b, which clearly indicates that some polymerization must be taking place in $CH_2C\ell_2$ solutions.

4) Optical Spectra

The optical spectra of VOT_2 were recorded in various media and portions of these spectra are shown in Figure 12a-12d. A

Figure 12a

The electronic spectrum of VOT_2 in a solution of pyridine recorded between 10,000 cm^{-1} and 25,000 cm^{-1}.

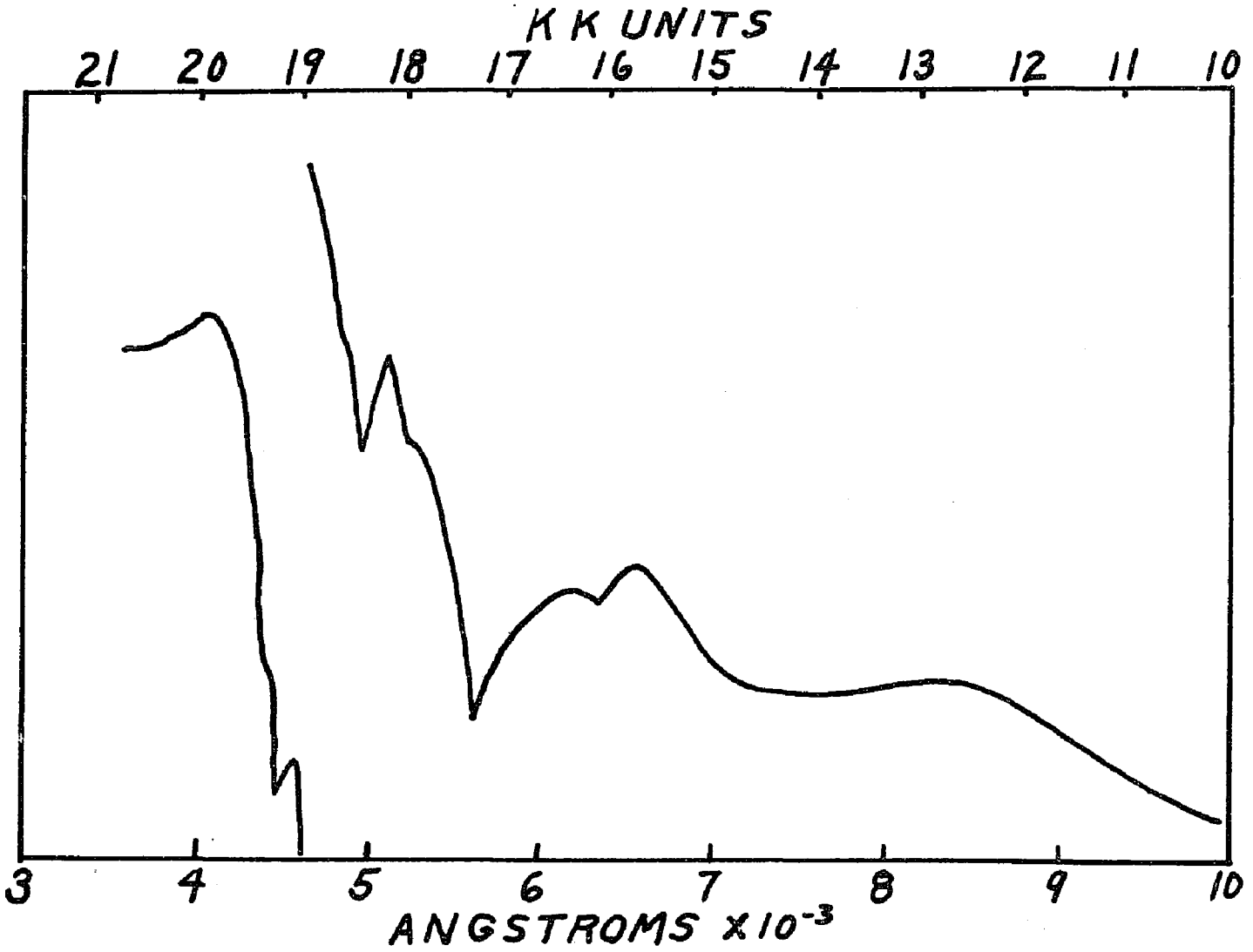
KK UNITS
21 20 19 18 17 16 15 14 13 12 11 10
3 4 5 6 7 8 9 10
ANGSTROMS X10⁻³

Figure 12b

The electronic spectrum of VOT_2 in nujol mull recorded between 10,000 cm^{-1} and 25,000 cm^{-1}.

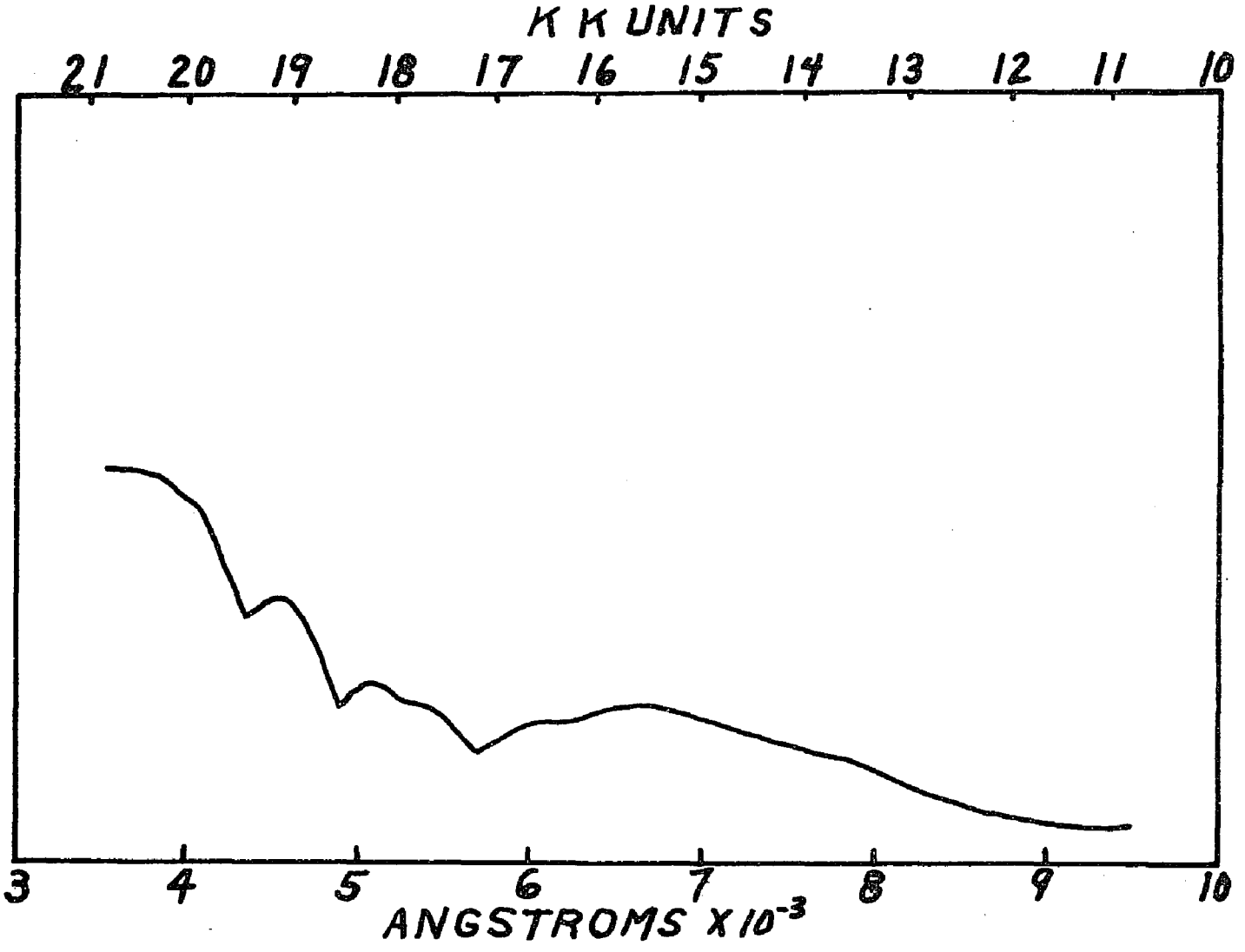
KK UNITS
21 20 19 18 17 16 15 14 13 12 11 10
3 4 5 6 7 8 9 10
ANGSTROMS X 10⁻³

Figure 12c

The electronic spectrum of VOT_2 in a solution of $CH_2C\ell_2$ recorded between 10,000 cm^{-1} and 25,000 cm^{-1}.

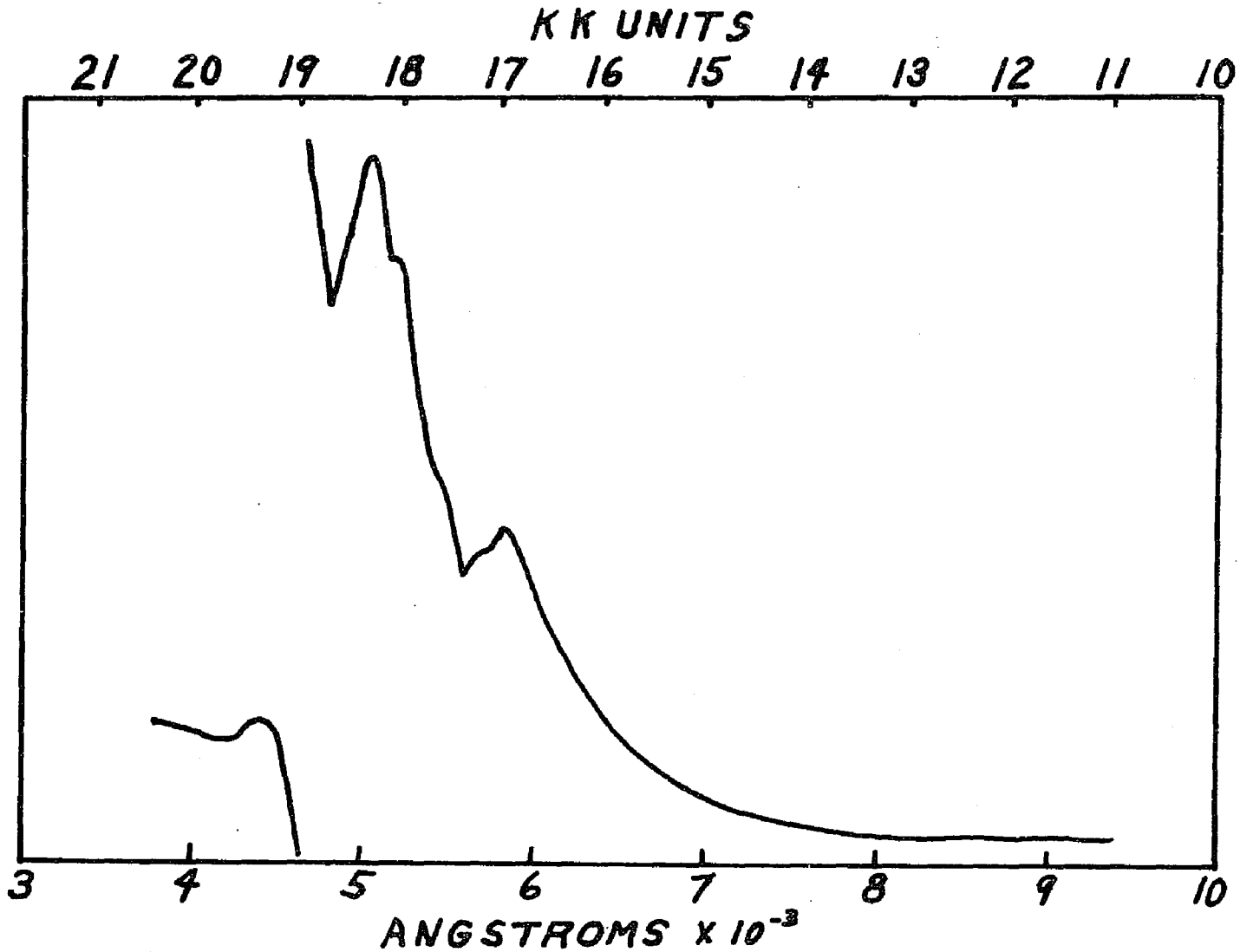
KK UNITS
21 20 19 18 17 16 15 14 13 12 11 10
3 4 5 6 7 8 9 10
ANGSTROMS X 10⁻³

Figure 12d

The electronic spectrum of VOT_2 which required four days in which to dissolve in $CH_2C\ell_2$. The spectrum was recorded between 10,000 cm^{-1} and 25,000 cm^{-1}.

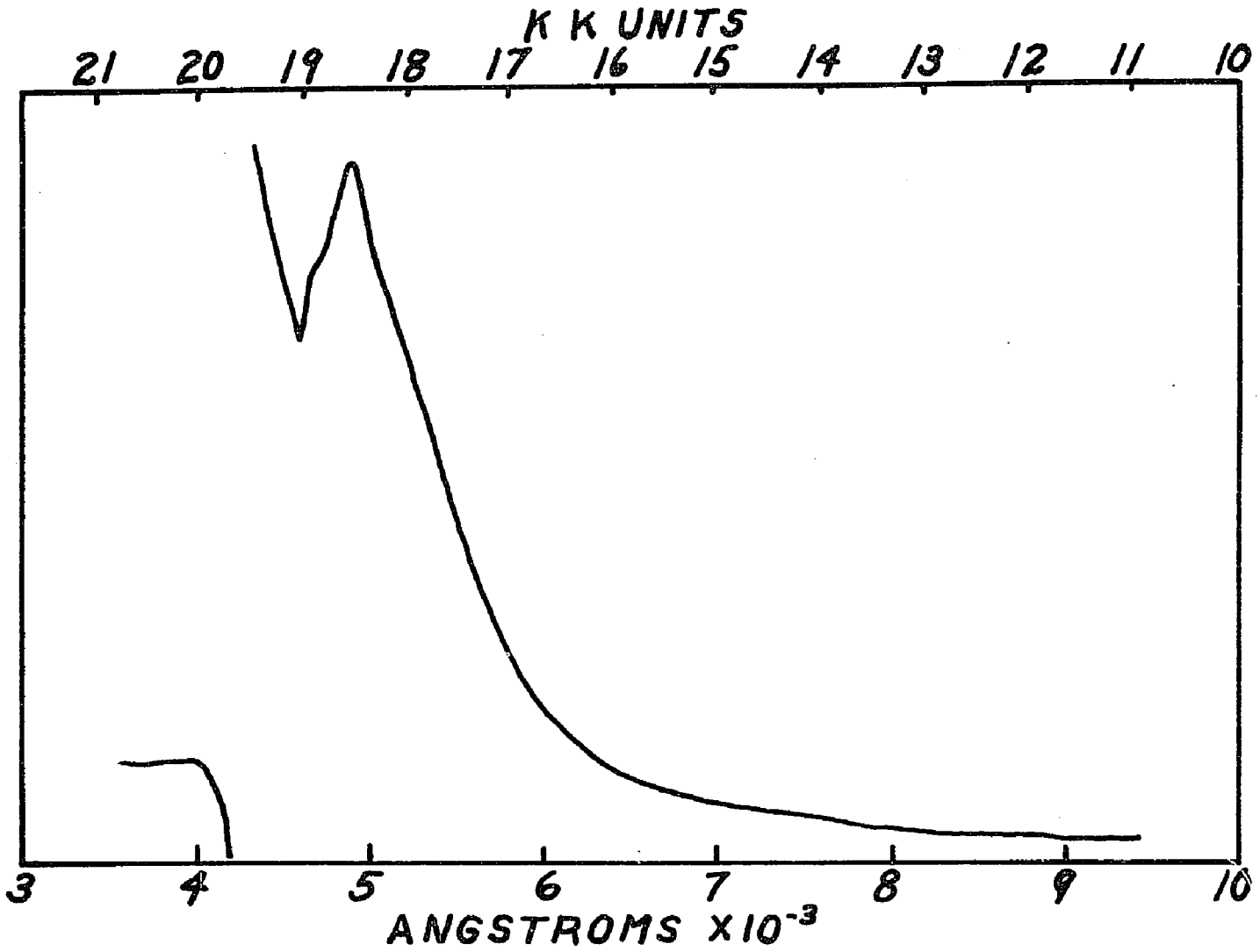
K K UNITS
21 20 19 18 17 16 15 14 13 12 11 10
3 4 5 6 7 8 9 10
ANGSTROMS X10⁻³

summary of the optical spectral data is given in Table XII.

Probably the most interesting aspects of Table XII are the energies for band 1, found for VOT_2 in nujol mull and in pyridine, and the fact that four bands (1-4) lie below 19,300 cm^{-1}. Relatively few references[3] have reported bands for VO^{2+} complexes down as low as 12,000 (band 1, VOT_2 in pyridine) but even fewer have reported four bands below 19,300 cm^{-1}. If one looks at the spectra data for vanadyl tropolonate which is assumed to have oxidized in $CH_2C\ell_2$, Table XIId, one can see that four bands (bands 5-8) appear above 19,300 cm^{-1} which have comparable shapes and positions to bands 5-8 recorded for VOT_2 in pyridine, nujol mull and $CHC\ell_3$. If bands 5-8 for the oxidized vanadyl tropolonate (a d^0 system) result from transitions which do not involve the excitation of the d^1 electron located in the b_2 VO^{2+} orbital (a similar hypothesis for the oxidation of $VO(aca)_2$ in solution is made by McGlynn et al.[53] to aid in the location of d-d bands), then it is possible that the four bands 1-4, found for VOT_2 in nujol mull and pyridine result from d-d transitions. The recent paper by Vanquickenborne and McGlynn[53] supports this possibility. Their semi-empirical MO calculations for $VOSO_4 \cdot 5H_2O$ give the following transitions below

19,300 cm^{-1}: $e_\pi \rightarrow b_2$, $a_1 \rightarrow b_2$, $b_2 \rightarrow e^*_\pi$. They place the $b_2 \rightarrow b_1^*$ ($xy \rightarrow x^2-y^{2*}$) transition somewhat higher than 19,300 cm^{-1} but are reluctant to assign it firmly since it should be quite sensitive both to the bond length and bond angle of the equatorial ligands attached to the VO^{2+} ion. In addition, ESR measurements suggest that this transition lies lower than their calculations have placed it. The spectrum of VOT_2 in $CH_2C\ell_2$ (prior to oxidation) is similar to VOT_2 in pyridine with two noticable exceptions. First, the peak at 12,000 cm^{-1} (band 1) found in pyridine solution has completely disappeared and secondly, bands 2 and 3 found at 15,380 cm^{-1} and 16,000 cm^{-1} in the pyridine solution have shifted to higher energies of 17,240 cm^{-1} and 17,540 cm^{-1}. No good explanation can be found for the disappearance of band 1 in the $CH_2C\ell_2$ solution. Band 1 is assigned as the $e^b_\pi \rightarrow b_2$ transtion which is the same assignment given the first band appearing the McGlynn-Vanquickenborne energy scheme for $VOSO_4 \cdot 5H_2O$. The shifting of bands 2 and 3, however, support the assignments made above that these bands are transitions $a_1 \rightarrow b_2$ and $b_2 \rightarrow e^*_\pi$. The more polar pyridine molecule attaches itself to the sixth position trans to the vanadyl oxygen; and, in doing so, it reduces the bond order of the V≡O (see also, infrared data for differences between $\nu(V\equiv O)$ for VOT_2 and $VOT_2 \cdot py$). In

doing so, the a_1 (d_{z2}) is raised in energy causing a lowering of the band 2 energy for the VOT_2 in a polar solvent. Since the $b_2 \rightarrow e^*_\pi$ involves transition to essentially d_{xz} and d_{yz} metal orbitals, these orbitals are likewise affected in a polar medium which results in the observed shift for band 3. The fourth band, band 4, shifts in a direction opposite that of bands 2 and 3. Since the tentative assignment above for band 4 was given as $b_2(d_{xy})$ to $b_1^* d_{x2-y2}$, then either the latter orbital must be lowered or the former orbital must be raised in energy in a polar solvent. Since it is known that VO^{2+} complexes of this type are square pyramidal, in which the equatorial ligands form angles of about 102^o with the major axis of rotation, it is very probable that these equatorial ligands, displaced downward from a position expected in an octahedral arrangement, expose the almost non-bonding d_{xy} orbital to the influence of a molecule such as pyridine. The effect is that the d_{xy} orbital is raised closer to the d_{x2-y2}^* orbital thus shifting band 4 to lower energy.

The above is by no means a firmly established assignment of the d-d transitions in VOT_2; this will require much more additional study. Enough unusual evidence, however, has been presented to warrent a closer look at the optical spectrum of VOT_2.

There does not appear to be any evidence in the observed optical spectra to support the proposition that VOT_2 is a polymer either in the solid state or in solution since all the transition shifts can be explained by previously reported calculations and other rationales.

The optical spectra of VOS_2 were recorded in pyridine, benzene and nujol mull between 10,000Å and 4000Å. These spectra are shown in Figure 13a, 13b and 13c and a summary of the bands is given in Table XIII. No attempt was made to analyze the origin of these peaks.

There is, however, one very important bit of information to be gained from the data given in Table XIII. If one compares the data in Table XIII, one can see that there is no appreciable shift of the bands when the solvent is changed from the non-polar benzene to the very polar pyridine solvent. Since some of these bands are obviously d-d transitions whose positions in the spectra have been shown by Selbin and Ortolano[78] to be highly dependent upon solvent attack on the sixth position, one would expect a much greater effect than was observed. One could conclude that the sixth position was very little affected when the solvent was changed from benzene to pyridine. If this is so, one must conclude that the

Figure 13a

The electronic spectrum of VOS_2 in a solution of pyridine recorded between 10,000 and 25,000 cm^{-1}.

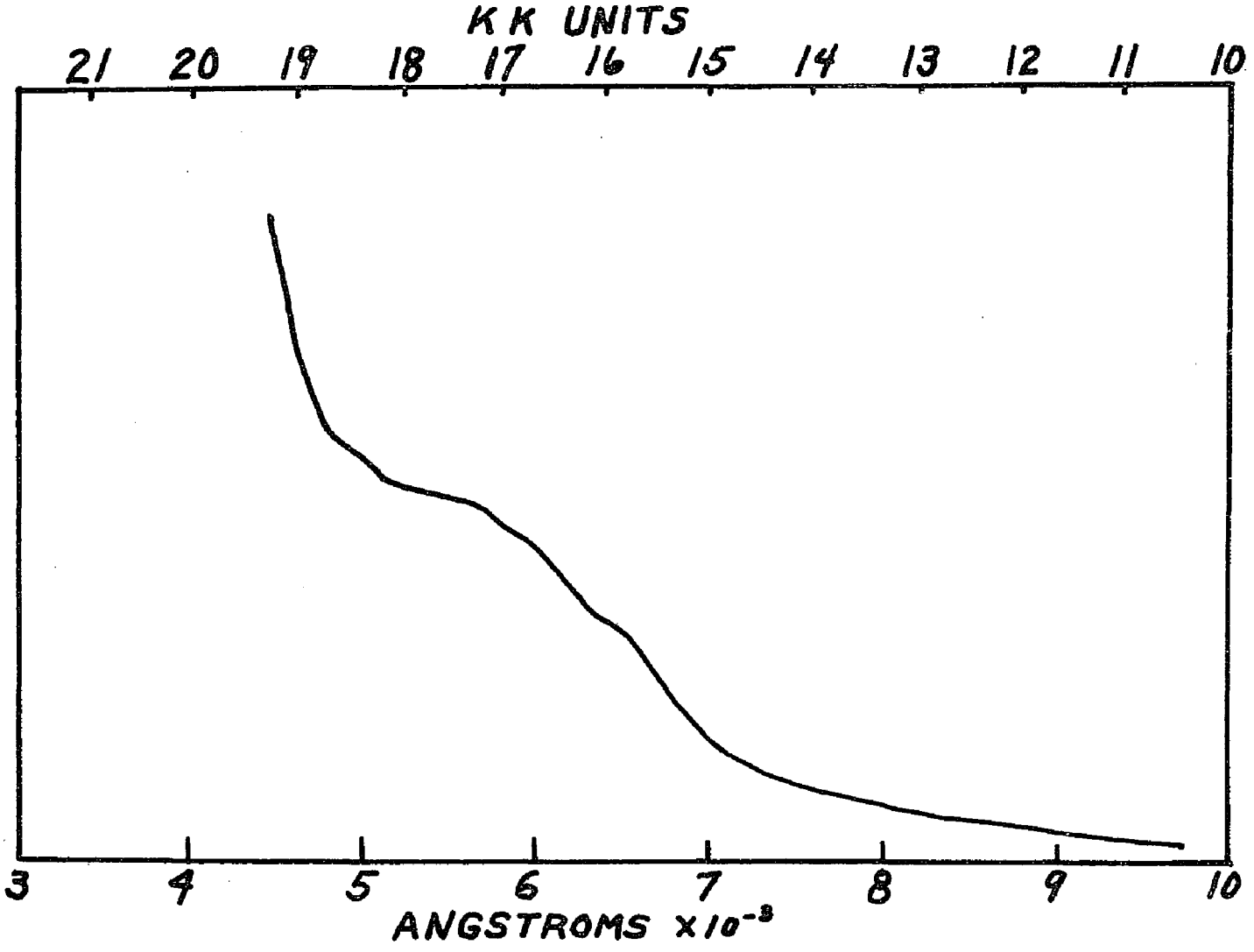
KK UNITS
21 20 19 18 17 16 15 14 13 12 11 10
3 4 5 6 7 8 9 10
ANGSTROMS x10⁻⁸

Figure 13b

The electronic spectrum of VOS_2 in a nujol mull recorded between 10,000 cm^{-1} and 25,000 cm^{-1}

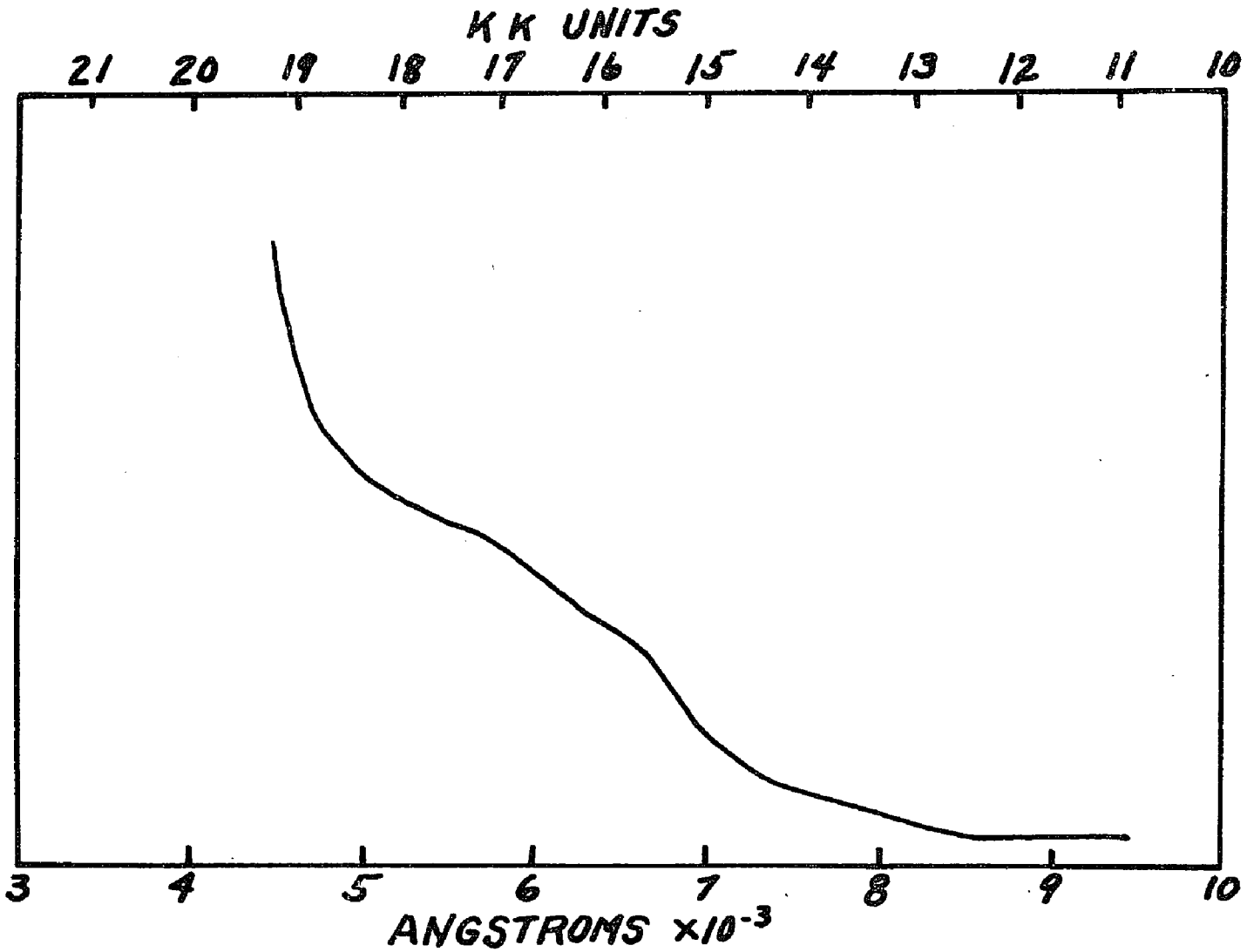
KK UNITS
21
20
19
18
17
16
15
14
13
12
11
10
3
4
5
6
7
8
9
10
ANGSTROMS X10-3

Figure 13c

The electronic spectrum of VOS_2 in a solution of benzene recorded between 10,000 cm^{-1} and 25,000 cm^{-1}

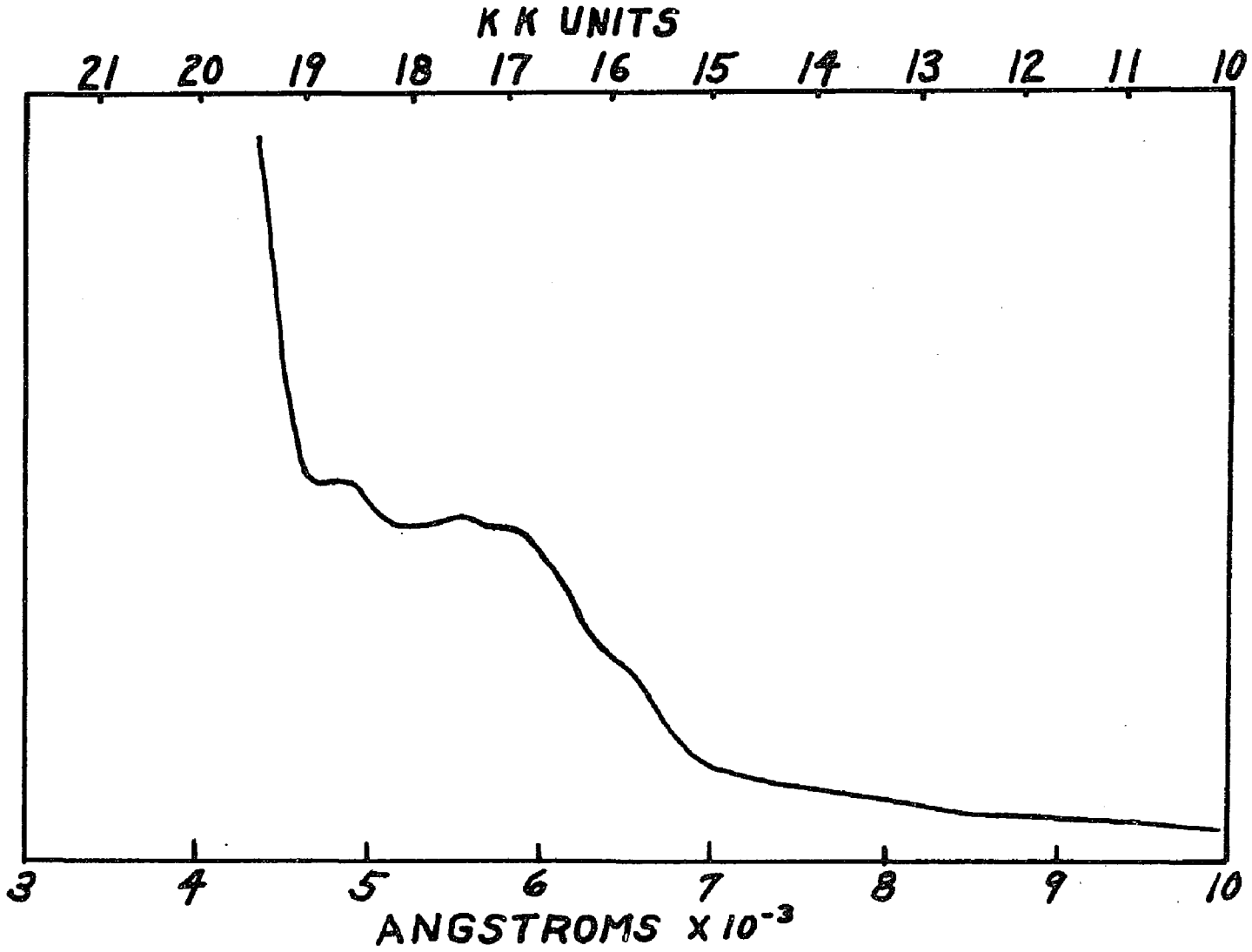
K K UNITS
21 20 19 18 17 16 15 14 13 12 11 10
3 4 5 6 7 8 9 10
ANGSTROMS X 10⁻³

sixth position is protected from solvent effects. A logical explanation would be the one given earlier in the discussion on solubilities; that is, the VOS_2 is a polymer whose structure is such that it does not permit access of the solvent molecule to the sixth position. Thus, in the case of VOS_2, the optical spectra seems to bear out the proposition that VOS_2 is polymeric in nature.

5) IR Spectra

The IR spectrum also indicates the presence of polymeric VOT_2 and monomeric $VOT_2 \cdot py$. In the region between 1500 cm^{-1} and 1600 cm^{-1}, all polymeric complexes of the tropolonate ion possess a peak which is not found in the monomeric tropolonate complexes.[70] Such a peak is observed at 1559 cm^{-1} in Figure 14a, which shows the IR spectrum of VOT_2 in nujol mull. In Figure 14b, which shows the IR spectrum of the monomer $VOT_2 \cdot py$ in nujol mull, this peak is not observed. In addition, the $\nu(V\equiv O)$ band for the possible polymer VOT_2 is at 984 cm^{-1} while the same $\nu(V\equiv O)$ in the monomer $VOT_2 \cdot py$ is found at lower energy, at 950 cm^{-1}. This shift is evidence for the fact that pyridine in the sixth position of the monomer weakens the $V\equiv O$ band from its strength in the polymeric molecule, where presumably there is not ligand trans to the oxygen.

Figure 14a

The infrared spectrum of VOT_2 in nujol mull
(A) between 1500 cm^{-1} and 1600 cm^{-1} and
(B) between 900 cm^{-1} and 1000 cm^{-1}.

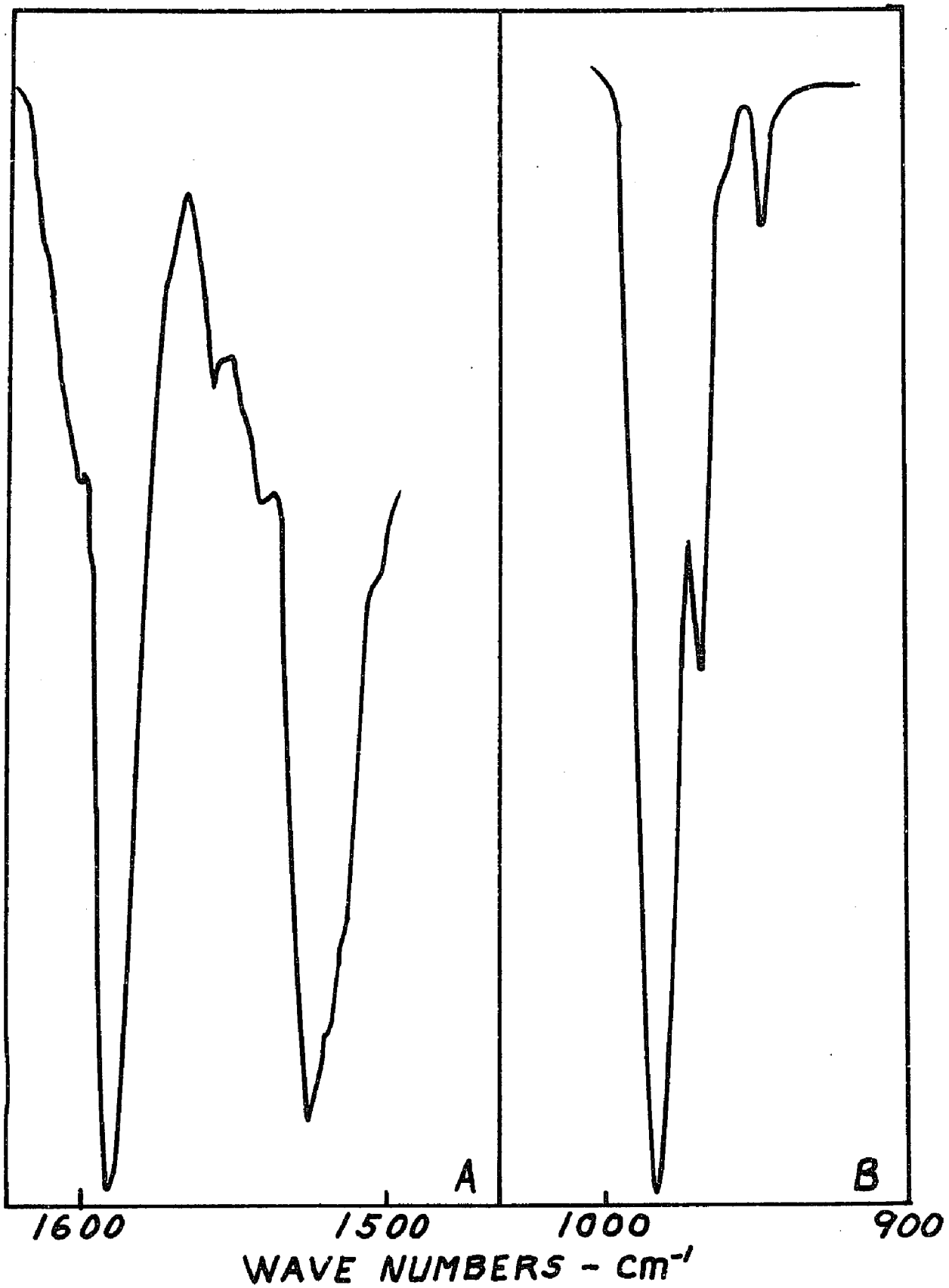
A
B
1600
1500
1000
900
WAVE NUMBERS - cm⁻¹

Figure 14b

The infrared spectrum of $VOT_2 \cdot py$ in nujol mull
(A) between 1500 cm^{-1} and 1600 cm^{-1} and
(B) between 900 cm^{-1} and 1000 cm^{-1}.

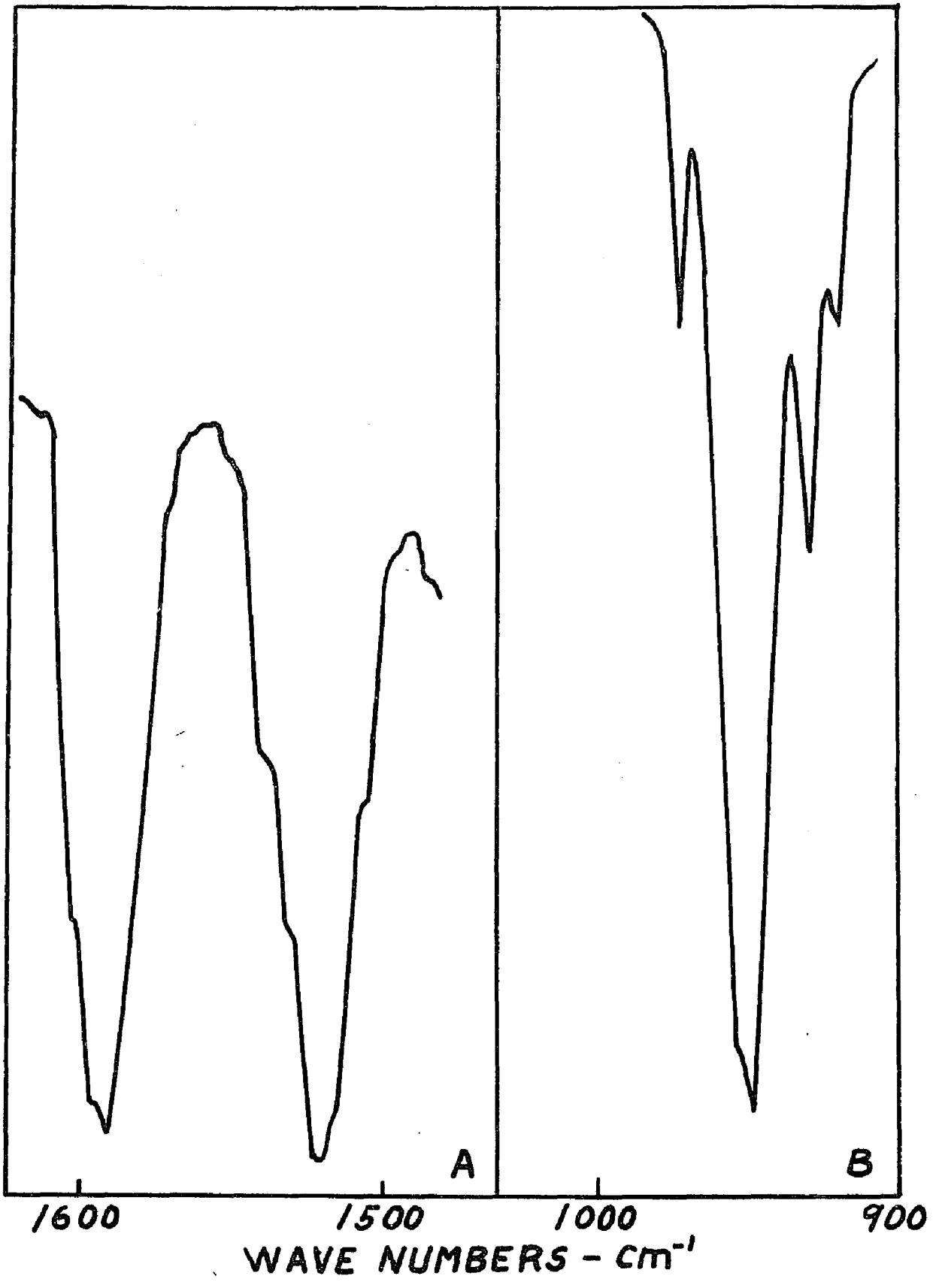
A
B
1600
1500
1000
900
WAVE NUMBERS - cm⁻¹

6) Magnetic Moment Determination

Magnetic moments of the solids VOT_2 and VOS_2 were determined by the Gouy method as described earlier. $VO(aca)_2$ was used as a standard for calibration since its magnetic moment is well established and it is a complex which is presumed to be very similar to VOT_2 and VOS_2. The μ_{eff}^{corr} = 1.21 BM was found for VOT_2 while the μ_{eff}^{corr} = 0.72 BM was found for VOS_2. Probably the strongest evidence which suggests the polymerization of VOT_2 and VOS_2 are these very low magnetic moments of 1.21 and 0.72 BM for a d^1 system such as the VO^{2+} ion.

The vanadyl tartrate studied extensively by Selbin and Morpurgo[79] was later shown to be a dimer by an x-ray diffraction study[80]. Its magnetic moment was found to be about 1.73 BM which would indicate very little signlet state character (electron spin-electron spin coupling) for the dimer. This can be understood if one consults the x-ray data. One finds that the two vanadium atoms of the dimer are connected through V-O-C-C-O-V linkage which results in a V-V distance of 4.3Å. This large V-V distance attenuates the effect of one unpaired electron on the other unpaired electron with the result that it has very little effect on the magnetic moment. Consider, however, the proposal made in this work that the vanadium

atoms of VOT_2 are held together by three-bonded oxygen atoms shown in (a).

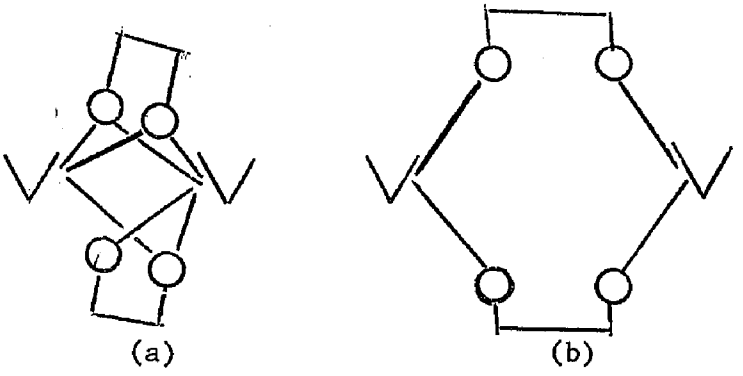

The V-V distance must be much shorter than in the case of the tartrate complex. This would naturally result in a stronger spin-spin coupling with a reduction of the magnetic moment. One must then conclude that these low magnetic moments for VOT_2 and VOS_2 not only indicate the strong possibility of polymerization but also that this polymerization probably results from three-bonded oxygen atoms between the vanadium atoms as shown in (a) rather than through the bonding system shown in (b).

7) ESR Spectra

The ESR spectra of VOT_2 were recorded in $CH_2C\ell_2$ solution, cyclohexanol solution, nujol suspension, and as a solid diluted by the tropolone ligand. These spectra are shown in Figures 15a-15b. The g factors for the solutions of $CH_2C\ell_2$ and cyclohexanol and for

Figure 15

The ESR spectrum of oxovanadium(IV) complexes. The ESR spectrum of VOT_2 in $CH_2C\ell_2$ is given in (A) and the ESR spectrum of VOT_2 in a suspension in nujol, as a solid diluted by tropolone ligand and as a dilute solution in cyclohexanol are given in (B). (Only one spectrum is shown for VOT_2 in all three media in B since they give essentially the same spectra). The ESR spectrum of vanadyl tartrate in aqueous solution, recorded by Belford et al.[81], is given in (C).

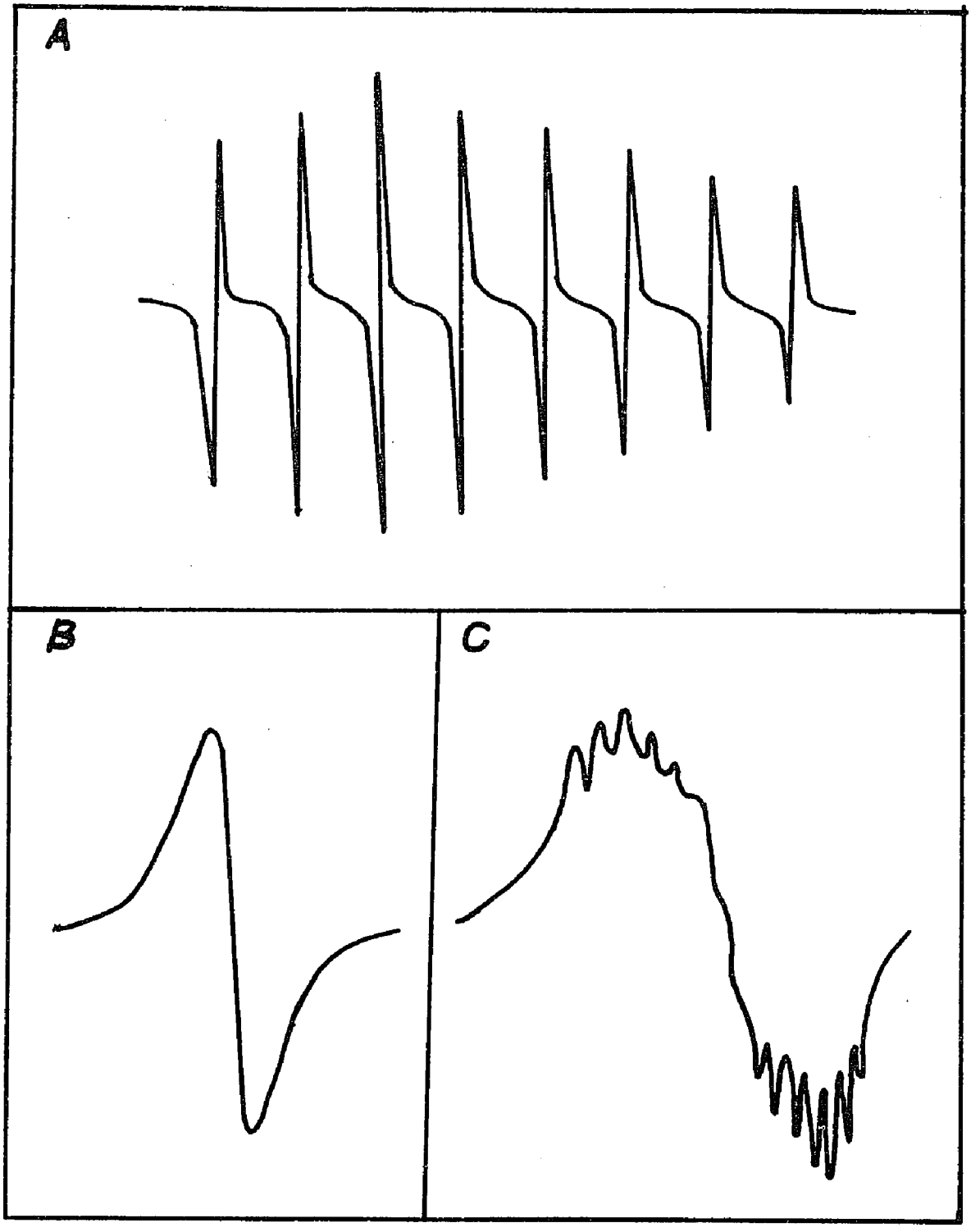
A
B
C

the dilute suspension in nujol were the same and were calculated to be $g_{avg} = 1.95$. The g factor for the solid diluted in tropolone was found to be g = 1.98. (There was a question concerning the functioning of the gaussmeter which might invalidate the latter value).

The ESR spectrum of VOT_2 in $CH_2C\ell_2$, Figure 15A, is very similar to those found for other monomeric vanadyl complexes in solution. There were eight sharp, almost equally spaced, peaks indicative of the d^1 unpaired electron split by the isotopically pure vanadium-51 nucleus with spin of $\frac{7}{2}$. There did not appear to be any signs of other hyperfine splitting or other spectral details which might indicate polymerization in $CH_2C\ell_2$ solution. This is in contrast to the magnetic moment data derived from the NMR experiment. ESR does not offer any evidence for the proposition that VOT_2 is a polymer in $CH_2C\ell_2$. With this knowledge, if VOT_2 does exist as a polymer in $CH_2C\ell_2$, it is at least largely dissociated and appears mostly as the monomer. This possibility prompted the author to obtain the spectrum in a still less polar medium, thus, a sample of the solid well-diluted by the ligand was run (Figure 15B). The spectrum showed a single peak with no hyperfine structure. Carrington[75] describes the appearance of a single line as resulting

from one of two possibilities. First, if the VOT_2/ligand ratio is not small enough, the VO^{2+} (d^1 electrons) ions are close enough to each other to cause an effective spatial dipole-dipole coupling which results in line broadening and loss of hyperfine splitting. This phenomena results because the close proximity of neighboring spin re-orientation prevents the observation of most hyperfine structure. Another possible reason for the appearance of the single peak, however, is the occurrance of electron exchange between unpaired electrons, each residing on two different butlike atoms which are coupled together to form a dimer. Such is the case, for example, of the two Cu^{++} ions paired together in the copper acetate complex. The exchange interaction is evidence that the two unpaired electrons are near enought to "wash out" the hyperfine structure associated with the electron-nuclear coupling of the metal atom, and in the case of dilute samples, it is used as a criterion for inferring dimerization.

To explain this phenomenon, one must propose the dimer as being composed of two normal ground state complexes bonded together with some overlap of the orbitals which are occupied by the unpaired electrons. The unpaired electrons spend most of their time in the neighborhood of their respective metal nuclei but, due to orbital

overlap of the orbitals containing the unpaired electrons, some time is spent by the unpaired electrons in the neighborhood of each other. In this situation, the electrons occupy either a singlet state (electrons paired) or they may occupy a triplet state (electrons unpaired) which usually occurs within kT in energy above the singlet state. The effect on the spectrum by the electrons when they are in the neighborhood of their respective metal nuclei is that of the monomer, that is, the spectrum would show hyperfine splitting of the single peak. If, however, the electrons spent enough time in the neighborhood of each other, they may pair up to occupy the singlet state during which time no resonance can occur. The effect on the spectrum is that the size of the peak is reduced from the peak of a pure monomer. (This condition also accounts for the observed low magnetic moment of a dimer). If, however, the temperature is sufficient to populate the low lying triplet state ($kT \sim S \rightarrow T$), the contribution of this state to the spectrum is to produce a single narrow band. Thus, at ambient temperatures, one usually observes a combination of the triplet state and the monomer ground state which usually appears as a broad band with no fine structure. If the temperature of resonance is reduced, the triplet state becomes depopulated with the result that the fine structure

for the interaction between the metal nucleus and the unpaired electron begins to appear on the spectrum. While in the triplet state, exchange interaction between the electrons occurs so that each electron "sees" two equivalent nuclei. If the temperature is low enough to observe fine structure, one usually observes not the fine structure due to one but rather two nuclei. In the case of VO^{2+} dimers (S of $^{51}V = \frac{7}{2}$), one observes a fifteen line spectrum rather than the eight line spectrum of the monomer. As an example, a recent ESR spectrum by Belford et al.[81] (Figure 15c) recorded on a solution of the dimer sodium vanadyl(IV) dℓ-tartrate, shows a large single peak whose general shape is not dissimilar to the single peak of VOT_2 in tropolone ligand. Super-imposed on this single structure was a hyperfine structure containing fifteen lines rather than the eight lines one would expect from a VO^{2+} ion with ^{51}V spin of $\frac{7}{2}$. Through exchange of the unpaired electrons, each electron "sees" two identical nuclei with the result that one observes 2nI+1 lines (n = 2; number of vanadium atoms) or a fifteen line hyperfine structure.

Not knowing if the single peak observed for VOT_2 in tropolone was a result of the dimerization of two molecules or whether the sample was too concentrated, it was then advisable to

to make a very dilute sample of VOT_2 suspended in nujol. Figure 15B shows this sample's spectra to be very similar to the solid sample. In addition, it was found that small quantities of VOT_2 would dissolve in cyclohexanol to give a light orange solution. After filtering the solution to insure that no solids remained, the ESR spectrum of VOT_2 was recorded in cyclohexanol (Figure 15B). This dilue solution exhibited the same single line appearing in the previous spectra. It would appear then that ESR does not offer any evidence for the existance of a polymer of VOT_2 in $CH_2C\ell_2$ at the temperature at which the spectrum was recorded. If polymerization is present in $CH_2C\ell_2$ as is suggested by the NMR experiment previously described, then the exchange between the polymer form and the monomer is such that its solution still gives the eight line ESR spectrum of the monomer. On the other hand, a more non-polar solution, such as cyclohexanol, a dilute solid and the nujol suspension, all give a bit of evidence for the existance of VOT_2 as a polymer (probably a dimer).

The ESR spectrum of VOS_2 was made in benzene and in a dilute mixture of its ligand (Figures 16 a and 16b). The average g factor for both was found to be $\langle g \rangle = 1.93$. The general shape in both the solid spectrum and the solution spectrum were very much

Figure 16a

The ESR spectrum of VOS_2 in a solution of benzene

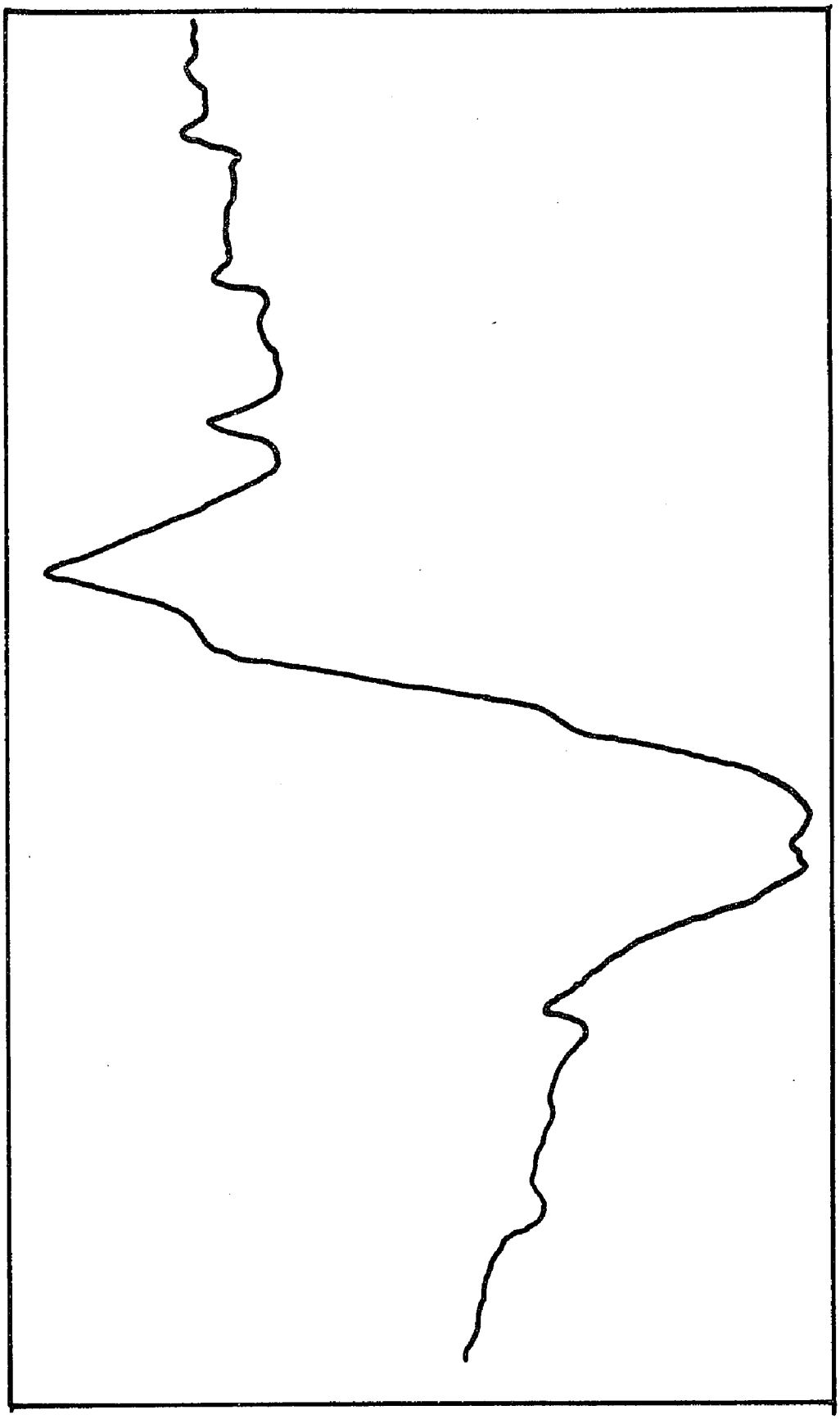

Figure 16b

The ESR spectrum of VOS_2 as a solid diluted with 5-mercapto-3-phenyl-1,3,4-thiadiazole-2-thione ligand.

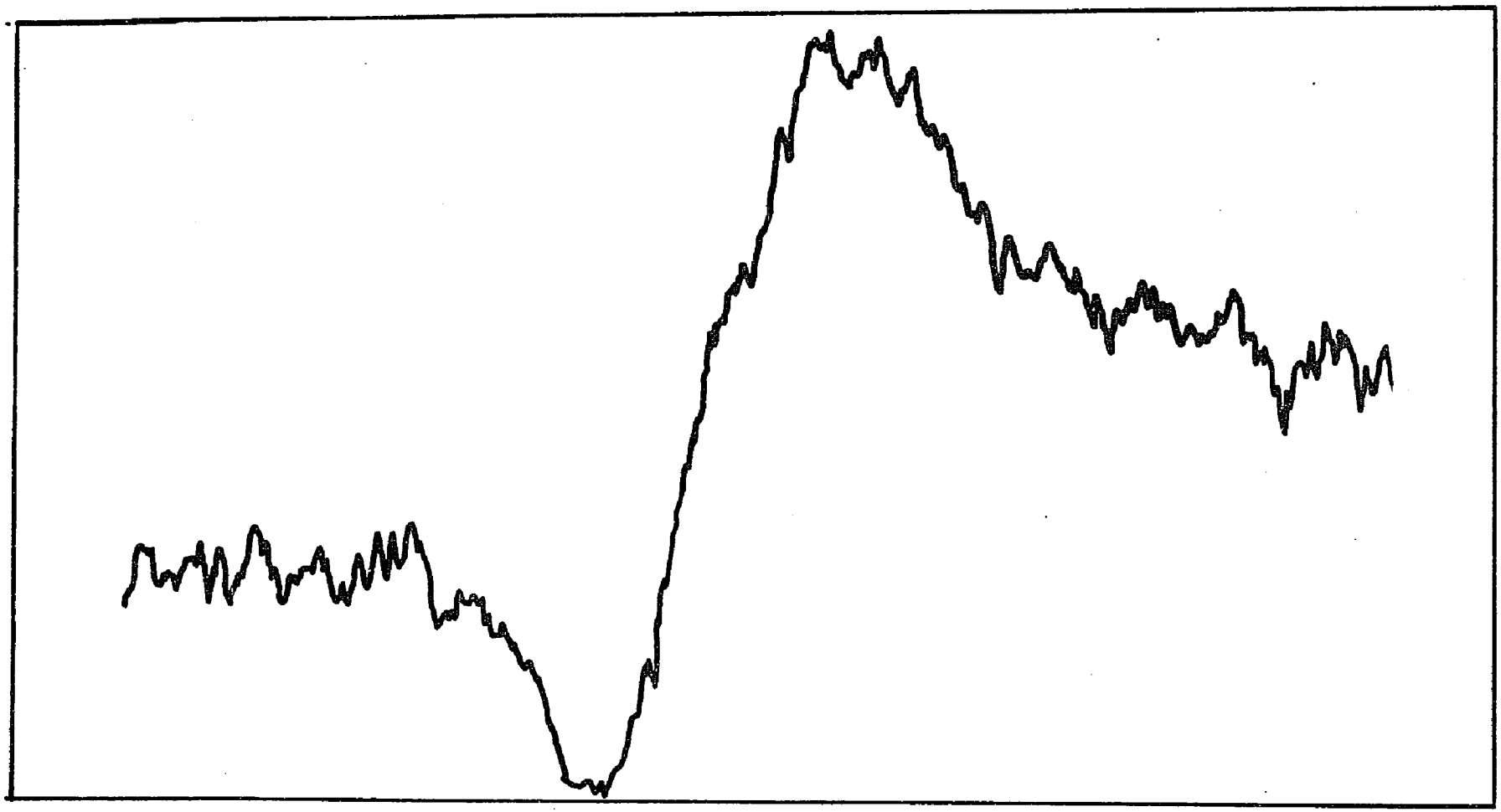

alike. This likeness in shape reinforces the conclusion drawn from the optical data that no extensive solvation effects on the structure of the molecule take place in solution and that the sixth position of VOS_2 is blocked, possibly by virture of the complex being a polymer. Other features, however, were more indicative of the existance of a polymer. First, the general shape of the spectrum was a single absorption band similar to that of VOT_2 and, using the rationale used to analyze the spectra of VOT_2, it can be said that VOS_2 is probably also a polymer. More important probably is the fine structure which seems to be developing in the spectra of both the solution and the solid sample. The spectra are too poorly defined to tell what type of hyperfine structure is developing, however. The ESR evidence for VOS_2 as a polymer is as strong, if not stronger, than that for VOT_2. The fact that it probably retains its polymeric character, regardless of the solvent in which it is dissolved (if, indeed, it is a polymer), makes VOS_2 a much better complex for future study than VOT_2. A future study should include a low temperature ESR investigation of these complexes with the expectation of finding a fifteen line spectrum (and the existance of the low lying triplet state); such a spectrum would make a more concrete case for the existence of polymerization in these complexes.

E. CONCLUSIONS

Muetterties states that "the facility with which an ion can form higher-coordination structures is some function of metal-ion size and charge"[70]. Large ion size and high charge are necessary requirements for high coordination to the metal ion. Meutterties[70] has given 0.68Å as probably the minimum ionic radius necessary for a trivalent ion to coordinate to a number of ligands higher than six. Although the formal charge of the vanadium atom of VO^{2+} is four, the π-donation of the vanadyl oxygen reduces the actual charge on the vanadium atom to a charge closer to three than four. The ion size for V^{3+} has been given to be 0.74Å[82] which would indicate that the ion size requirement and charge are met in order that VO^{2+} species coordinate to coordination numbers higher than six. A presumably seven-coordinate complex of V^{5+} (VOT_3) was prepared by Muetterties *et al.*[68] which, if it is true, should reinforce the claim that the VO^{2+} species possesses the necessary charge and ionic radius to coordinate to a number above six.

An additional requirement of Muetterties for inferring polymerization (with resulting high coordination) is that of low solubility in common solvents. Polymerization is concluded to be through three-centered oxygen bonds, thus it can be seen that a

six-coordinated polymeric complex is in actuality at least a seven- or higher-coordinated complex. Both VOT_2 and VOS_2 meet these solubility requirements and, thus, could possess higher-than-usual coordination. The NMR data given in Figure 12b shows the gradual reduction of the magnetic moment of VOT_2 as the amount of $CH_2C\ell_2$ in the mixed solvent (DMSO/$CH_2C\ell_2$) is increased. Extrapolating out to pure $CH_2C\ell_2$, one can see that a significant reduction in μ_{eff} is found. This is a strong indication that the magnetic moment reduction results from some type of polymerization in solution. The question of the extent to which the VOT_2 in solution has been oxidized places some doubt on the conclusion that VOT_2 contains polymeric species in the $CH_2C\ell_2$ solution.

The molecular weight determination of VOT_2 in $CH_2C\ell_2$ is too doubtful to be of value due to low solubilities, and no conclusions will be drawn from these data.

Although the optical spectral data of VOT_2 offers no evidence of polymerization in solution, the unusual number of low energy peaks makes this complex an interesting one for future study. The complex VOS_2 gives essentially the same optical spectrum in a non-polar solvent (benzene) as it does in the very polar solvent pyridine. The peaks which normally are well-shifted as a result of

a strongly attached sixth position ligand do not show signs of this shift for VOS_2 in pyridine. This lack of peak shifting is evidence for the proposition that no pyridine molecules can reach the sixth position of VOS_2 because of its polymeric structure.

It is believed that the polymeric structure of VOT_2 in the solid state is destroyed in a solution of polar solvents. The IR spectrum should reflect differences between the monomer and the polymer. A substantial shift of the $\nu(V{\equiv}O)$ of VOT_2 was observed in the IR spectrum of $VOT_2{\cdot}py$. This shift, down in energy for the monomeric $VOT_2{\cdot}py$, would be expected if the polymer VOT_2 were destroyed in solution and a pyridine molecule were allowed to attack the sixth position. In addition, a peak appearing in tropolonate IR spectra which is characteristic of the polymeric species but is not found in monomeric complexes was found in VOT_2 but not in $VOT_2{\cdot}py$.

Two portions of experimental evidence which most strongly support the polymeric structure, and hence, high coordination of VOT_2 and VOS_2 are magnetic moment and ESR data. The magnetic moments of VOT_2 and VOS_2 were found to be 1.21 BM and 0.72 BM, respectively. These low moments probably result from a large spin coupling of the d^1 electrons as polymerization brings the VO^{2+} ions closer together.

The single line ESR spectra found for VOT_2 in the solid state in a dilute nujol suspension and in a solution of cyclohexanol suggest that the complex could exist as a polymer. Although one might conclude that the single line spectra (without hyperfine splitting) resulted from a sample too highly concentrated with VO^{2+} ions, such an explanation for the single line spectrum of VOT_2 in cyclohexanol could not be the case since the sample was a dilute solution. The ESR spectra of VOS_2 were even more indicative of polymerization in that not only did the general shape of the spectra appear as a single line, but also there was evidence of developing hyperfine structure on the peaks of the fine structure. A complete temperature study of both the magnetic moments and ESR would be necessary to validate the above findings. The ultimate answer, of course, will lie with complete structural determination of these complexes by x-ray crystallography.

TABLE XII

THE OPTICAL SPECTRAL DATA OF VOT_2

	Solvent	1	2	3	4	5	6	7	8
a)	Nujol Mull	15,660	15,380	16,130	19,010	19,610	21,500		26,320
b)	Pyridine	12,020 (ϵ-52)	15,380	16,000	19,230	19,640	21,700	22,730	25,000
c)	$CH_2C\ell_2$		17,240	17,540	18,350	19,050	19,610	20,620	21,500
d)	$CH_2C\ell_2$*					20,580 (ϵ=250)	21,280 (ϵ=210)	22,470	22,730

* The disolution of VOT_2 in $CH_2C\ell_2$ required four days; NMR shows the solution to be diamagnetic with vanadium in V(IV) oxidation state.

a) Energies are given in cm^{-1}.

b) No extinction coefficients are given for bands which appear as shoulders.

TABLE XIII

THE OPTICAL SPECTRAL DATA OF VOS_2

Solvent	1	2	3	4
a) Pyridine	15,630	17,240	17,860	20,200
b) Nujol Mull	~15,000	---	---	---
c) Benzene	15,380	17,090	17,760	20,160

No extinction coefficients are given since all bands were found to be shoulders.

The nujol mull spectrum was too poorly defined to locate any but the first band.

BIBLIOGRAPHY

1. G. Booth, "Advances in Inorganic Chemistry and Radiochemistry", Vol.6, pp.1-69, edited by H.J. Emeleus and A.G. Sharpe, Academic Press, New York, N.Y., 1964.

2. D. Nicholls, Coord. Chem. Rev., 1, 379 (1966).

3. J. Selbin, Coord. Chem. Rev., 1, 293 (1966); Chem. Rev., 65, 153 (1965).

4. R.J.H. Clark, U. Lewis, and R.S. Nyholm, J. Chem. Soc., 2460 (1962).

5. R.J.H. Clark, J. Chem. Soc., 5699 (1965).

6. R.J.H. Clark, M.H. Greenfield and R.S. Nyholm, J. Chem. Soc., 1254 (1966).

7. A.K. Majundar, A.K. Mukherjee, and R.G. Bhattacharya, J. Inorg. Chem., 26, 386 (1964).

8. B.W. Fitzsimmons, P. Gans, B. Hayton, and B.C. Smith, J. Inorg. Nucl. Chem., 28, 915 (1966).

9. F.A. Hart and J.E. Newbery, J. Inorg. Nucl. Chem., 26, 1334 (1966).

10. S.M. Horner, S.Y. Tyree and D.L. Venzky, Inorg. Chem., 1, 844 (1962).

11. G. Vigee and J. Selbin, unpublished results.

12. B.J. McCormick, Inorg. Nucl. Chem. Letters, 3, 293 (1967).

13. J. Selbin, G. Maus, and D.L. Johnson, J. Inorg. Nucl. Chem., 29, (1967).

14. L. Orgel, "An Introduction to Transition-Metal Chemistry", pp.136-156, John Wiley and Sons, Inc., New York, N.Y., 1964.

15. A. Fowles, Proc. Int. Conf. Coord. Chem., 8, 208-209 (1964).

16. R. Holm and E. King, Inorg. Chem., 2, 219 (1963).

17. N.S. Garifyanov and B.M. Kozyrev, Theor. i Eksperim. Khim., Akad. Nauk, USSR, 1, 525 (1965).

18. B. McCormick, Inorg. Nucl. Chem. Letters, 3, 293 (1967).

19. A. Davison, N. Edelstein, R. Holm and A. Maki, J. Am. Chem. Soc., 86, 2799 (1964).

20. H.Gray and E. Billig, J. Am. Chem. Soc., 85, 2019 (1963).

21. F.J. Welcher, "Organic Analytical Reactions", Vol.IV, p.82, R. Van Nostrand, New York, N.Y., 1948.

22. J. Selbin, Chem. Rev., 65, 153 (1965).

23. R.S. Drago, J. Am. Chem. Soc., 87 (1965).

24. N. Bloembergen, Physica, 16, 95 (1950).

25. H.M. McConnell, J. Chem. Phys., 24, 764 (1956).

26. H.M. McConnell, J. Chem. Phys., 29, 1361 (1958).

27. R.G. Shulman and V. Jaccarino, Phys. Rev., 108, 1219 (1957).

28. D.R. Eaton, J. Am. Chem. Soc., 87, 3102 (1965).

29. R.S. Drago, "Physical Methods in Inorganic Chemistry, p. 239 , Reinhold Publishing Co., New York, N.Y.

30. D.R. Eaton, A.D. Josey, W.D. Phillips and R.E. Benson, J. Chem. Phys., 37, 347 (1962).

31. J.A. Happe and R.L. Ward, J. Chem. Phys., 39, 5, 1211 (1963).

32. W.D. Horrocks, R.C. Taylor and G.N. Lamar, J. Am. Chem. Soc., 86, 3031 (1964).

33. A.J. Freeman, Phys. Rev. Letters, 6, 343 (1961).

34. W.D. Horrocks and R.W. Kluiber, J. Inorg. Chem., 5, 152 (1966).

35. W.D. Horrocks and R.W. Kluiber, J. Am. Chem. Soc., 88, 1399 (1966).

36. D.R. Eaton, A.D. Josey, R.E. Benson, W.D. Phillips and T.L. Cairns, J. Am. Chem. Soc., 84, 4100 (1962).

37. A. Forman, J.N. Murrell and L.E. Orgel, J. Chem. Phys., 31, 1129 (1959).

38. T.S. Davis and J.P. Fackler, J. Inorganic Chem., 5, 242 (1966).

39. W.D. Horrocks and R.W. Kluiber, J. Am. Chem. Soc., 88, 1399 (1966).

40. H.F. Holtzclaw, R.C. Larson and R.C. Hennery, J. Inorg. Chem., 5,

41. W.D. Horrocks and R.W. Kluiber, J. Am. Chem. Soc., 87, 5350 (1965).

42. R.S. Drago, J. Am. Chem. Soc., 88, 2455 (1966).

43. R.S. Drago, J. Am. Chem. Soc., 88, 2966 (1966).

44. A.C. Adams and E.M. Larsen, J. Inorg. Chem., 5, 814 (1966).

45. A.C. Adams and E.M. Larsen, J. Inorg. Chem., 5, 277 (1966).

46. D.F. Evans, J. Chem. Soc., 2003 (1956).

47. C.J. Ballhausen and H.B. Gray, Inorg. Chem., 1, 111 (1962).

48. S.P. McGlynn, D.G. Carroll and A.T. Armstrong, J. Chem. Phys., 44, 1865 (1966).

49. J. Selbin, L.H. Holmes and S.P. McGlynn, J. Inorg. Nucl. Chem., 25, 1359 (1963).

50. D. Kivelson and S.K. Lee, J. Chem. Phys., 41, 1896 (1964).

51. M. Zerner and M. Gouterman, Inorg. Chem., 5, 1699 (1966).

52. H.G. Hecht and T.S. Johnson, J. Chem. Phys., 46, 23 (1967).

53. L.G. Vanquickenborne and S.P. McGlynn, to be published.

54. R.E. Benson and W.D. Phillips, in "Advances in Magnetic Spectroscopy", Vol.1, Academic Press, New York, N.Y., 1965, pp.103,148.

55. B.B. Wayland and W.L. Rice, Inorg. Chem., 5, 54 (1966).

56. R. Hausser and G. Laukien, Z. physik, 153, 294 (1959).

57. J. Reuben and D. Fiat, Inorg. Chem., 6, 579 (1967).

58. K. DeArmond, B.B. Garett and H.S. Gutowsky, J. Chem. Phys., 42, 1019 (1965).

59. H.E. Radford, Phys. Rev., 126, 1035 (1962).

60. K. Wüthrich and R.E. Connick, Inorg. Chem., 6, 683 (1967).

61. E.L. Mutterties and C.M. Wright, Quart. Revs., 21, 109 (1967).

62. F.A. Cotton, Quart. Rev., 20, 389 (1966).

63. H. Schafer, Angew. Chem., 76, 833 (1964).

64. N.V. Sidgwick and H.M. Powell, Proc. Roy. Soc. (A), 176, 153 (1940).

65. R.J. Gillespie and R.S. Nyholm, Quart. Rev., 11, 339 (1957).

66. E.L. Muetterties and C.M. Wright, J. Am. Chem. Soc., 86, 5132 (1964).

67. E.L. Muetterties and C.M. Wright, J. Am. Chem. Soc., 87, 21 (1965).

68. E.L. Muetterties and C.M. Wright, J. Am. Chem. Soc., 87, 4706 (1966).

69. E.L. Muetterties and C.M. Wright, J. Am. Chem. Soc., 88, 305 (1966).

70. E.L. Muetterties and C.M. Wright, J. Am. Chem. Soc., 88, 4856 (1966).

71. J. Selbin and J.D. Ortego, J. Inorg. Nucl. Chem., 30, 313 (1968).

72. P.M. Selwood, "Magneto Chemistry", Interscience Publishers, Inc., 2nd Edition, 1956.

73. B.N. Figgis and J. Lewis, in J. Lewis and R.G. Wilkin's "Modern Coordination Chemistry", Interscience Publishers, Inc., New York, N.Y., 1960, pp.400-445.

74. K. Frei and H.J. Bernstein, J. Chem. Phys., 27, 1891 (1962).

75. A. Carrington and A.D. McLachlan, "Introduction to Magnetic Resonance", Harper and Row Publishers, New York, N.Y., 1967.

76. A. Carrington, Quart. Rev., 17, 67 (1963).

77. M. Bersohn and J.C. Baird, "Electron Paramagnetic Resonance", W.A. Benjamin, Inc., New York, N.Y., 1966.

78. J. Selbin and T. Ortolano, J. Inorg. Nucl. Chem., 26, 37 (1964).

79. J. Selbin and L. Morpurgo, J. Inorg. Nucl. Chem., 27, 673 (1965).

80. J.C. Forrest and C.K. Prout, J. Chem. Soc. (A), 1967.

81. R. Tapscott and L. Belford, Inorg. Chem., 6, 735 (1967).

82. C.G. Phillips and R.P. Williams, "Inorganic Chemistry", Oxford University Press, New York, N.Y., 1965.

VITA

Gerald S. Vigee was born in Crowley, Louisiana on March 4, 1931 and graduated from Crowley High School in 1948. From 1950 to 1954 he attended the United States Military Academy at West Point, New York and upon graduation, was commissioned a 2/Lt of Artillery in the United States Army. Following five years service in the army, he attended Louisiana State University and received a B.S. degree in 1960. Prior to returning to Louisiana State University for work towards a Ph.D. in chemistry, he received a M.S. degree in chemistry from the University of Southwestern Louisiana.

He is married to Wilhelmina Rist Vigee from which two sons, John and David, and a daughter, Noelle, were born.

EXAMINATION AND THESIS REPORT

Candidate: Gerald S. Vigee

Major Field: Chemistry

Title of Thesis: Preparation and Optical and NMR Spectral Studies of Some Unusual Complexes of Oxovanadium(IV)

Approved:

Joel Selbin
Major Professor and Chairman

Max Goodrich
Dean of the Graduate School

EXAMINING COMMITTEE:

W M Baddley

Eugene W. Berg

James H. Atherton

William T. Burnett Jr

Date of Examination:

May 2, 1968